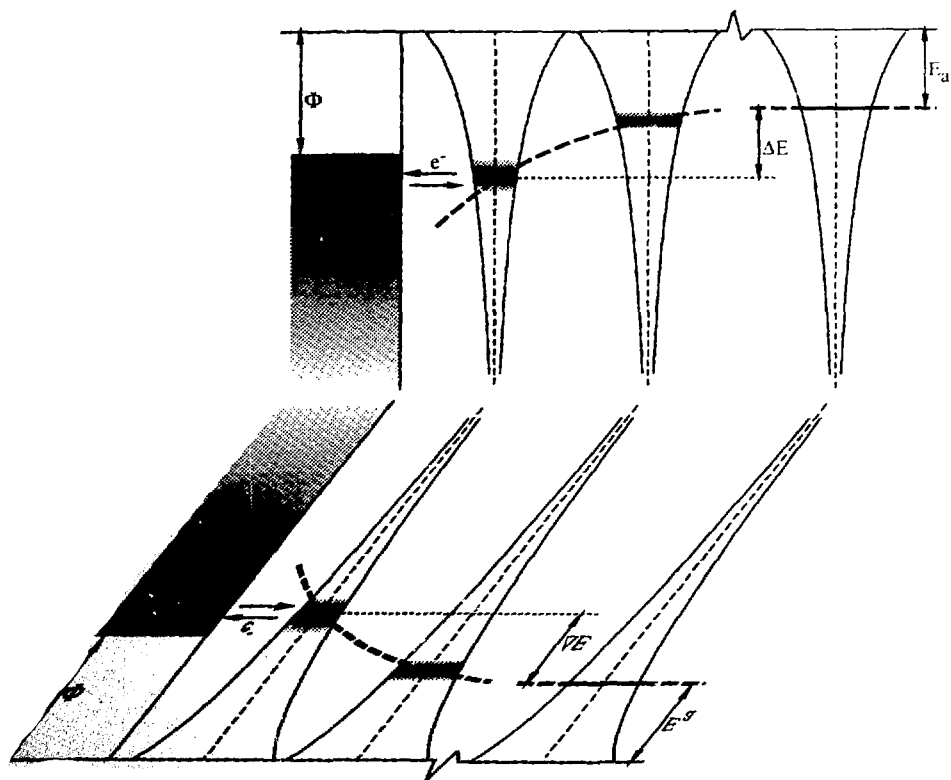
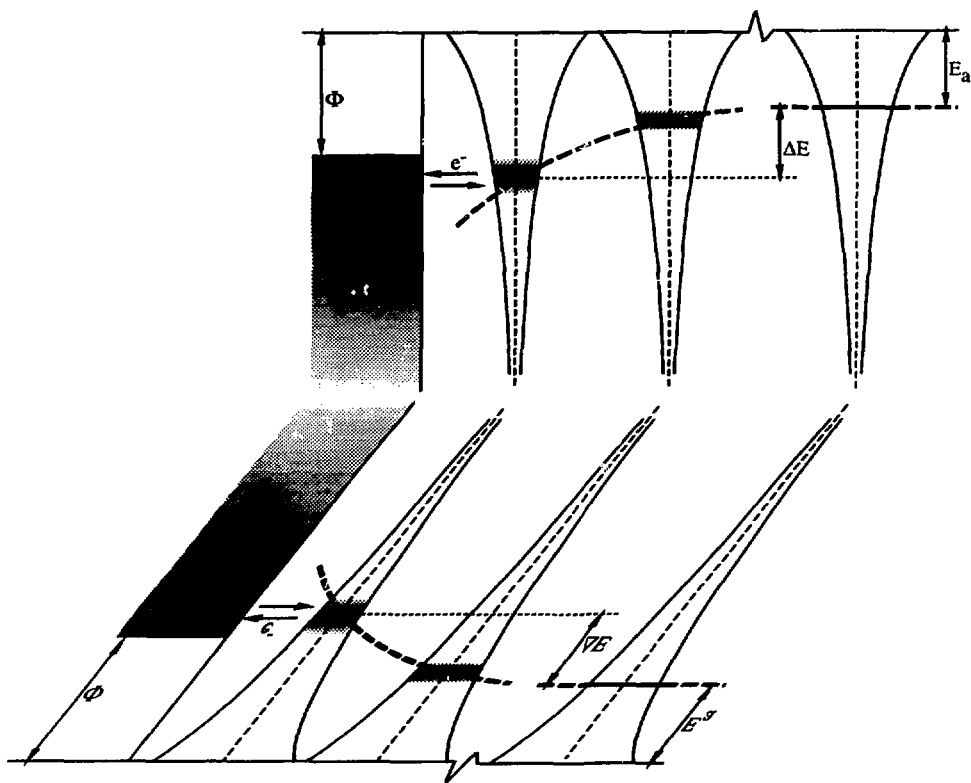


NEGATIVE ION SOURCERY

INIS-mf--11550

*Ron van Os*

NEGATIVE ION SOURCERY



Ron van Os

NEGATIVE ION SOURCERY

EEN BRON VAN NEGATIEVE IONEN

(met een samenvatting in het Nederlands)

*Proefschrift ter verkrijging van de graad van doctor
aan de Rijksuniversiteit te Utrecht
op gezag van de Rector Magnificus, Prof. Dr. J.A. van Ginkel
ingevolge het besluit van het College van Dekanen
in het openbaar te verdedigen
op 24 mei 1989 des namiddags te 2:30 uur*

*door
Carolus Franciscus Adrianus van Os*

*promotores: Prof. Dr. F.W. Saris, Rijksuniversiteit Utrecht (RUU).
Prof. Dr. J. Los, Universiteit van Amsterdam (UvA).*

co-promotor: Dr. Ir. P.W. van Amersfoort, FOM instituut voor Plasma Fysica, Rijnhuizen.

The work described in this thesis was mainly performed at the FOM-Institute for Atomic and Molecular Physics, Kruislaan 407, NL-1098 SJ Amsterdam, The Netherlands, as part of the research program of the association agreement between the Stichting voor Fundamenteel Onderzoek der Materie (FOM) and EURATOM, with financial support from the Nederlandse Organisatie voor Wetenschappelijk Onderzoek (NWO) and EURATOM.

This thesis is based upon the following articles:

Chapter 2:

- *NEGATIVE ION FORMATION DURING THE SCATTERING OF A PROTON BEAM FROM A BARIUM SURFACE UNDER GRAZING ANGLES OF INCIDENCE*
C.F.A. van Os, H.M. van Pinxteren, A.W. Kleyn and J. Los, to be submitted to J. Appl. Phys.
- *INTERFERENCES IN THE RESONANT CHARGE EXCHANGE BETWEEN A PROTON AND A BARIUM METAL SURFACE*
C.F.A. van Os and J. Los, to be submitted to Surf. Sci. Lett.

Chapter 3:

- *NEGATIVE ION FORMATION AT A BARIUM SURFACE IN CONTACT WITH A HYDROGEN PLASMA*
C.F.A. van Os, R.M.A. Heeren and P.W. van Amersfoort, Appl. Phys. Lett. **51** (1987) 1495
- *NEGATIVE ION FORMATION AT A BARIUM SURFACE EXPOSED TO AN INTENSE POSITIVE-HYDROGEN ION BEAM*
C.F.A. van Os, P.W. van Amersfoort and J. Los, J. Appl. Phys. **64** (1988) 3863.

Chapter 4:

- *MODELLING OF H⁻ SURFACE CONVERSION SOURCES; DIFFUSION AND SPUTTERING LIMITED CONVERTERS*
C.F.A. van Os, C. Leguijt and J. Los, to be submitted to J. Appl. Phys.
- *IMPORTANCE OF HEAVY ION BOMBARDMENT FOR H⁻ ION FORMATION IN SURFACE CONVERSION SOURCES*
C.F.A. van Os and P.W. van Amersfoort, Appl. Phys. Lett. **50** (1987) 662.
- *THE ROLE OF CESIUM-ION BOMBARDMENT IN THE FORMATION OF NEGATIVE HYDROGEN IONS ON A CONVERTER SURFACE*
C.F.A. van Os, E.H.A. Granneman and P.W. van Amersfoort, J. Appl. Phys. **61** (1987) 5000

Chapter 5:

- *TRANSPORT OF NEGATIVE IONS PRODUCED AT A BARIUM SURFACE LOCATED WITHIN A MULTICUSP ION SOURCE*
C.F.A. van Os, A.W. Kleyn, L.M. Lea, A.J.T. Holmes and P.W. van Amersfoort, accepted for publication in Rev. Sci. Instrum. (April 1989).

Chapter 6:

- *H⁻ FORMATION VIA SURFACE CONVERSION AT A BARIUM SURFACE IN A HIGH POWER DC ENVIRONMENT*
C.F.A. van Os, C. Leguijt, R.M.A. Heeren, J. Los and A.W. Kleyn, accepted for publication in J. Opt. Eng. (May 1989).

CONTENTS

PREFACE	1
1. INTRODUCTION	3
1.1. Neutral beam injection	5
1.2. Volume production of negative ions	8
1.3. Negative surface ionization	9
2. FUNDAMENTALS OF NEGATIVE SURFACE IONIZATION	13
2.1. Introduction	13
2.2. Theory	14
2.3. Experimental arrangement	17
2.4. Results and Discussion.	18
2.4.a. Charge exchange with the barium surface	18
2.4.b. Interferences in the charge exchange process	22
2.4.c. Influence of hydrogen adsorption on the charge exchange	26
2.5. Conclusions	26
Appendix 2.1	27
3. SURFACE CONVERSION AT A BARIUM SURFACE	31
3.1. Introduction	31
3.2. Formation of negative ions	33
3.3. Experimental set-up	36
3.3.a. ALICE, Amsterdam Light Ion Conversion Experiment	36
3.3.b. The detector	37
3.3.c. The barium converter	39
3.4. Experimental results	39
3.5. Discussion	43
3.5.a. The conversion efficiency	43
3.5.b. The hydrogen coverage of the converter surface	44
3.6. Summary	49
Appendix 3.1	50
4. SURFACE CONVERSION AT A CESIATED TUNGSTEN SURFACE	53
4.1. Introduction	53
4.2. Theory	55
4.2.a. Ionization probability	56
4.2.b. Sputtered flux	57

4.3 Experimental arrangement	58
4.3.a. Cesium coverage of a tungsten surface immersed in a cesium seeded hydrogen discharge	59
4.3.b. Porous tungsten converter with liquid cesium supply	62
4.4. Experimental results	63
4.5 Discussion	66
4.6. Conclusions	69
Appendix 4.1	70
 5. TRANSPORT OF NEGATIVE IONS THROUGH A BUCKET SOURCE	 73
5.1. Introduction	73
5.2. Theoretical considerations regarding surface ionization	74
5.2.a. Resonant charge exchange (RCE)	74
5.2.b. Implantation, sputtering and diffusion at the converter surface	75
5.3. Experimental arrangement	76
5.3.a. The Culham source test stand	76
5.3.b. The barium converter	77
5.4. Experimental results	78
5.4.a. Extracted positive ion current density reaching the surface	80
5.4.b. Surface production of negative ions	81
5.4.c. Transport of surface produced negative ions	81
5.4.d. Enhancement of volume produced negative ion current	84
5.5. Discussion	85
 6. HIGH FLUX SURFACE CONVERSION AT A BARIUM SURFACE	 89
6.1. Introduction	89
6.2. Experiments	91
6.3. Discussion	92
6.4. Summary	94
 7A. SUMMARY	 97
 7B. SAMENVATTING (SUMMARY IN DUTCH)	 99
 7C. ЗАКЛЮЧЕНИЕ (SUMMARY IN RUSSIAN)	 101
 CURRICULUM VITAE	 104
 NAWOORD	 104

'Man's search for energy to meet his needs has proceeded since the dawn of civilization. At least some of our international friction is directly traceable to disputes over possession of the areas favored with abundant energy resources. Classical conquest and exploitation rarely are undertaken for barren areas alone. The acquisition of land endowed with energy and material resources motivates much of our present strife. It is to be hoped that the nuclear processes of fission and fusion may permanently solve at least the need for energy and thus contribute substantially to the peaceful relations among mankind.

The demands for energy are now increasing so rapidly that the present reserves of nonnuclear fuels of all types, particularly coal and oil, seem very small indeed when measured against the use anticipated over even the next few decades. It would therefore be prudent to develop the use of nuclear fuels, which represent stores of energy vastly greater than those of all nonnuclear fuels.'

The text printed above is the introduction to a book by David J. Rose and Melville Clark, Jr. entitled "Plasma and Controlled Fusion" published in 1961. It clearly illustrates the romantic view of scientists of those days about nuclear energy. Today, 28 years after this book was published, the hazards of nuclear fuels have shattered this romantic view. Nuclear fission plants went up into smoke, Tsjernobyl (USSR), were close to melt down, Harrisburg (USA) or polluted an entire lake with radioactive products, Windscale (UK). The production of staggering quantities of highly radioactive waste is continuing without a proper and environmentally safe method of disposal. Furthermore, the exploitation of nuclear fission resulted in a world in which peaceful relations are guarded by a vast nuclear arsenal.

However, nuclear energy has conquered a place in our society and we have become dependent on this form of energy production. We have learned to live with the hazards of nuclear energy. This doesn't mean that we have come to terms with nuclear energy. There is still a long way to go before the nuclear waste problem is solved, and fusion as a viable means to produce peaceful energy has still to be proven.

Nowadays, with a still increasing energy consumption, it is in my opinion impossible to abandon nuclear fuels as a means to produce energy without considerably reducing our standards of living. Apart from this, uncontrolled use of our limited conventional energy sources, may result in a large scale devastation of our natural environment (acid rain, greenhouse effect). I feel that there is a enormous lack of realization that our energy greedy society is busy consuming our resources at a pace which cannot be kept by technological advances. This means that compromises are made: We use nuclear fission without having a proper means for the disposal of radioactive waste, we increased the burning of coal realizing that it contributes to a possible greenhouse effect.

However, technological progress is still being made both in the field of nuclear fuels and in the field of alternative energy sources (solar energy, wind energy, tide wave energy, earth heat energy, ect.). Lets focus on the methods of producing energy from nuclear fuels. What progress is needed ? Basically there are two ways of gaining energy via nuclear processes; fission and fusion. Fission is already in use on a wide scale producing energy and highly radioactive waste. It's evident that a large effort is needed in solving the waste problem. Fusion however is in a development stage. No controlled fusion has ever been demonstrated on a scale useable for energy generation. There are some aspects about fusion which motivate a large scale research effort in this field. It is believed that the waste problem of fusion is less hazardous compared to fission. The fusion process itself produces no radioactive waste, only harmless and probably useful helium gas. However, due to the high neutron fluxes penetrating everywhere, activation of the whole reactor results in a large quantity of radioactive waste. Although the amount of nuclear waste would be of the same order compared to fission, the life time of the products is smaller, considerably smaller, of the order of several decades. Due to this shorter life time, the storage or disposal problem of the waste is less complex. But nonetheless also for fusion there is a waste problem ! A more political reason is that with fusion, no byproducts are produced which can be used for nuclear bombs, and finally, no meltdown problems are expected, since the fusion process can be halted within seconds.

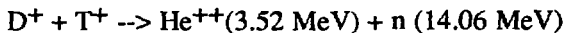
The afore mentioned reasoning that waste problems, proliferation violation and running hazards might be smaller for fusion compared to fission is more or less overshadowed by economical reasoning. It is predicted that the price for fusion energy is higher compared to fission energy. Fortunately, this aspect has as yet not resulted in a large reduction of the fusion research program. Why is the predicted price of fusion so high ? The answer is simple, a fusion machine in the sense of a magnetically confined fusion plasma, is huge, complex and therefore expensive. The development of such a huge machine can therefore not be done by one country by itself. International collaboration and joint funding are essential. This has been recognized and acted upon.

'The president and the General Secretary noted with pleasure the commencement of work on a conceptual design of an International Thermonuclear Experimental Reactor (ITER) under the auspices of the IAEA, between scientists and experts from the United States, USSR, European Atomic Energy Community and Japan. The two leaders noted the significance of this next step towards the development of fusion power as a cheap, environmentally sound and essential inexhaustible energy source for the benefits of all mankind'

The above text is a fusion extract from the joint statement of the Geneva Summit between the leaders of the United States and the USSR held in 1985. The reader may feel the same romantic tone in this statement as there was in the quoted text from 1961 at the beginning of this introduction. I sincerely hope that fusion once in operation does not turn out to be another nuclear disillusion.

The work described in this thesis is invoked by current research programs in the field of nuclear fusion. A brief introduction to fusion is given, anticipated problems related to current drive of the fusion plasma are pinpointed and probable suggestions to overcome these problems are described. One probable means for current drive is highlighted; Neutral Beam Injection (NBI). This is based on injecting a 1 MeV neutral hydrogen or deuterium beam into a fusion plasma. Negative ions are needed as primary particles because they can easily be neutralized at 1 MeV. The two current schemes for production of negative ions are described, volume production and negative surface ionization. The latter method is extensively studied in this thesis.

From the equivalence of mass and energy $E = mc^2$ (931 MeV/atomic mass unit), we see that energy can be extracted from any source only by decreasing the mass of the system. Reactions leading to a decrease of the mass can quickly be found by inspection of the energy available per nucleon. The quantity is measured by the packing fraction P , defined by $P = (M - A)/A$ where M is the actual mass in atomic units and A is the nuclear mass number. In Fig. 1.1 we plotted the packing fraction for several nuclides.¹ Zero on the ordinate is derived from the fact that the oxygen mass is 16 atomic mass units. Clearly, energy can be obtained either by splitting very heavy nuclides (today's fission) or fusing light ones (tomorrow's fusion). The most viable fusion reaction is the merging of a deuterium and a tritium nucleon;



The amount of energy released when one gram of a deuterium-tritium mixture fuses is equal to the amount of energy produced by burning 10.000 liter of organic

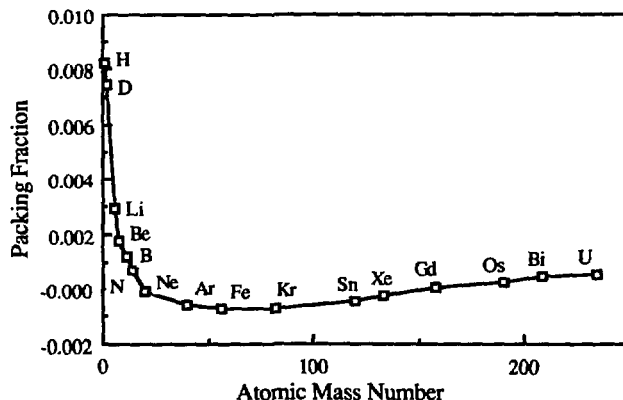


Fig 1.1. The packing fraction (energy available per nucleon) versus the mass number.

oil. In order to obtain this merging the density and the energy of the primary particles should be high enough to bring the particles sufficiently close together. Two schemes to obtain high energies and densities are investigated. The first method is based on implosion of a small pellet which contains the active nuclides, and is called *inertia fusion*. It involves the development of large high power (laser, electromagnetic and particle) beams which are aimed at small glass bulbs filled with deuterium-tritium mixtures or frozen deuterium-tritium droplets. A second approach is based on the creation of a dense and highly energetic plasma which is magnetically confined, and is called *magnetically confined fusion*. The majority of this research is focussed on plasmas created within a tokamak. We will restrict ourselves to the latter form; magnetically confined fusion using a tokamak like geometry.

A tokamak is basically a large scale transformer, where the secondary winding is the fusion plasma. This fusion plasma is confined in a toroidal magnetic field. The plasma current is inductively driven by powering of the primary winding. The schematic arrangement of the JET (Joint European Torus) tokamak is shown in Fig. 1.2.² It consists of a toroidal vacuum chamber (the torus) within a large iron yoke. The vacuum vessel is surrounded by magnetic field coils to produce the toroidal magnetic field for the confinement of the inner plasma. Since the secondary plasma current is inductively driven, there is a clear limit to the operation time of a tokamak, at current it is generally less than 10 seconds. For running a tokamak in a DC mode additional schemes are needed to sustain the plasma current. A mechanism generally referred to as *current drive*.

Current drive can be obtained by injection of energetic particles or by incident electro magnetic waves. Four schemes for current drive have evolved; γ_{CD} denotes the current drive efficiency;

- I. *Neutral Beam Injection (NBI)*. A high energy beam is injected along the axis of the fusion plasma (1 MeV, 100 MWatt, $\gamma_{CD} \approx 0.3-0.4$). This beam should be composed of neutral particles in view of the strong magnetic fields which are present in and around the tokamak. The incident beam drives the plasma current by transfer of momentum from the energetic beam particles to the plasma particles. Recent experimental results have shown that NBI is capable of increasing the plasma temperature. The beam can also be used to fuel the plasma. The energy of the beam should be sufficiently high to penetrate to the center of the plasma and not too high in view of "shine-through" problems.
- II. *Electron Cyclotron Resonance Heating (ECRH)*. An electromagnetic wave is coupled into the plasma at a frequency identical to the electron cyclotron resonance frequency (200 GHz, 130 MWatt, $\gamma_{CD} \approx 0.1$). In this way the energy of the electrons can be increased resulting in a higher plasma temperature. However a source which produces this high frequency at this high power rating has still to be developed

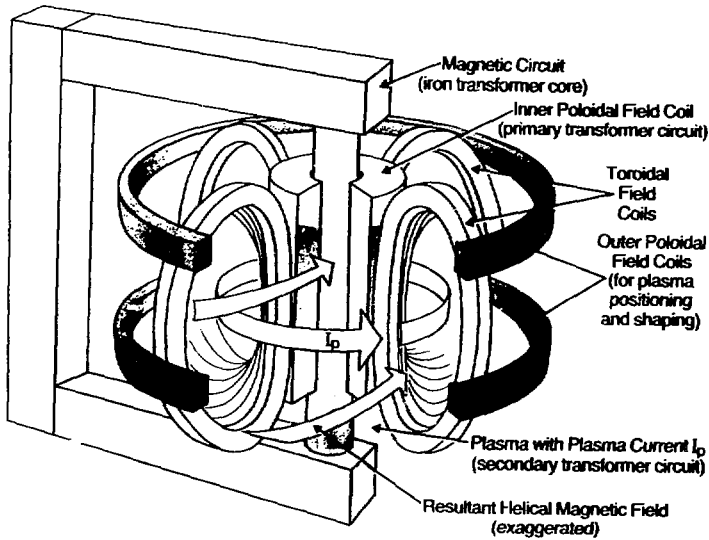


Fig 1.2. The schematic set-up of the JET-TOKAMAK (Joint European Torus).

III. *Ion Cyclotron Resonance Heating (ICRH)*. Again a electromagnetic wave is coupled into the plasma with a frequency equal to the ion cyclotron resonance frequency (35-100 MHz, 100 MWatt, $\gamma_{CD} \approx 0.3$). Experiments have shown that with this scheme the ion temperature can be lifted.

IV. *Lower Hybrides (LH)*. The frequency of these electromagnetic wave is such that it does not penetrate to the axis of the fusion plasma (2.5 GHz, $\gamma_{CD} \approx 0.3-0.4$). However, this scheme seems to be a good candidate for profile control of the fusion plasma and for current drive of the outer region of the plasma.

The estimated costs of all four forms of current drive are of the order of US\$ 2 per Watt. The availability for these methods at present is 80 % for NBI, 60 % for ECRH, 87 % for ICRH and 90 % for LH. Furthermore, the estimated power efficiencies of these methods are 21 % for NBI, 20 % for ECRH, 33 % for ICRH and 33 % for LH. The work in this thesis is related to the first form of current drive and we will therefore elaborate on this form and not discuss the other schemes for current drive.

1.1. Neutral beam injection

Experiments at JET (Joint European Torus) have shown that NBI can heat the plasma. The maximum beam energy they used for these experiments was 120 keV and a neutral beam power of 15.3 MWatt. This beam is produced by extraction of positive deuterium ions from a P.I.N.I. (Plug In Neutral Injector) multicusp bucket plasma source at 120 kV and subsequent neutralization in a gas cell. The produced beam is passed through a magnetic field to remove any charged particles and

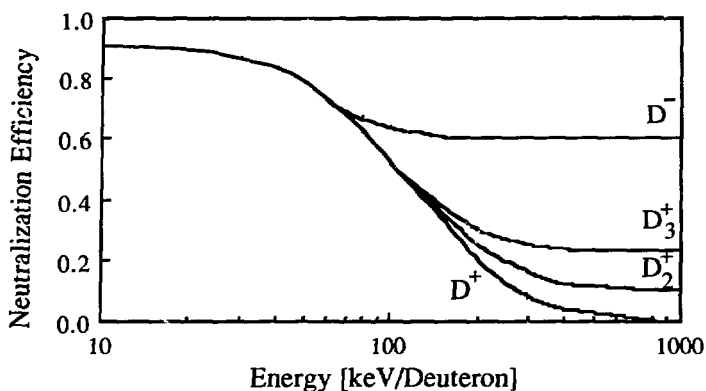


Fig 1.3. The neutralization fraction as a function of the beam energy for positive and negative deuterium ions vs the beam energy.

subsequently injected into the torus. The positive ion current needed to obtain the afore mention neutral power adds up to 240 A of deuterium ions, a current of 60 A per P.I.N.I.

For an efficient current drive, it is generally believed that the beam energy should be higher, of the order of 1 MeV. For such high energies the neutralization cross sections for deuterium ions becomes very small as depicted in Fig. 1.3.³ This makes the efficiency of an NBI system based on positive ions unacceptable. The only solution for this problem is to use negative deuterium ions as the intermediate particles for acceleration. The neutralization cross section for D^- is also given in Fig. 1.3 and amounts to about 60 percent for a beam energy of 1 MeV. It is anticipated that for the next generation of tokamaks the NBI power needed would be of the order of 100 MWatts (NET, Next European Torus, ITER, International Thermonuclear Experimental Reactor). This means a total negative ion current of the order of 150 A if one uses conventional gas neutralizers. If one would use a plasma neutralizer, which is estimated to give a neutralization for negative ions of the order of 85 percent, the current needed is somewhat smaller. Another promising method is the use of a laser to neutralize the negative ions, since the electron affinity of a negative hydrogen ion is only 0.75 eV. A neutralization of 100 percent should be feasible. However, a high intensity laser with a large beam diameter is needed which is at the moment not available.

Fig. 1.4 gives the conceptual set-up of a neutral beam injector for ITER.⁴ In view of the large area the sources will occupy to get the high current needed for NBI, the length of the beam lines is considerable; 50 m. The neutralizers are mounted directly behind the accelerator. Therefore no electrostatic lens system is needed to transport the beam to the torus. However, the divergence of the neutral beam should be very small in order to get the entire beam trough the relatively small duct in the torus. A maximum value of 0.17 degrees is anticipated. A second reason why the beam line has a length of 50 m is to reduce the neutron flux at the sources.

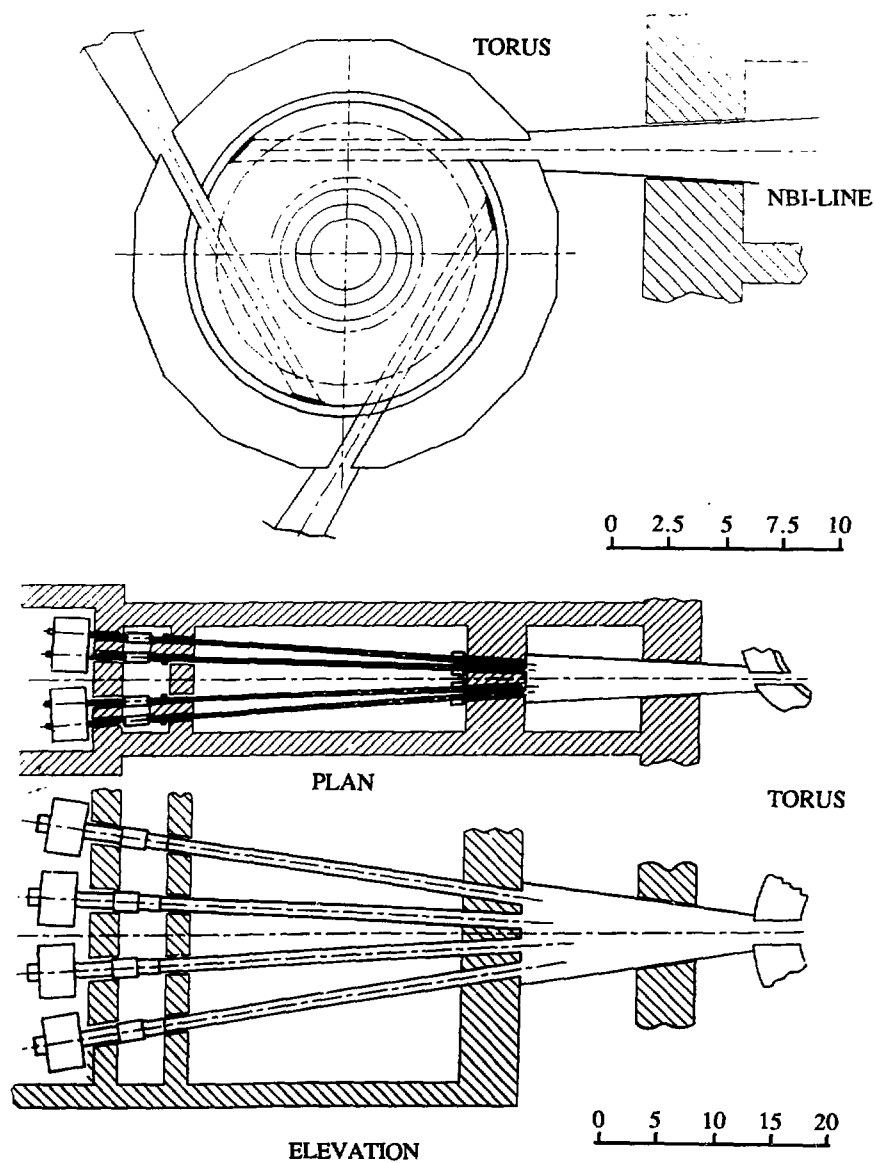


Fig 1.4. A conceptual design of a neutral beam injector for ITER, the scale unit is meters.

For a positive ion extraction from a multicusp bucket plasma source these currents are "easily" obtained, and the physics well understood. However, negative ion sources which are capable of delivering large currents are still under investigation. Two different production mechanisms are at present being explored, volume production and surface conversion. We will elaborate further on these two production methods in the following sections.

1.2. Volume production of negative ions

Positive hydrogen or deuterium ions can easily be extracted from a multicusp bucket plasma source. Reversal of the extraction potential results in the extraction of a large current of electrons but also of negative ions apparently present in the bucket source. The observation of the existence of negative ions in a plasma was established long ago; around 1959.⁵ From that time on, many improvements have resulted in a reduction of the electron to negative ion current ratio and a subsequent larger negative ion current.^{6,7} In understanding the physical limitations of volume sources, as this type of source is called, it is necessary to know the processes that produce these negative ions. It is generally believed that the dominant production of negative ions in a bucket source is a two step process.^{8,9} The first step is the vibrational excitation of molecules by energetic electrons,^{10,11} followed by dissociative attachment of the vibrationally excited molecules by slow electrons¹²

- I. $e^-_{\text{fast}} + \text{H}_2 \rightarrow e^- + \text{H}_2^*$, (vibrational excitation, $e^-_{\text{fast}} > 15 \text{ eV}$)
- II. $e^-_{\text{slow}} + \text{H}_2^* \rightarrow \text{H}^- + \text{H}$ (dissociative attachment, $e^-_{\text{slow}} \approx 1 \text{ eV}$).

Eenshuistra *et al.* have recently measured the vibrational distribution of hydrogen molecules up to $v=5$ which confirmed the above reaction scheme.¹³ In view of the different requirements for the electron energies for the different production steps, the bucket source is divided into two regions by means of a magnetic filter as shown schematically in Fig. 1.5. The region around the filaments, where the electron

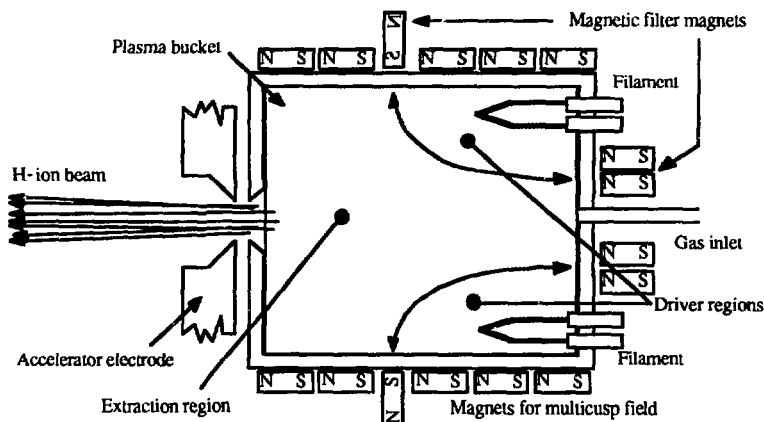


Fig 1.5. The schematic set-up of a volume source. The bucket is separated into a driver region and an extraction region by means of a magnetic field (the filter).

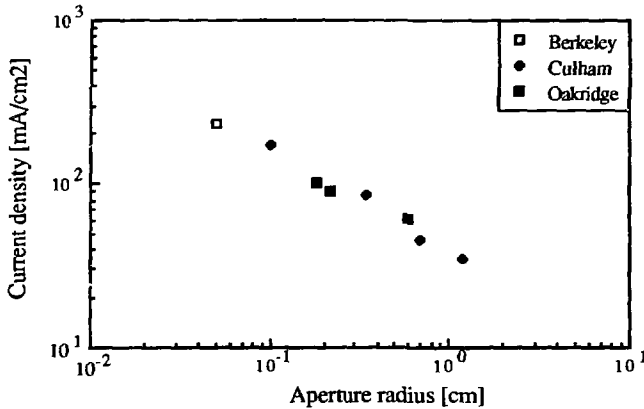


Fig 1.6. The extracted negative ion current density as a function of the extraction diameter for various volume sources.

temperature is relatively high, is called the driver region. The region behind the magnetic filter has a low electron temperature and is called the extraction region. A fractional negative ion density of 70 percent of the positive ion density has been reported to exist in the extractor of such a source.¹⁴

The process itself uses hydrogen molecules as intermediate to the formation of negative ions. This requires a relatively high neutral gas pressure in the source and results in a large gasloading of the accelerator. The effect of this intrinsic problem of volume sources is best illustrated in Fig. 1.6 where we plotted the extracted negative ion current density for several volume sources as a function of extraction aperture.¹⁵ We observe a strong decrease of the current density as the aperture becomes larger. This is believed to be related to stripping of the extracted negative ions on the gas effusing from the source.

A second important property of a volume source is the "temperature" or the transverse energy of the extracted negative ion beam. For a typical volume source the calculated temperature of the negative ions is of the order of a few tens of an eV. This results in a reasonable emittance of the source which makes it quite useful for NBI.

A Japanese volume source has produced 1.6 A at an extraction voltage of 3 kV and a accelerator voltage of 31 kV. Their set-up consist of a large multicusp bucket source with a magnetic filter and 209 extraction apertures with a diameter of 9 mm. The average current density they obtained is 15 mA/cm².¹⁶ Future developments are to increase the number of extraction holes to 259 with a diameter of 11.3 mm and to hopefully extract a negative ion current of 3 A.¹⁷

1.3. Negative surface ionization

In order to populate the empty affinity level of a hydrogen atom one needs a source of electrons which have an energy of -0.75 eV. In the conduction band of metals there is an abundance of electrons which have these negative energies, although they have a stronger bond equal in energy with the work function of the

metal surface. The work function of most metals is in the range of 2.5 to 5 eV. However, when a hydrogen atom is brought into the vicinity of a metal surface, the affinity level drops and broadens due to the attractive interaction with the image of the affinity level in the metal.^{18,19} Close to the surface the affinity level is lowered such that it is below the work function. At this point the electronic states in the metal conduction band are resonant with the affinity level, which means that charge can be transferred. Or in other words, a negative ion can be formed.

The negative surface ionization probability is a strong function of the work function of the metal surface, the lower the work function the higher the probability of forming a negative ion.²⁰ A practical use of this effect is to scatter a positive ion beam from a low work function surface. The incident proton is efficiently neutralized in the incoming channel and subsequently ionized with a certain probability in the outgoing channel. Experiments using a beam with currents of the order of a few nano ampere, which is scattered from a partially cesiated tungsten surface, have shown that negative ion formation probabilities as high as 60 percent are possible.²¹

A practical source set-up which uses this principle is a so-called surface conversion source.^{22,23} A general concept is drawn in Fig. 1.7, it basically consists of a plasma which is brought into contact with a negatively biased low work function surface. Positive ions are extracted from the plasma sheath and are either back scattered or implanted in the surface. The incoming flux of positive plasma particles can also sputter already adsorbed particles from the surface. The processes of back scattering and sputtering both result in a flux of particles leaving the surface which have a probability of being negatively ionized. Once a negative ion is formed close to the surface it is accelerated across the plasma sheath in the direction of the extraction aperture.

The process described above is not dependent on molecules; this means that this process has not the intrinsic problem of needing a high neutral gas pressure as mentioned for volume sources. However, since the negative ions are formed in

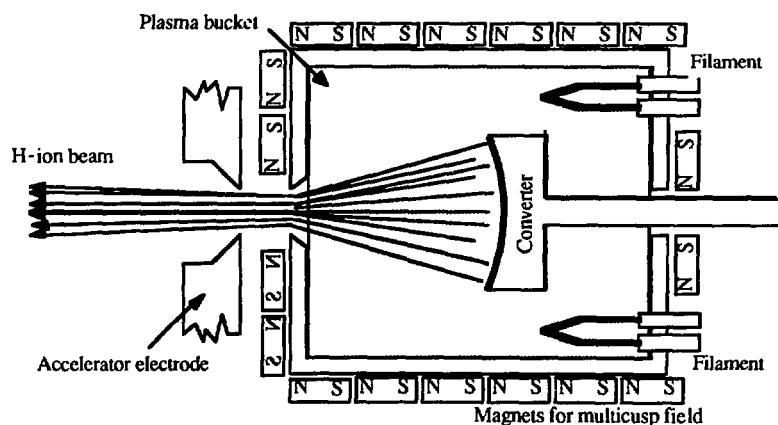


Fig 1.7. A schematic set-up of a surface conversion source.

either a sputtering process or a back scattering process, the transverse energy of these ions is relative high, especially when compared to the low transverse energy expected for volume sources. The feature of running the source with a low neutral gas pressure makes this source interesting for NBI. However, the problem of the relatively high transverse energy should not be underestimated.

Work on semi-DC surface conversion in the Soviet Union resulted in a negative ion current density of the order of 60 mA/cm^2 for a cesiated molybdenum converter²⁴ using geometrical focussing.²⁵ In very short pulsed experiments, 100-150 ns, they observed negative ion current densities of the order of 200 A/cm^2 .²⁶

The work in this thesis extensively describes the physics related to negative surface ionization. Chapter 2 describes a detailed study of negative ion formation during the scattering of a proton beam at a barium surface.^{27,28,29} Quantum mechanical models developed so far are not applicable to this system; therefore suggestions and examples are given for modelling of this particular system. Chapter 3 describes the operation of ALICE with a pure barium metal converter.³⁰ Extensive modeling of the hydrogen household of this system was necessary in order to understand the scaling of the negative ion yield with incident positive ion current on the converter.^{31,32,33} Chapter 4 covers the operation of our surface conversion source ALICE (Amsterdam Light Ion Conversion Experiment) employing a porous tungsten converter through which liquid cesium can diffuse in order to obtain the necessary cesium coverage of the surface.^{34,35} This method of cesium supply has evolved from a theoretical study of the cesium equilibrium coverage of a tungsten surface in a cesium seeded hydrogen discharge.³⁶ Chapter 5 gives experimental data of the attenuation of a surface produced negative ion beam by neutral gas. Furthermore the divergence of the surface produced negative ion beam is estimated from these data.³⁷ The combination of surface production and volume production at low source filling pressures is shown experimentally. Finally, chapter 6 shows the scaling of the negative ion yield with incident positive ion current on the converter over an extended range using a barium converter in MEGALICE (MEGA Light Ion Conversion Experiment).³⁸

References

- ¹ D.J. Rose and M. Clark, Jr. *Plasma and Controlled Fusion*, M.I.T. Press, (61-8814) 1961.
- ² JET Annual Report 1987.
- ³ K.H. Berkner, R.V. Pyle and J.W. Stearns, *Nuclear Fusion* **15**, 249, 1975.
- ⁴ A.J.T. Holmes, JDC-meeting, 12-13 juli, Cadarache, 1988 (unpublished).
- ⁵ C.D. Moak, H.E. Banta, J.N. Thurston, J.W. Johnson and R.F. King, *Rev. Sci. Instrum.* **30**, 694 (1959).
- ⁶ K.W. Ehlers, B.F. Gravin and E.L. Hubbard, *Nucl. Instrum. Methods* **22**, 87 (1963).
- ⁷ Y.I. Belchenko, G.I. Dimov and V.G. Dudnikov, *Novosibirsk Report No.* 66-72 (1972).
- ⁸ V.V. Kuchinskii, V.G. Mishakov, A.S. Tibilov and A.M. Shutkin, *Opt. Spectrosc.* **39**, 598 (1975).
- ⁹ M. Allan and S.F. Wong, *Phys. Rev. Lett.* **41**, 1791 (1978).
- ¹⁰ C. Gorse, M. Capitelli, J. Bretagne and M. Bacal, *Chem Phys.* **93**, 1 (1985).

- 11 J.R. Hiskes, A.M. Karo and P.A. Willman, *J. Vac. Sci. Technol.* **A3**, 1229 (1985).
- 12 J.R. Hiskes, *Comments AT. Mol. Phys.* **19**, 59 (1987).
- 13 P.J. Eenshuistra, R.M.A. Heeren, A.W. Kleyn and H.J. Hopman, submitted to *Phys. Rev. A*.
- 14 A.J.T. Holmes, G. Dammertz and T.S. Green, *Rev. Sci. Instrum.* **59**, 1697 (1985).
- 15 R. McAdams, A.J.T. Holmes, A.F. Newman and R. King, *Proc. of the IIIrd European Workshop on Production and Application of Light Negative Ions*, February 17-19, Amersfoort, Netherlands, 1988, p15.
- 16 T. Inoue et al, *Proc. of the 7th Int. Conf. on Ion Implantation Technology (ITT'88)*, June 7-10, Kyoto, Japan, 1988.
- 17 Y. Ohara, private communication.
- 18 E.G. Overbosch, B. Rasser, A.D. Tenner and J. Los, *Surf. Sci.* **92**, 310 (1980).
- 19 B. Rasser and D.M. Newns, *Surf. Sci.* **108**, 253 (1981).
- 20 J.N.M. van Wunnik, J.J.C. Geerlings, E.H.A. Granneman and J. Los, *Surf. Sci.* **131**, 17 (1985).
- 21 J.J.C. Geerlings, P.W. van Amersfoort, L.F.Tz. Kwakman, E.H.A. Granneman, J. Los and J.P. Gauyacq, *Surf. Sci.* **157**, 151 (1985).
- 22 A.I. Herscovitch and K. Prelec, *Rev. Sci. Instrum.* **52**, 1459 (1981).
- 23 K.N. Leung and K.W. Ehlers, *Rev. Sci. Instrum.* **53**, 803 (1982).
- 24 Yu. I. Belchenko, G.I. Dimov, V.G. Dudnikov and A.S. Kupriyanov, *Revue Phys. Appl.* **23** (1988) 1847.
- 25 Yu. I. Belchenko and A.S. Kupriyanov, *Revue Phys. Appl.* **23** (1988) 1885.
- 26 P.S. Mikhalev, V.A. Papadichev, V.N. Pashentsev, I.V. Tyapkin, S.A. Pikuz and T.A. Shelkovenko, *Proc. of IIIrd European workshop on the Production and Application of Light Negative Ions*, Februari 17-19, Amersfoort, Netherlands, 1988, p231.
- 27 C.F.A. van Os, H.M. van Pinxteren A. W. Kleyn and J. Los, to be submitted to *J. Appl. Phys.*
- 28 C.F.A. van Os and J. Los, to be submitted to *Surf. Sci. Lett.*
- 29 C.F.A. van Os, H.M. van Pinxteren and J. Los, *Proc. of IIIrd European workshop on the Production and Application of Light Negative Ions*, Februari 17-19, Amersfoort, Netherlands, 1988, p166.
- 30 C.F.A. van Os, R.M.A. Heeren and P.W. van Amersfoort, *Appl. Phys. Lett.* **51**, 1495 (1987).
- 31 C.F.A. van Os, C. Leguyt, P.W. van Amersfoort and J. Los, *Proc. of IIIrd European workshop on the Production and Application of Light Negative Ions*, Februari 17-19, Amersfoort, Netherlands, 1988, p149.
- 32 C.F.A. van Os, P.W. van Amersfoort and J. Los, *J. Appl. Phys.* **64**, 3863 (1988).
- 33 C.F.A. van Os, C. Leguyt, A.W. Kleyn and J. Los, *Proc. of the 15th Symposium on Fusion Technology*, 19-23 september, Utrecht, Netherlands, 1988.
- 34 C.F.A. van Os, E.H.A. Granneman and P.W. van Amersfoort, *J. Appl. Phys.* **61**, 5000 (1987).
- 35 C.F.A. van Os and P.W. van Amersfoort, *Appl. Phys. Lett.* **50**, 662 (1987).
- 36 C.F.A. van Os, C. Leguyt and J. Los, to be submitted to *J. Appl. Phys.*
- 37 C.F.A. van Os, A.W. Kleyn, L.M. Lea, A.J.T. Holmes and P.W. van Amersfoort, accepted for publication in *Rev. Sci. Instrum.*
- 38 C.F.A. van Os, C. Leguyt, R.M.A. Heeren, J. Los and A.W. Kleyn, to be published in *J. Opt. Eng.*

FUNDAMENTALS OF NEGATIVE SURFACE IONIZATION

A fundamental study of the formation of negative hydrogen ions via resonant charge exchange in scattering a proton beam from a barium surface is presented. Experiments in a UVV apparatus show that negative ion fractions in the outgoing beam are as high as 35 percent for an incoming proton beam with an energy of 1 keV. The measured negative ion fractions are in good agreement with model calculations. In these calculations is taken into account; (i) the polarization of the negative hydrogen ion in the vicinity of the surface, (ii) the parallel velocity effect and (iii) the deceleration-acceleration of the hydrogen particle in the neighborhood of the turning point. Moreover, oscillations observed in the measured data as a function of scatter angle could be accounted for by a description based upon a stationary phase approximation around the turning point. Finally, measurements show that the adsorption of hydrogen on the surface has no influence on the charge exchange process.

2.1. Introduction

Negative hydrogen ion sources based on surface conversion have been investigated in great detail over the past ten years.^{1,2,3,4} This interest in negative ions was invoked by its probable application in future fusion experiments. In these experiments, high energy neutral beams are needed for heating and current drive of the thermonuclear-plasma. Neutral beams with an energy of the order of 0.5 to 1 MeV can only be produced, with an acceptable efficiency, by using negative ions as primary particle.⁵ A different application of surface conversion is the detection of low energetic (5..1000 eV) hydrogen atoms and molecules.⁶ Apart from applications, surface conversion has been the subject of extensive experimental and theoretical study, with the aim of understanding the resonant charge transfer process resulting in a negative hydrogen ion. The first approach is that of Hiskes.⁷ He assumes that the negative hydrogen ion is formed close to the surface, while at larger distances it partly decays to neutral hydrogen. This empirical description doesn't include the broadening of the affinity level nor does it include the metallic nature of the surface. However, it clearly illustrates the basics of the process. A different approach, which is the basis of the model used in this paper, is the description of the time evolution of the negative ion formation probability with a classical master equation which has been suggested by Overbosch *et al.*⁸ and by Rasser *et al.*⁹ Geerlings *et al.*¹⁰ showed that this approach is the semi-classical limit of a quantum mechanical model describing the time evolution of the wave function amplitude.¹¹

The majority of the theoretical modelling and experiments have been done on cesiated surfaces, in order to obtain the required low work-function metal surface.^{12,13} Recently, a pure barium metal converter has been employed in a surface conversion source.¹⁴ The negative ion yields are comparable with those

obtained with cesiated surfaces.¹⁵ This observation invoked a more fundamental study of the charge exchange between a hydrogen atom and a barium metal surface. The experimental method used is scattering a proton beam of moderate energy from a barium covered W(110) surface in a UHV environment. The negative ion fractions are determined as a function of the outgoing angle in the range of 90 to 50°, the incident angle is kept constant at 80°. The results of the experiments and a theoretical model for this system are presented in this paper. All parameters and equations used in this paper are expressed in atomic units.

2.2. Theory

We will assume that the affinity level is the only level interacting with the metal conduction band. In principle the resonant transfer of electrons between a metal surface and a positive ion, which can form a stable negative ion, is a two electron process. However, the energy difference between the ionization- and affinity level in the case of hydrogen, is such that the neutralization and the formation of a negative ion can be considered to be uncorrelated. The latter has been checked experimentally by scattering different incident species, e.g. H^- , H_2^+ and H_3^+ , from a cesiated W(110) surface with the same energy per nucleon and measuring the ionization probability, which proved to be independent of the incoming species.¹⁶ We assume that the incoming proton is neutralized into an excited state in the incoming trajectory, and Auger deexcited close to the surface.¹⁷

In Fig. 2.1 we have schematically drawn a potential diagram of the charge exchange process in the outgoing trajectory, after the neutralization has taken place and the atom is in its ground state. The z -axis is normal to the surface. When a

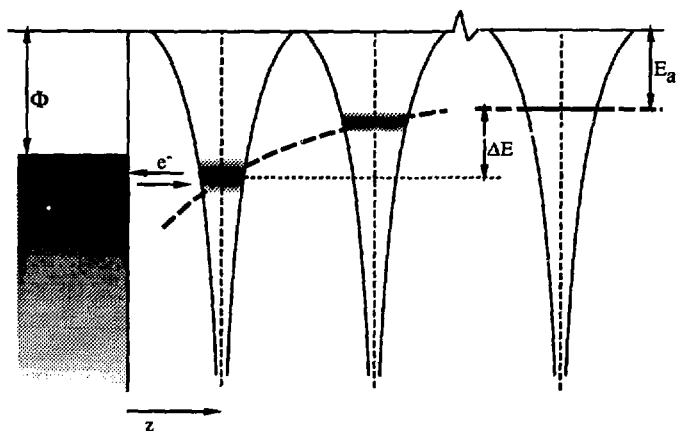


Fig. 2.1 Electron energy level diagram for the interaction of a hydrogen atom with a metal surface.

hydrogen atom is brought close to a metal surface the originally sharp affinity level is shifted and broadened into a band of finite width. The shift is caused by the interaction between the atom and its mirror image induced in the metal. To first order the level shift ΔE is determined by the classical image potential

$$\Delta E = \frac{1}{4(z+k_s^{-1})} \quad [2.1]$$

where z is the atom-surface distance and k_s^{-1} the electrostatic screening length.¹⁸ The electrostatic screening of the image charge by the metal electrons causes a shift of the classical image plane with respect to the surface. The model calculations and measurements of Geerlings *et al.* have shown that this description may be used for this case.¹⁹

We cannot directly employ the model of Geerlings *et al.* for the case of barium because the interaction in this case is very close to the surface ($z \approx 2 a_0$) compared to a cesiated W(110) surface where the interaction region is in the range of 4 to 6 a_0 . In order to accommodate for this close interaction we made some modifications in the model described by Geerlings *et al.* Firstly, we took into account the polarization α_H of the negatively charged atom. A value of 65 a_0^3 is reported in literature.²⁰ This results in a more accurate description of the bending of the affinity level close to the surface. Adding the polarization potential to the energy shift (Eq. [2.1]) we get

$$\Delta E = -\frac{1}{4(z+k_s^{-1})} - \frac{\alpha_H}{2(2(z+k_s^{-1}))^4} \quad [2.2]$$

The affinity level can be shifted below the Fermi level at small values for z . As a consequence, it becomes degenerated with the occupied metal states, so that resonant charge transfer can take place. The initially sharp affinity level is broadened due to this interaction. The electrons tunnel between the metal states and the affinity level with a given transition frequency, $\omega(z)$, which according to Heisenberg's uncertainty principle, results in a broadening of the affinity level with a width $\Delta(z)$. This transition frequency can be calculated from Fermi's golden rule in first order perturbation theory,

$$\omega(z) = \Delta(z) = 2\pi \sum \rho(E_a(z)) |<ilV|k>|^2. \quad [2.3]$$

The sum has to be taken over all metal states $|k>$ in the conduction band. $|i>$ is the negative ion state and ρ is the density of metal states, which varies within the free electron model as $\epsilon_k^{1/2}$. V is the unperturbed core potential of the atom.²¹ $\Delta(z)$ can be approximated as an exponentially decaying function of z ,¹⁷

$$\Delta(z) = \Delta_0 \exp(-\alpha z). \quad [2.4]$$

The broadened affinity level has a Lorentzian line profile.²² At this point it is worthwhile to note, that the level width, e.g. the transition frequency, is a function of the density of states in the metal surface. The higher the density of states, e.g. the Fermi energy, the higher the transition frequency.

In table 2.1, we collected the figures for the work function and the density of states for barium and W(110) covered with 0.6 monolayers of cesium. The work function of barium compared to the cesiated tungsten is more than 1 eV higher,

Table 2.1. The work function and Electron density at the Fermi level for barium and cesiated tungsten.

Material	Work function [eV]	Electron density at Fermi level [a ₀ ⁻³]
Barium	2.5	2.44 x 10 ⁻³
0.5 monolayer Cesium	1.45	1.03 x 10 ⁻³

however the density of states is more than two times that of the cesiated tungsten. It is well known from literature that the higher the work function, the lower the negative ion yield. However, the high density of states for barium, resulting in a higher transition frequency, may partly compensate for the effect of the difference in work function.

From the overlap of the shifted and broadened affinity level and the conduction band, we are able to calculate the equilibrium charge state, $N(z)$, as a function of z .²³ In case of a moving hydrogen atom the charge state $P^-(\infty)$, after reflection from the surface, can be computed by integrating the following rate equation, known as the classical master equation,

$$\frac{dP^-}{dz} = \frac{\Delta(z)}{v_{\perp}} (N(z) - P^-(z)), \quad [2.5]$$

where v_{\perp} denotes the normal velocity of the hydrogen atom. The result of this integration is the following classical expression for the ionization probability;

$$P^-(\infty) = P^-(z_0) \exp\left(-\int_{z_0}^{\infty} \frac{\Delta(z)}{v_{\perp}} dz\right) + \int_{z_0}^{\infty} \frac{N(z)\Delta(z)}{v_{\perp}} \exp\left(-\int_z^{\infty} \frac{\Delta(z')}{v_{\perp}} dz'\right) dz \quad [2.6]$$

where $P^-(\infty)$ is the ionization probability at infinity and $P^-(z_0)$ the probability to have a negatively charged hydrogen atom at the turning point (z_0). Eq. [2.6] is the classical solution of a quantum mechanical model via the equation of motion according to Eq. [2.5]. The first term is called the memory-term, the second term describes the creation of negatively charged hydrogen in the outgoing trajectory.

In our calculations we use a stationary phase approximation around the crossing point (i.e. the distance at which the affinity level crosses the work function the outgoing trajectory), of the quantum mechanical model following the method discussed by Geerlings *et al.*¹⁰. This results in a similar expression for the ionization probability as Eq. [2.6]. However, the equilibrium charge $N(z)$ is now replaced by a function $F(z)$, which is the overlap integral of the broadened affinity level at position z , and the occupied part of the metal conduction band, taking into account the effect of parallel velocity,²⁴ and the Fermi distribution as a function of the surface temperature. The stationary phase method is only valid if the following condition is fulfilled at every distance of the atom to the surface;

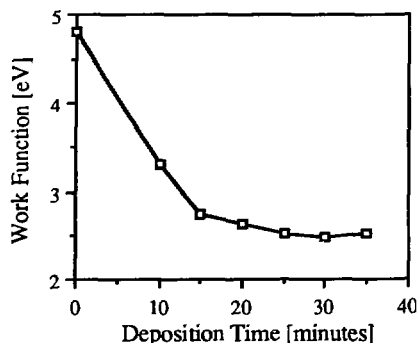


Fig. 2.3 The work function of the W(110) surface, as measured with a Kelvin probe, vs the barium deposition time.

To determine the work function of the surface as a function of the barium coverage, we use a Kelvin probe. In Fig. 2.3 we have plotted the measured work-function as a function of the barium deposition time. After some time the work-function of the surface saturates which corresponds with a barium coverage of at least one monolayer²⁶. All experiments have been done for a barium coverage of the W(110) surface of at least one monolayer, which corresponds to a work function of 2.5 eV.

2.4. Results and Discussion.

In this section we will describe the experimental results we obtained in scattering a proton beam under grazing angles from a barium surface. Furthermore, the effect of adsorption of hydrogen at the surface on the charge exchange is studied.

2.4.a. Charge exchange with the barium surface

Based on the theory described above, we expect a strong dependence of the ionization probability on the normal velocity, i.e. the ionization probability increases with normal velocity. Therefore, we measured the ionization probability as a function of the normal velocity by changing the detection angle. Fig. 2.4 presents these measurements of the negative ion fraction under grazing angles for a primary energy of 1000, 500 and 250 eV. We fitted the experimental data with the model discussed above. A least squares fitting procedure is used, with the turning point and the screening length as free parameters.

In the region where the probability model is valid, for grazing angles of

Table 2.2 The screening length calculated from our measurements and from theory.

Method	Screening length [a_0]		
	1000 eV	500 eV	250 eV
Experimentally	2.8	2.4	2.3
Thomas - Fermi	2.1		
Wojciechowski	1.7		
Crossing levels	2.2		

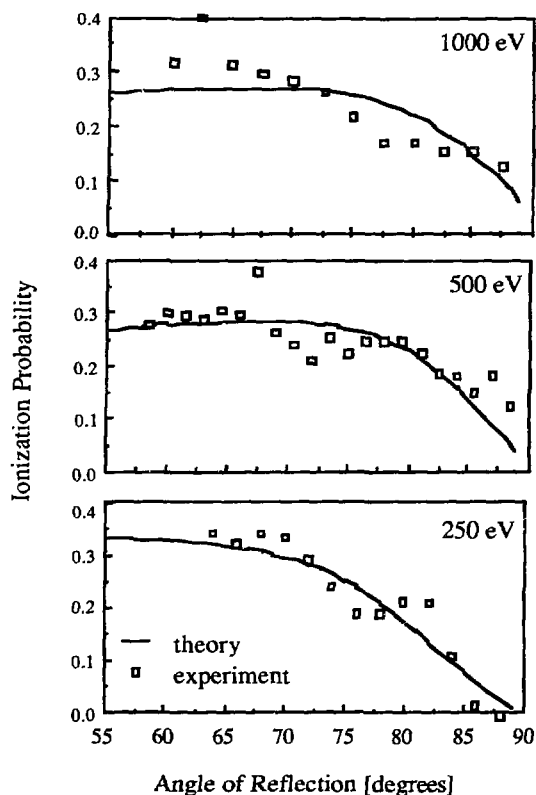


Fig. 2.4 The measured negative ion fractions in the outgoing beam vs scatter angle for three different beam energies, 1000, 500 and 250 eV. The solid line depicts the results from model calculations and the open symbols are the measurements. The ambient pressure is below 10^{-9} Pa and the angle of incidence is 80° .

reflection, the ion yield increases with increasing energy, as predicted by this model. Table 2.2 shows the screening lengths we have calculated from the measurements. In this table we also included the screening lengths which are calculated from Thomas-Fermi screening and from the formula of Wojciechowski and the screening length estimated from the assumption that the affinity level should merge with the bottom of the valence band.^{27,28} The turning points we found from the fit with the experimental data were for all three energies of the order of zero. This is from a physical point of view rather unsatisfying, therefore a closer analysis of Eq. [2.5] has been undertaken especially in the region close to the surface.

An atom which back scatters from a surface has to reverse its normal velocity, e.g. on the incoming trajectory it decelerates, stops at the turning point and in the outgoing trajectory accelerates again to its final energy. The distances at which this occurs is generally of the order of three Bohr radii distance from the surface. In our system, the interaction between a hydrogen atom and the barium surface takes place very close to the surface. Therefore, the effect of the accelerating hydrogen atom has to be taken into account. So we need to know the strength of the repulsive potential to calculate the turning point and elaborate further on the physical parameter which determines the turning point.

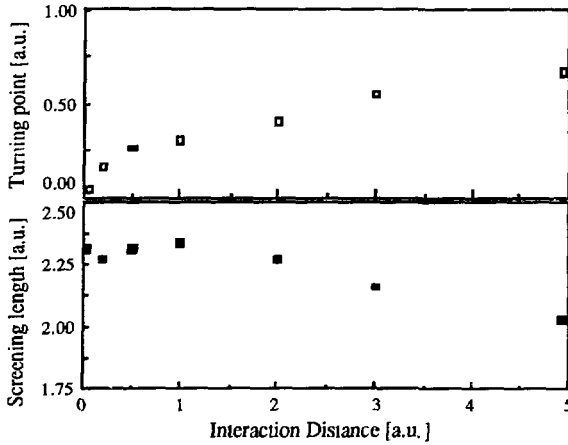


Fig. 2.5 The resulting screening length and turning point vs the interaction distance from a fit with the 250 eV measurements.

Firstly, we examined the case in which the turning point is defined by the incoming normal velocity of the hydrogen atom. This means that the turning point is constant over the whole range of outgoing angles. We used a free two parameter fit to determine the turning point and the screening length as a function of the strength of the repulsive potential.

We implemented the following expression for the varying normal velocity of the hydrogen atom into our model, which is based upon an exponentially repulsive potential,

$$v_{\perp}(z) = v_{\perp} \sqrt{1 - \exp\left(-\frac{1}{\gamma}(z - z_0)\right)} \quad [2.8]$$

Here, γ denotes the decay constant of the exponential potential or the interaction distance, and $v_{\perp}(z)$ denotes the normal velocity of the hydrogen atom at distance z . Subsequently, we used the afore mentioned least-square two-parameter fit where we varied the value of the interaction distance γ . The resulting screening length and turning point versus the interaction distance for an incident beam energy of 250 eV are depicted in Fig. 2.5. We see a strong increase of the turning point with increasing γ .

This can be explained by analyzing Eq. [2.6]. The second term on the right hand side of this equation basically consists of the integration over z of a negative ion production term: $N(z)\Delta(z)/v_{\perp}$ multiplied by an exponentially decaying term: $\exp(-|\Delta(z')/v_{\perp}|dz')$. $N(z)$ and $\Delta(z)$ are rapidly decreasing functions of z . The negative ion production term increases with decreasing normal velocity in the vicinity of the surface. The exponential decay term decreases with increasing normal velocity. In the case of an accelerating atom, the negative ion is formed at low normal velocity, which gives a high production term, and rapidly accelerated to its final value for which the decay term is closer to unity. Subsequently, the calculated ionization probability, according to Eq. [2.6], for a constant normal velocity is lower compared to the ionization probability calculated for an accelerating atom for the same value for the turning point and the screening length.

Table 2.3. The screening length and turning point calculated from our measurements for three different values of the interaction distance of the potential.

Interaction distance		$\gamma = 1$	$\gamma = 2$	$\gamma = 3$
250 eV,	k_s^{-1}	2.34	2.27	2.17
	z_0	0.30	0.41	0.56
500 eV,	k_s^{-1}	2.31	2.26	2.07
	z_0	1.00	1.12	1.18
1 keV,	k_s^{-1}	3.36	3.25	3.29
	z_0	0	0	0

We used the afore mentioned fitting procedure to calculate the screening length and turning point from the measured negative ion fraction, i.e. the ionization probability. Since, in this approach the ionization probability is fixed we expect the effect of an acceleration of the atom to become apparent in the two fit parameters, which is depicted in Fig. 2.5. For small interaction distances we see that the starting point of the integration, the turning point, moves away from the surface and the screening length slightly decreases. The correlation coefficient, i.e. the quality of the fit, for an interaction distance in the range $0-8 a_0$ is constant within 12 %. For large interaction distances, the turning point reduces and the screening length increases. This indicates that the decay of the formed charge state is too strong to obtain the measured ionization probability. The turning point moves inwards in order to correct for this. Note, that the correlation coefficient, i.e. the quality of the fit, decreases for interaction distances larger than $8 a_0$. The same behavior is seen for the 500 eV and 1 keV measurements. The results of the calculations are summarized in table 2.3. One would expect to see a decrease of the turning point with increasing normal velocity, which tendency is absent in table 2.3.

Therefore, as mentioned above, a second approach has been examined in which we vary the turning point as a function of the normal energy with which the atom leaves the surface. In order to calculate the turning point we use the method based on planar channeling of ions at a solid surface. The trajectory of scattered projectiles results from planar channeling in the collective potential²⁹:

$$V_{pl} = 2 \pi Z_1 Z_2 e^2 a_F N_s f_{pl}\left(\frac{z}{a_F}\right) \quad [2.9]$$

where the screening is taken into account by the Moliere approximation³⁰

$$f_{pl}\left(\frac{z}{a_F}\right) = 1.17 \exp(-0.3 \frac{z}{a_F}) + 0.46 \exp(-1.2 \frac{z}{a_F}) + 0.02 \exp(-6 \frac{z}{a_F}) \quad [2.10]$$

and

$$a_F = \frac{0.885}{(\sqrt{Z_1} + \sqrt{Z_2})^{2/3}} \quad [2.11]$$

is the "Firsov screening parameter"³¹ for a projectile-target combination Z_1, Z_2 and N_s is the planar density of atoms at the surface (for barium $6 \times 10^{14} \text{ cm}^{-2}$). Fig. 2.6a shows this planar potential as a function of the distance from the surface. With this potential we can calculate the turning point as a function of the energy with which

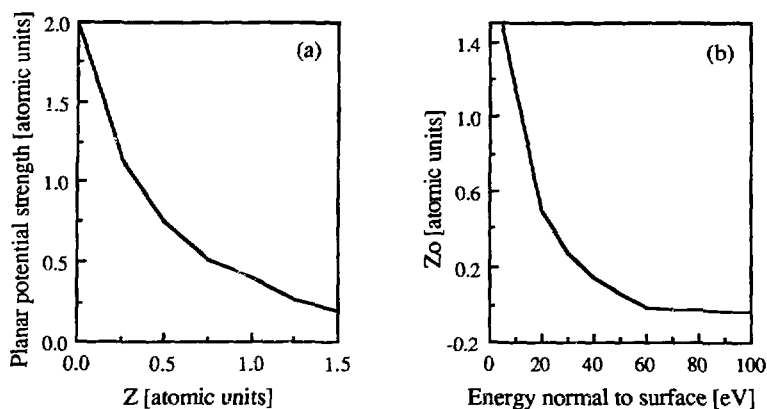


Fig. 2.6 a) The planar channeling potential as a function of the distance z to the surface. b) The calculated turning point as a function of the energy of the particle leaving normal to the surface.

the $h\nu$ hydrogen ion leaves normal to the surface, see Fig. 2.6b. From this calculation we can derive the following expression for the turning point as a function of normal velocity:

$$z_0 = 4400 v_{\perp}^{-0.72} - 1 \quad [2.12]$$

which is valid for normal velocities in the range from 10^4 to 2×10^5 m/s. We incorporated Eq. [2.11] into Eq. [2.6] and fitted our experimental data with a least square one parameter fit, with the screening length as parameter, as a function of the interaction length γ . The overall correlation between theoretical values and experimental data improved by at least 40 percent (300 percent for the 1 keV measurements). The optimum value for the interaction distance γ was in the range from 2 to 3 a_0 for the 250 and 500 eV measurements and between 3 and 5 a_0 for the 1 keV measurement. The γ^{-1} values agree reasonably with the exponential decay factor from the first and dominating term of the left hand side of Eq. [2.10]. The screening lengths obtained with this procedure are for 250 eV, 2.2 a_0 , for 500 eV and 1 keV, 2.9 a_0 . One would expect that the screening length is independent of the incident beam energy. Calculations for the 250 eV measurements with a screening length of 2.9 a_0 show a rather large deviation from the experimental values. The correlation between theoretical values and experimental data reduced by more than 80 percent.

2.4.b. Interferences in the charge exchange process

Closer examination of the experimental data, especially the measurements for 250 eV, exposes oscillations of the ionization probability as a function of scatter angle. The beam current we used in our experiment is sufficiently low to assume that these oscillations are not caused by some kind of collective (i.e. more than one hydrogen particle) process at the surface. Therefore, it is concluded that the

observed oscillations are related to interferences of the incoming and outgoing trajectory of the hydrogen atom. This is the first time that such a behavior is seen in resonant charge exchange in the wide band approximation.

The theory as described in this paper so far cannot account for such oscillations. Therefore, a closer examination of the condition formulated in Eq. [2.7] has been undertaken. The crossing point in the case of a barium surface is at an atom metal-surface separation of about $2 a_0$. The condition according to Eq. [2.7] gives a value of 0.6 if we neglect the polarization term in Eq. [2.2]. This value is close to unity which means that the semi classical description we used may be incorrect. However, if we take into account the polarization term according to Eq. [2.2] this value reduces due to a strong increase of $|\partial \epsilon_a / \partial z|$. This explains why we obtained a satisfactory agreement between the experimental data and theory in the previous section.

However, it is expected that closer to the surface condition [2.7] is no longer met and a closer examination on the validity of the stationary phase approximation around the crossing point is necessary. In the previous section we showed that when we incorporate a changing normal velocity according to Eq. [2.8] in the semi-classical model, reasonable consistency in terms of calculated turning points and fitted screening lengths are obtained. With an expression for the normal velocity according to Eq. [2.8] we see that an atom scattering from a metal surface spends a considerable time around the turning point, since, at this point its velocity is decreasing and subsequently increasing. Around the turning point, the time needed for an electron to tunnel through the potential barrier is of the same order as the time the atom collision time. Therefore, the turning point could well be used as the stationary phase approximation point. However, the two stationary phase points (i.e one for the incident trajectory and one for the outgoing trajectory) are close together, which means that for an accurate description the stationary phase approximation should be done up to the second order. In this section we will show that when we use a second order stationary phase approximation around the turning point, oscillations of the ionization probability versus normal velocity can be seen in the resulting expression for the ionization probability.

Our starting point is the following quantum mechanical expression^{11,32} for the charge state as a function of the time, t , of the moving hydrogen atom,

$$P^-(t) = P^-(-\infty) \exp\left(-\int_{-\infty}^{\infty} \Delta(t') dt'\right) + \frac{1}{\pi} \int_{-\infty}^{\infty} f(\epsilon, T) \left| \int_{-\infty}^t \sqrt{\frac{\Delta(t')}{2}} \exp(-i\epsilon t' - \int_{t'}^t \left(i\epsilon_a(t'') + \frac{\Delta(t'')}{2}\right) dt'') dt' \right|^2 d\epsilon \quad [2.13]$$

where ϵ is the electron energy, ϵ_a is the energy of the affinity level and $f(\epsilon, T)$ is the Fermi distribution. The first term in this equation is the so-called memory term

which is equal to zero since we start with atoms, i.e. $P^-(-\infty) = 0$. We expand $\varepsilon_a(t)$ up to the second order around the turning point, z_0 , ($t = t_0$),

$$\varepsilon_a(t) = \varepsilon_a(t_0) + (t - t_0) \frac{\partial \varepsilon_a}{\partial t} \Big|_{t_0} + \frac{(t - t_0)^2}{2} \frac{\partial^2 \varepsilon_a}{\partial t^2} \Big|_{t_0}. \quad [2.14]$$

The first order time derivative of the affinity level is zero in the turning point. The second order time differential can be converted into distance differential taking into account the variation of the normal velocity with distance according to Eq. [2.7]. This yields

$$\varepsilon_a(t) = \varepsilon_a(t_0) + \frac{(t - t_0)^2}{2} \frac{v_{\perp}^2}{2\gamma} \frac{\partial \varepsilon_a}{\partial z} \Big|_{z_0}. \quad [2.15]$$

Furthermore, in order to calculate the integration over t'' in Eq. [2.13] assume an exponential decay of the level width, according to Eq. [2.4] and a changing normal velocity according to Eq. [2.8]. For $t = \infty$, i.e. for the final charge state $P^-(-\infty)$ this yields

$$\int_{t'}^{\infty} \frac{\Delta(t'')}{2} dt'' = \frac{\Delta(z_0)}{2v_{\perp}} \left(\frac{1}{\alpha} + \frac{1}{2} \frac{1}{(\alpha + \gamma^{-1})} + \frac{3}{8} \frac{1}{(\alpha + \gamma^{-1})^2} + \dots \right) \quad [2.16]$$

If the effect of a changing normal velocity according to Eq. [2.8] is not included in this derivation one would only have found the first term of the sum. Since, the effect of the changing normal velocity in this approximation is small we only used the first term of the sum in our calculations. With these approximations we are now able to calculate the integral over t' in Eq. [2.13] as described in the appendix 2.1. The resulting expression for the final charge state is;

$$P^-(-\infty) = \frac{2\pi\Delta(z_0)}{q^{1/3}} \exp\left(-\frac{\Delta(z_0)}{\alpha v_{\perp}}\right) \int_{-\infty}^{\infty} f(\varepsilon, T) \text{Ai}^2\left(\frac{\varepsilon_a(z_0) - \varepsilon}{q^{1/3}}\right) d\left(\frac{\varepsilon}{q^{1/3}}\right) \quad [2.17]$$

$$\text{with } q = \frac{v_{\perp}^2}{2\gamma} \frac{\partial \varepsilon_a}{\partial z} \Big|_{z_0}$$

This expression has in principle an oscillatory term; the Airy function. We fitted the experimental data for an incident beam energy of 250 eV with this equation using the screening length obtained from the method described in the previous section and varied the strength and the interaction length of the planar potential as fit parameters. Furthermore, in the calculations we limited ourselves to turning points which are larger than $0.25 a_0$. The result of the calculation for a screening length of $2.3 a_0$ and a surface temperature of 0 K is shown in Fig. 2.7 together with the experimental data. Around a scatter angle of 75 degrees there is a "kink" in the calculated curve due to the afore mentioned limitations we used on the position of the turning point. The derived interaction length is $0.9 a_0$ and the potential strength is 0.65 atomic units which differs not much from the calculated values from Eq. [2.10]. We used the afore mentioned values to calculate the ionization probability

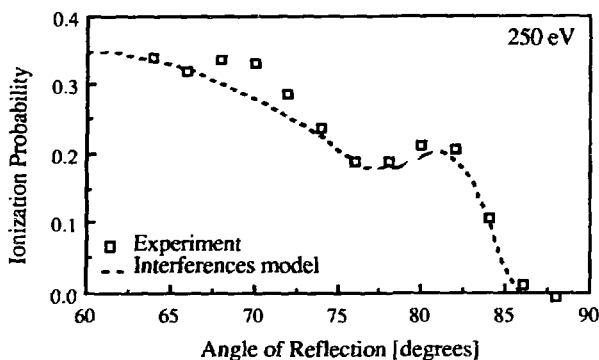


Fig. 2.7 The ionization probability vs the scatter angle for an incident beam energy of 250 eV. The dotted line is the result of a second order model calculation based on the discussed model.

for an incident beam energy of 500 and 1000 eV. The result of this calculation is plotted in Fig. 2.8. We see that for higher energies the oscillations become less apparent which tendency is also seen in the experimental data in Fig. 2.4.

The oscillation in the calculated curve is not coming from the Airy function, but is the result of the turning point shifting through the "freezing" point. When the turning point coincides with the "freezing" point, one expects a high ionization probability, when it is further away from the surface we expect a lower probability decreasing to zero at larger atom metal surface separation. When the turning point is between the "freezing" point and the metal surface we expect a decrease of the ionization probability. Both tendencies are seen both in the experimental data and the theoretical curve. However, at shorter atom metal-surface separation we observe an increase of the ionization probability. Note that at this point there is a significant deviation of the calculated curve and the experimental data. However, it

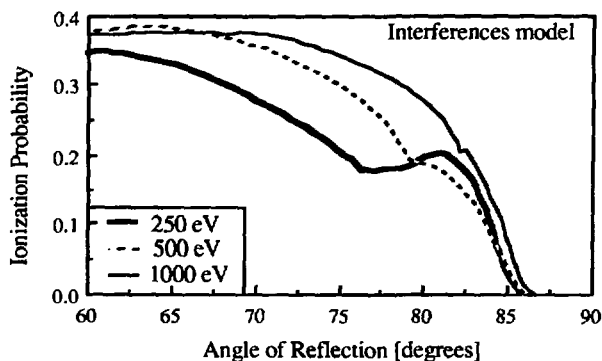


Fig. 2.8 The calculated ionization probability for three different beam energies. The parameters for the repulsive potential have been calculated from the 250 eV measurement and used to calculate the 500 and 1000 eV curves.

is in this region where the above modeling which assumes a decreasing affinity level with decreasing atom surface separation becomes less correct. Ossicini and Bertoni show that close to the surface the affinity level no longer decreases with decreasing separation, but flattens out and becomes constant with atom metal separation.³³ With this description, close to the surface the factor $\partial \epsilon_a / \partial z$ in q is close to zero which means that the Airy function blows up in this region thus giving a considerable oscillatory contribution in this region. A description which incorporates the dependence of the affinity level as a function of the atom metal separation as described by Ossicini and Bertoni would presumably give a more detailed and complete model of the resonant interaction close to the surface. However, such a calculation is beyond the scope of this article.

2.4.c. Influence of hydrogen adsorption on the charge exchange

In a surface conversion source, the converter is heavily "polluted" with hydrogen. It is therefore worthwhile to measure the effect of this contamination on the charge exchange process. For a W(110) surface covered with half a monolayer of cesium, a decrease of almost a factor of two after an exposure to 900 Langmuirs of hydrogen has been measured.^{34,35} We used two different schemes for measuring the effect of adsorbed hydrogen on the charge exchange process.

At first we adsorbed hydrogen on the clean W(110) surface and checked with the Kelvin probe to see whether we had really fixed a layer of hydrogen on the tungsten surface. After this step we adsorbed barium on top of this system, with a thickness of approximately 0.4 monolayers. With a surface prepared in this way we measured the negative ion fraction of the outgoing beam. The same measurement was done for a surface which was only covered with 0.4 monolayers of barium. The measured negative ion fractions coincide within 3 percent, which is better than the experimental error of the data.

Another scheme we have used is to expose the barium surface to 1000 Langmuirs of hydrogen and measure the negative ion fraction before and after adsorption. This scheme didn't influence the negative ion yield either. The latter might be related to a very low sticking probability of hydrogen on barium. However, even after an exposure to several thousands Langmuirs of hydrogen no change in the negative ion fraction was observed. From these two experiments we therefore conclude that adsorbed hydrogen on top or underneath the barium layer doesn't affect the charge exchange process. A similar behavior was found for a W(110) surface covered with a full monolayer of cesium.

2.5. Conclusions

Under grazing angles of incidence and scattering there is a good agreement between theory and experiment. For these grazing angles the particles follow a predictable path, for which a description in terms of a "classical" turning point is valid. The particle trajectories close to the surface have to be calculated in great detail since the resonant charge exchange takes place in this region. The method of defining the turning point as a function of the normal velocity of the outgoing particle gives a more consistent model compared to a turning point calculated

directly from the incident normal energy. The calculation of the turning point is based on a rather simple single repulsive exponential potential. Furthermore, we have shown that using a second order stationary phase approximation around the turning point, one can get an idea of the details of the charge exchange process located very close to the metal surface.

For incident energies in the range of 250 to 1000 eV negative ion fractions in the reflected beam are as high as 30 percent despite the relatively high work function of barium compared to cesiated tungsten surfaces. This is related to the high electron density (i.e. the high density of states) for barium which is twice that for cesium.

Adsorption of hydrogen on barium has no effect on the charge exchange process. This is important for the application of barium in a surface conversion source where the converter is exposed to very large fluxes of positive hydrogen ions and molecular hydrogen.

Summarizing, the fundamental study on resonant charge exchange between a barium metal surface and a hydrogen atom presented here, very clearly indicates that the application of barium as a converter surface in a surface conversion source is feasible. Furthermore, the experiments give more insight in the effect of the electron density of the metal surface on resonant charge exchange and the consequences of a varying normal velocity of the atom in the outgoing trajectory.

Acknowledgments

The authors wish to thank, H. J. Timmer for his overall technical support and G. N. van der Leek for his assistance in the build-up of the computer control and data-acquisition systems of the experiment. The work described here was performed as part of the research program of the association agreement between the Stichting voor Fundamenteel Onderzoek der Materie (FOM) and EURATOM, with financial support from the Nederlandse Organisatie voor Wetenschappelijk Onderzoek (NWO) and EURATOM.

Appendix 2.1

In this appendix we will show how we can calculate the following integral in Eq. [2.12],

$$\int_{-\infty}^{\infty} \sqrt{\frac{\Delta(t')}{2}} \exp(-i\epsilon t' - \int_{t'}^{\infty} (i\epsilon_a(t'') + \frac{\Delta(t'')}{2} dt'')) dt' \quad [2.A1]$$

Using the stationary phase approximation around the turning point, according to Eq. [2.15], and taking only the first term of the sum yields

$$G(v_{\perp}, z_0) \int_{-\infty}^{\infty} \exp(-i(\epsilon t' + \int_t^{\infty} \epsilon_a(t'') dt'')) dt' \quad [2.A2]$$

with $G(v_{\perp}, z_0) = \sqrt{\frac{\Delta(z_0)}{2}} \exp(-\frac{\Delta(z_0)}{2\alpha v_{\perp}})$.

We can expand the $\epsilon_a(t'')$ around the turning point following Eq. [2.14]. Substitution of this expression yields

$$G(v_{\perp}, z_0) \int_{-\infty}^{\infty} \exp(-i(\epsilon t' + \int_t^{\infty} \epsilon_a(t_0) - \frac{(t'' - t_0)^2}{2} \frac{v_{\perp}^2}{2\gamma} \frac{\partial \epsilon_a}{\partial z} |_{z_0} dt'')) dt' \quad [2.A3]$$

which can be rewritten as

$$G(v_{\perp}, z_0) \exp(i(\epsilon - \epsilon_a)t_0) \int_{-\infty}^{\infty} \exp(i(\epsilon_a - \epsilon)(t' - t_0) + \frac{i(t' - t_0)^3}{6} \frac{v_{\perp}^2}{2\gamma} \frac{\partial \epsilon_a}{\partial z} |_{z_0}) dt' \quad [2.A4]$$

The remaining integral is an Airy function:

$$G(v_{\perp}, z_0) \frac{2\pi}{q^{1/3}} \text{Ai}\left(\frac{\epsilon_a - \epsilon}{q^{1/3}}\right) \exp(i(\epsilon - \epsilon_a)t_0 - i\pi) \quad \text{with} \quad q = \frac{v_{\perp}^2}{2\gamma} \frac{\partial \epsilon_a}{\partial z} |_{z_0} \quad [2.A5]$$

Substitution of this result in equation [2.12] yields the ionization probability as given in Eq. [2.17]

References

- 1 P.J.M. van Bommel, J.J.C. Geerlings, J.N.M. van Wunnik, P. Massmann, E.H.A. Granneman and J. Los, J. Appl. Phys. **54** (1983) 5676.
- 2 P.J. Schneider, K.H. Berkner, W.G. Graham, R.V. Pyle and J.W. Stearns, Phys. Rev. **B23** (1981) 941.
- 3 A. Pargellis and M. Seidl, Phys. Rev. **B25** (1982) 4356.
- 4 M. Seidl and A. Pargellis, Phys. Rev. **B26** (1982) 1.
- 5 H. Horiike, Y. Ohara, Y. Okumara, T. Shibata and S. Tanaka, Japan Atomic Energy Report, JEARI-M 86-064 (1986) unpublished.
- 6 P.J. Schneider, W. Eckstein and H. Verbeek, Physica Scripta **T6** (1983) 35.
- 7 J. R. Hiskes, XIVth International Conference on Phenomena in Ionized Gases, Grenoble, July (1979).
- 8 E.G. Overbosch, B. Rasser, A.D. Tenner and J. Los, Surf. Sci. **92** (1980) 310.
- 9 B. Rasser, J.N.M. van Wunnik and J. Los, Surf. Sci. **118** (1982) 697.
- 10 J.J.C. Geerlings, J. Los, J.P. Gauyacq and N.M. Temme, Surf.Sci. **172** (1986) 257.

- 11 R. Brako and D.M. Newns, *Surf. Sci.* **108** (1981) 253.
- 12 J.N.M. van Wunnik, J.J.C. Geerlings, E.H.A. Granneman and J. Los, *Surf. Sci.* **131** (1983) 17.
- 13 J.L. Desplat and C.A. Papageogopoloulos, *Surf. Sci.* **92B** (1980) 97.
- 14 C.F.A. van Os, R.M.A. Heeren and P.W. van Amersfoort, *Appl. Phys. Lett.* **51** (1987) 1495.
- 15 C.F.A. van Os, P.W. van Amersfoort and J. Los, accepted for publication in *J. Appl. Phys.* (October 1988).
- 16 E.H.A. Granneman, J.J.C. Geerlings, J.N.M. van Wunnik, P.J. van Bommel, H., J. Hopman and J. Los, *Proc. of the third int. conf. on Production and Neutralization of Negative Ions and Beams*, Edited by K. Prelec, Brookhaven (1983).
- 17 S. Horiguchi, K. Koyama and Y.H. Ohtsuki, *Phys. Stat. Sol.* **87** (1978) 757.
- 18 R. Gomer and L.W. Swanson, *J.Chem.Phys.* **38** (1963) 1613.
- 19 J.J.C. Geerlings, P.W. van Amersfoort, L.F.Tz. Kwakman, E.H.A. Granneman, J. Los and J.P. Gauyacq, *Surf. Sci.* **157** (1985) 151.
- 20 Landolt-Bornstein, *6.Aufl., 1. Band, 1. Teil*, Springer Verlag, 1950, p401.
- 21 J.W. Gadzuk, *Surf.Sci.* **6** (1967) 133.
- 22 B. Rasser, J.N.M. van Wunnik and J. Los, *Surf.Sci.* **118** (1982) 697.
- 23 B. Rasser and M. Remy, *Surf.Sci.* **93** (1980) 223.
- 24 J.N.M. van Wunnik, R. Brako, K. Makoshi and D.M. Newns, *Surf. Sci.* **126** (1983) 618.
- 25 F.J. Rogers, H.C. Graboske and D.J. Harwood, *Phys. Rev. A* **1** (1970) 1577.
- 26 B.J. Hopkins and B.J. Smith, *J.Chem.Phys.* **49** (1968) 2136.
- 27 N.D. Lang and A.R. Williams, *Phys.Rev.* **B18** (1978) 616.
- 28 J.K. Nørskov, *Phys.Rev.* **B20** (1979) 446
- 29 D.S. Gemmell, *Rev. Mod. Phys.* **46** (1974) 129.
- 30 G. Moliere, *Z. Naturforsch.* **2A** (1947) 133.
- 31 O.B. Firscov, *Sov. Phys. JETP* **33** (1958) 133.
- 32 W. Bloss and D. Hone, *Surf. Sci.* **72** (1978) 277.
- 33 S. Ossicini and C.M. Bertoni, *Surf. Sci.* **178** (1986) 244.
- 34 P.W. van Amersfoort, J.J.C. Geerlings, R. Rodink, E.H.A. Granneman and J. Los, *J. Appl. Phys.* **59** (1986) 241.
- 35 J.P. Gauyacq and J.J.C. Geerlings, *Surf. Sci.* **128** (1987) 245.

SURFACE CONVERSION AT A BARIUM SURFACE

A fundamental study of the formation of negative hydrogen ions via surface conversion is presented. Employed is a novel type of converter, namely a pure barium metal surface. In spite of the high work function of barium compared to more conventional cesiated converters, considerable yields of negative ions were produced. Conversion efficiencies up of 4 % are obtained, which is of the same order as for cesiated converters. The high negative-ion yield is probably related to the electron density of barium which is almost twice that of cesium. This is confirmed by model calculations and by UHV-scattering experiments under well defined conditions. Furthermore, calculations showed that the hydrogen coverage of the converter increases with increasing flux of positive hydrogen ions to the surface. This behavior is confirmed experimentally. Seeding the hydrogen plasma with argon has no significant effect on the conversion efficiency. This is believed to be related to the competition between the lowering of the surface hydrogen coverage and the increase of the hydrogen desorption rate, both due to the higher sputter coefficient of argon compared to hydrogen.

3.1. Introduction

Formation of negative hydrogen ions via resonant charge exchange at a metal surface has been widely studied over the last decade. The motivation for this research lies in the field of thermonuclear fusion, where negative ions find application as intermediate step in the production of intense beams of neutral atoms. These beams can be used to diagnose particle densities and momentum distributions of a fusion plasma. In this paper, a fundamental study of the charge transfer process at a barium converter surface, which is in contact with a hydrogen plasma, is presented. Our results are also of interest for other devices, in which the dynamic interaction of plasma particles with a metal surface plays a role. Examples of such devices are etching and deposition reactors, as are nowadays used in the production of semiconductor components, coated glasses etc.

A typical negative-ion source consists of an isolated metal electrode, the so-called converter, which is immersed in a hydrogen plasma.^{1,2,3} The converter is usually biased at a negative potential of a few hundred volts. This causes a flux of positive hydrogen ions from the surrounding plasma to flow towards the converter surface. These arrive at the surface with an energy proportional to the converter potential minus the plasma potential. The latter depends on the kind of discharge used. For a bucket-type plasma the plasma potential is of the order of a few volts positive, whereas for a Penning-like geometry of the discharge (as employed in our experiment) it is negative. The major part of the incident flux is implanted into the converter surface, the remaining part is scattered. Implanted hydrogen particles can come to the surface via diffusion or via removal of substrate material by sputtering. Hydrogen atoms, which have arrived at the surface, are subsequently sputtered by

the incident flux. A fraction of the scattered and sputtered particles can become negatively charged via charge exchange with the converter. It is well known, that this fraction strongly depends on the work function of the converter surface; the lower the work function the higher the negative ion yield.⁴ Negative ions formed in the vicinity of the surface are accelerated across the plasma sheath and subsequently "self-extracted" through an aperture.⁵

In most experiments on surface production of negative ions, the low work function of the converter is obtained by adsorption of cesium on a molybdenum or tungsten substrate.⁶ Two methods are used to obtain the coverage, (i) admitting cesium vapor to the discharge chamber and (ii) employing a converter which is made from porous material through which liquid cesium can diffuse. The latter method results in a much smaller pollution of the plasma with cesium, since, with this scheme, cesium only flows into the plasma via sputtering by incident hydrogen ions. A plasma, which is not seeded with cesium, enables one to single out the charge exchange process for hydrogen. Furthermore, to such a plasma, heavy ions like xenon or argon can be added to simulate the effect of cesium ions present in seeded discharges. Van Os and van Amersfoort carried out such an experiment and concluded that cesium not only serves as a means to lower the work function, but also plays an important role in the sputtering of hydrogen from the converter surface.⁷ These sputtered hydrogen particles, which leave the surface with relatively low energies, have a large probability for becoming negatively charged. Thus, the work function of the converter is important but does not solely control the negative-ion formation probability in a surface-conversion source. This insight led to the idea to use a barium-metal converter and to admit some heavy gas, like argon, to increase the sputtering of hydrogen from the surface. The advantage of this approach is, that electrical breakdowns in the source and in the extraction region, which are a consequence of the presence of large amounts of cesium vapor, are eliminated to a large extent.

A clean barium surface has a work function of 2.5 eV. This is large compared to tungsten covered with half a monolayer of cesium, which has a work function of 1.45 eV. However, to maintain a coverage of half a monolayer on a surface which is constantly bombarded by plasma particles is difficult, if not impossible. Van Amersfoort *et al.* did calculations on the equilibrium cesium coverage of a converter surface immersed in a cesium seeded hydrogen plasma.⁸ The calculations showed that a coverage higher than 0.24 monolayers is not feasible if the converter is only cesiated via vapor deposition. Tompa, Carr and Seidl reported a cesium coverage, as a result of implantation of cesium into tungsten, of the order of half a monolayer for low incident energies.⁹ In their experiment, implanted cesium particles caused a surface coverage after removal of substrate material via sputtering. In a typical surface-conversion source the converter is operated at a negative bias of 100 to 200 Volts. For these values, the coverage measured by Tompa *et al.*, is also lower than half a monolayer. Therefore, in a practical set-up, it is questionable if the coverage has the optimum value for the charge-exchange process, which according to van Wunnik *et al.* amounts to a 0.6 monolayers.⁴ Moreover, the coverage is a function of the discharge parameters and the converter potential. The advantage of barium, in this respect, is its constant work function.

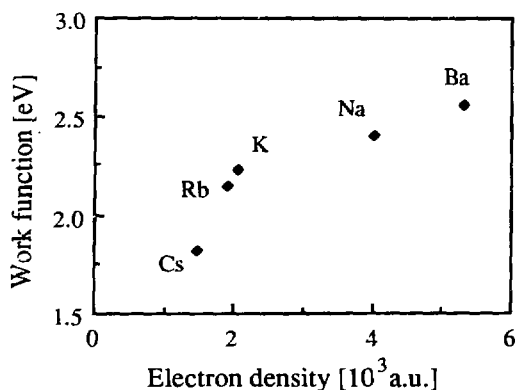


Fig. 3.1. The electron density versus the work function for several (alkali) metals.

Besides the work function, a second important quantity in the charge exchange process, is the width of the conduction band (e.g. the Fermi energy) of the converter. For barium the Fermi energy is 3.65 eV, whereas for a full monolayer of cesium on tungsten it amounts to 1.96 eV. This implies that the electron density of barium is much higher than the electron density of cesiated tungsten. This is illustrated in Fig. 3.1, which has been taken from Wojciechowski.¹⁰ In this figure the work function of barium and several alkali metals is plotted versus their electron density. The beneficial effect of a higher electron density for the negative-ion formation process is the subject of the study presented here.

In this paper, section 3.2 describes the application of the existing theory on resonant charge exchange to a barium surface. For this application, measurements were done in a well-controlled UHV scattering experiment. Our surface-conversion source, which is equipped with a pure barium-metal converter, is described in section 3.3. Experimental results obtained with this source are presented in section 3.4. In addition, section 3.5 contains a comparison of our barium converter with more conventional cesium-covered converters, and a discussion of the equilibrium hydrogen coverage of the converter surface.

3.2. Formation of negative ions

The negatively biased converter is exposed to a flux of positive hydrogen ions extracted from the surrounding plasma. In the vicinity of the converter surface, these ions are efficiently neutralized, probably via resonant neutralization into an excited state, followed by Auger de-excitation to the ground state. Subsequently, the atom is either implanted into the surface or scattered with a negligible energy loss. Incident hydrogen ions can also sputter adsorbed hydrogen atoms from the surface. Thus, the flux of hydrogen atoms leaving the surface has an energy ranging from a few eV to the incident energy, which is a few hundred eV. A fraction of the outgoing flux can become negatively charged via resonant charge exchange with the metal. In this section we shall discuss the functional relationship between the energy with which the atom leaves normal to the surface and the ionization probability. In order to estimate this ionization probability, we scattered a proton beam at a

bariated tungsten surface under grazing angles of incidence and extrapolated the experimental results, with a model on resonant charge exchange, to particles leaving normal to the surface.

In calculating the ionization probability for a stationary atom located at a distance z from a metal surface, the shift of the affinity level due to the attractive interaction with its image charge in the metal has to be taken into account. In first order this shift can be expressed as

$$\Delta E_a^{(1)} = \frac{e^2}{4\pi\epsilon_0} \frac{1}{4(z+k_s^{-1})} \quad [3.1]$$

where e is the electron charge, ϵ_0 is the dielectric permittivity of vacuum and k_s^{-1} is the electrostatic screening length in the metal.¹¹ When the atom moves closer to the metal surface, the affinity level crosses the work function of the metal. Subsequently, metal electrons can tunnel between the conduction band and the affinity level of the atom. The affinity level broadens due to this interaction. The corresponding level width $\Delta(z)$ depends exponentially on the distance z to the surface,

$$\Delta(z) = \Delta(0) \exp(-\beta z) \quad [3.2]$$

where β can be calculated using the theory of Gadzuk.¹² According to this theory, the transition frequency depends strongly on the Fermi energy, i.e. on the width of the conduction band of the metal. A higher Fermi energy corresponds to a higher transition frequency.

In the so-called stationary phase approximation,¹³ the ionization probability, η_H for scattered (or sputtered) atoms can be expressed as

$$\eta_H = \frac{1}{v_{\perp}} \int_{z_0}^{\infty} N^-(z) \Delta(z) \exp\left(\frac{-1}{v_{\perp}} \int_z^{\infty} \Delta(z') dz'\right) dz \quad [3.3]$$

where $N^-(z)$ is the ionization probability for stationary atoms, which is determined by the overlap of the broadened affinity level and the metal conduction band¹⁴ and v_{\perp} is the particle velocity normal to the surface. In Eq. (3), the ionization probability is only a function of the velocity of the atom normal to the surface. However, it was shown by van Wunnik *et al.*, that the velocity of the hydrogen atom parallel to the surface also influences the ionization probability.¹⁵ This effect can be introduced in Eq. (3) by shifting the Fermi sphere in k -space. In Eq. [3.3] only the equilibrium charge $N^-(z)$ is affected by this shift. In our calculations the parallel velocity was taken into account.

Geerlings *et al.*, used the screening length to fit the theory with experimental data. For the turning point they used the Bohr radius of the hydrogen atom ($z_0=1 a_0$).¹⁶ This procedure gave a good agreement between theory and experiments for scattering hydrogen from a W(110) surface covered with half a monolayer of cesium. We used the same procedure to fit the experimental data, obtained in the same experiment,¹⁶ for scattering hydrogen from a W(110) surface which was fully covered with barium. However, there was a large discrepancy between the

Table 3.1 The work function and the Fermi energy in eV for a half and a full monolayer cesium coverage on W(110), and for a thick layer of barium on W(110). The latter contains at least one monolayer.

Coverage	Fermi Energy [eV]	Work Function [eV]
0.5 monolayer Cs	1.59	1.45
1 monolayer Cs	1.96	2.15
thick Ba layer	3.69	2.50

experimental values and the calculated.

This is probably related to the fact that for bariated tungsten, the region in which the electron is captured is closer to the surface than for W(110) covered with half a monolayer of cesium. This can be understood by examining the crossing point of the affinity level and the work function of the metal. If the work function is higher, the crossing point lies closer to the metal surface, which implies that the electron is captured closer to the surface. The values for the work function and Fermi energy for cesiated tungsten and barium are gathered in table 3.1.

In order to increase the accuracy of our model calculations in the region close to the surface, we introduced an additional term, similar to Eq [3.2], to describe the effect of polarization of the H^- ion due to the attractive interaction with its image charge. This additional term leads to a more precise description of the bending of the affinity level close to the surface. The second-order shift of the affinity level can be expressed as

$$\Delta E_a^{(2)} = \frac{e^2}{4\pi\epsilon_0} \left(\frac{1}{4\pi} \frac{\alpha}{2(2(z+k_s^{-1}))^4} \right) \quad [3.4]$$

where α denotes the polarizability of the H^- ion, which has a value of $65 a_0^3$.¹⁷ The total shift of the affinity level is the sum of Eqs. [3.1] and [3.4]. Secondly, instead of using only the screening length as a fit parameter we chose for a more pragmatical fitting procedure. We employed a free two-parameter least-squares fit, where the additional free parameter is the turning point, z_0 .

The experimental data used for fitting the theory are obtained from NIOBE (Negative Ion Beam Experiment).¹⁸ In this UHV experiment, a well defined proton beam, of the order of 10^{-11} A, is scattered from a thoroughly cleaned and subsequently bariated W(110) surface under grazing angles of incidence. The negative ion fraction of the scattered beam is determined as a function of the angle of reflection with an angular resolution of 1 degree. A dispenser is mounted in front of the W(110) surface to create a (sub)monolayer coverage of barium.

In Fig. 2.4 in chapter 2, the negative ion fraction for primary energies of 250, 500 and 1000 eV are depicted together with the theoretical curve derived from the two-parameter fit. For the 250 eV data, the screening length, k_s^{-1} , is $2.3 a_0$ and the turning point, z_0 , is $3 \times 10^{-4} a_0$. The screening length has to satisfy a physical requirement. It was shown in Refs. 19 and 20, that the affinity level approximately joins the bottom of the conduction band for $z=0$. Substitution of $z=0$ into Eq. (5) and taking into account the electron affinity of the hydrogen atom ($E_a = 0.75$ eV), yields a screening length of $2.2 a_0$. Thomas-Fermi screening yields a value of $2.1 a_0$.

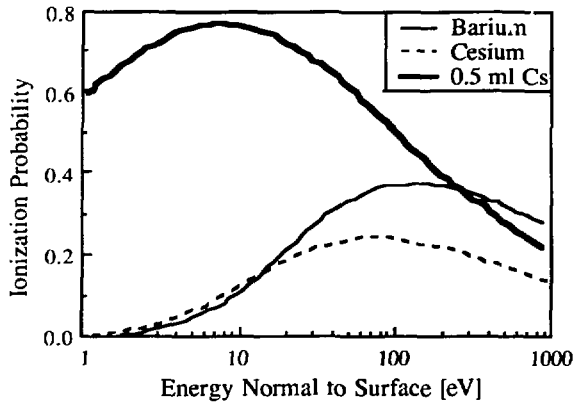


Fig. 3.2. The calculated negative-ion formation probability for hydrogen atoms leaving the surface along the normal versus energy. The solid line is for half a monolayer cesium coverage, the dashed line is for a full monolayer cesium coverage and the chain-dashed line for a thick barium coverage of the W(110) surface.

This is in good agreement with the value found from our fit. At this point it is worthwhile to note, that the coadsorption of hydrogen and barium on W(110) does not influence the ionization probability, as was also observed during experiments with a W(110) surface covered with a full monolayer of cesium.²¹ For half a monolayer coverage of cesium on W(110), the negative-ion fraction decreased with a factor of three after the coadsorption of hydrogen of the order of 1000 Langmuir of hydrogen.²¹

As we stated in the beginning of this section, our goal is to derive a relationship between the energy with which a hydrogen atom leaves the surface and the probability that this atom becomes negatively charged. Therefore, we used Eq. [3.3] with the screening length and the turning point found from the fit to calculate the probability for an atom moving normal to the surface. The result of this calculation is depicted in Fig. 3.2. Note, that for hydrogen atoms leaving the surface with a relatively high energy, barium gives a reasonable ionization probability, as was also pointed out in Ref. 22. For completeness, the curve for half a monolayer and a full monolayer coverage of cesium are also included. Care should be taken in interpreting Fig. 3.2, because the calculation moves close to the edge of the validity of the underlying theory. Therefore, Fig. 3.2 is only meant to qualitatively illustrate the effect of the wider conduction band and the higher work function of barium compared to cesium.

3.3. Experimental set-up

In this section we shall briefly discuss the surface conversion source ALICE (Amsterdam Light Ion Conversion Experiment), which was discussed more extensively in Ref. 23. The newly installed magnetic analyzer, which is capable of measuring the energy and the mass of the "self-extracted" negative-ion beam, is discussed. In addition, the new barium converter is described.

3.3.a. ALICE, Amsterdam Light Ion Conversion Experiment

Fig. 3.3 shows a schematic drawing of ALICE. A hydrogen plasma, produced by

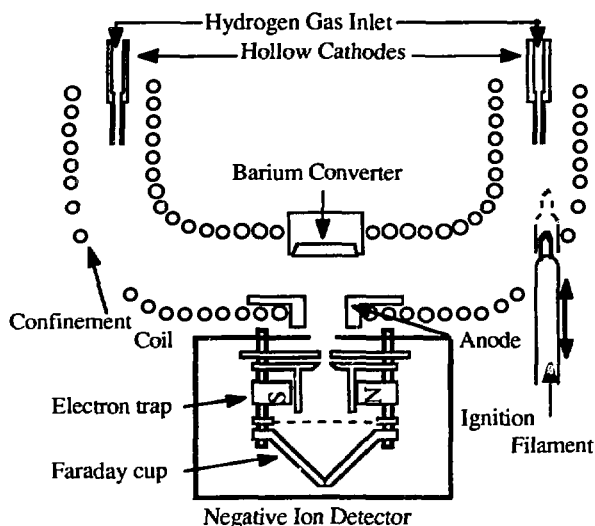


Fig. 3.3. Experimental set-up of the Amsterdam Light Ion Conversion Experiment, ALICE.

a hollow-cathode arc discharge, is confined by a magnetic field which is bent into a U-shape. This is done to provide easy access to the plasma and to reduce deposition of cathode material (tantalum) on the converter surface. The field of the confining coil is usually between 100 and 400 Gauss. The discharge is equipped with two cathodes. However, all measurements presented here, are obtained using only one cathode. The arc current can be adjusted between 5 and 50 A. The converter is mounted parallel to the anode. The converter is biased at a potential varying from 0 to -450 V. The "self-extracted" negative ions travel through the aperture into the detector. Recently, a data acquisition system was installed, which largely reduces the time needed to obtain experimental data with sufficient statistics.

3.3.b. The detector

Fig. 3.4 contains a schematic drawing of the new detector. It consists of a total-current collector with an aperture with a width of 2 mm and a height of 1 mm, an electron collector with an aperture of the same size to collimate the incoming beam, a negative-ion collector and two Faraday cups. The magnetic field can be varied from 0 to 4000 Gauss. The whole detector is mounted in an optically closed box. There are three modes in which this new detector can operate. By setting the magnetic field to approximately 100 Gauss and measuring the currents on the total-current collector, the electron collector and the negative-ion collector, the extracted negative-ion current can be determined. The second mode of operation is used to determine the energy of the extracted ions. In this case, the current detected in Faraday cup I is measured as a function of the magnetic field. The resolution in this mode amounts to $\Delta E/E = 13.4\%$. The third mode is used to determine the mass distribution of the extracted beam. For this measurement, the incident particles are

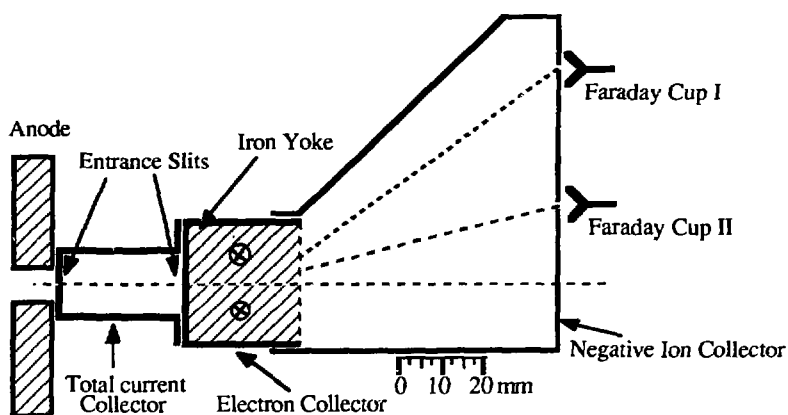


Fig. 3.4. A schematic drawing of the new detector. The incoming beam is collimated by two slits and subsequently momentum analyzed with a variable magnetic field.

accelerated to 1 keV, between the total current collector and the electron collector, and the current detected in Faraday cup II is measured as a function of the magnetic field. The resolution in this mode amounts to $\Delta m/m = 19.9\%$. Two Faraday cups are used because we require different detection ranges in the different modes.

Our detector can also be used to mass-analyze a positive current which is *directly* extracted from the plasma by reversing all potentials. Fig. 3.5 shows the mass distribution of a hydrogen plasma. Clearly visible are the H^+ , H_2^+ and H_3^+ peaks, which one would expect from a hydrogen plasma. Fig. 3.5 has been measured without a bias on the converter, which explains why no Ba^+ peak is present. At this point it is worthwhile to note that in the case of a pure argon plasma and a converter bias potential of -200 V, barium was observed in the mass distribution, whereas, for a pure hydrogen plasma barium was not observed. It is remarked, that the sputter coefficient for 200-eV argon and hydrogen ions incident on barium is

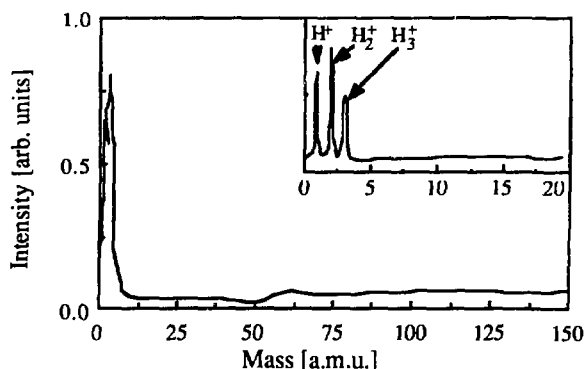


Fig. 3.5. The mass distribution of a beam extracted directly from a hydrogen plasma. In the insert, an enlarged view is given for the mass range 0 till 20 a.m.u. The ambient hydrogen pressure is 0.1 Pa. The arc current is 20 A and the arc voltage is -100 V. The field used to confine the plasma is 200 Gauss. The converter is not biased.

estimated to be of the order of 2 and 0.01, respectively,²⁴ which difference of two orders of magnitude explains the lack of barium in the case of a pure hydrogen plasma. Note, that an argon plasma can be used to "clean" the barium surface due to the high sputter rate.

3.3.c. The barium converter

For a bias potential of -400 V the converter extracts a current of the order of 1 A from the plasma. This implies that of the order of 400 Watt is dissipated on its surface. This power has to be transported from the barium surface to the cooling system, so that there should be a good heat contact between the surface and its cooled support. The set-up we use consists of a water-cooled movable copper support onto which a copper block, with a surface area of 20 x 60 mm and a thickness of 20 mm, can be mounted. At the front of this copper block, a 5-mm deep basin is milled. The basin is filled with pieces of barium and then heated slightly above the melting temperature of barium (640 °C) under an inert atmosphere. The liquid barium then fills the basin and the whole system is cooled down to room temperature. After this step the surface is flattened and polished. A converter prepared in this way proved to be satisfactory under all operating conditions. After mounting the converter in the vacuum vessel, the distance between the center of the discharge and the converter surface is adjusted to obtain a converter current of the order of 1 A at a bias of -200 V. As mentioned before, the barium surface is cleaned in-situ using an argon discharge and a converter bias of -200 V. During the cleaning procedure, the current drawn by the converter is continuously monitored. When this current reaches a saturation value, the arc is switched to hydrogen.

3.4. Experimental results

This section covers measurements done with our barium converter. The measurements of the conversion efficiency, η_H^* , have been done with the old detector which was discussed in Ref 23. All subsequent measurements of the energy and mass distribution were done with the new detector.

The plasma density in the neighborhood of the converter surface can be estimated by measuring the ion saturation current. The current drawn by the converter versus the converter potential is depicted in Fig. 3.6. For low converter potentials we see an increase of the current while for high potentials it more or less saturates. From the onset of the current from zero, we can estimate the plasma potential, which amounts to approximately -50 V. This is a rather high value, probably due to the Penning-like geometry of the discharge. We have a magnetic field parallel to the anode which prevents electrons from moving freely towards it. This causes the plasma potential to become negative to enable the flow of electrons to the anode. Note, that the electrical current to the converter consist of three parts, namely (i) the incoming flux of hydrogen ions on the converter, (ii) secondary electrons emitted due to this incoming flux and (iii) negative hydrogen ions produced at the surface. The latter constitute only a few percent of the incoming beam and can be neglected in interpreting Fig. 3.6. The secondary electrons return

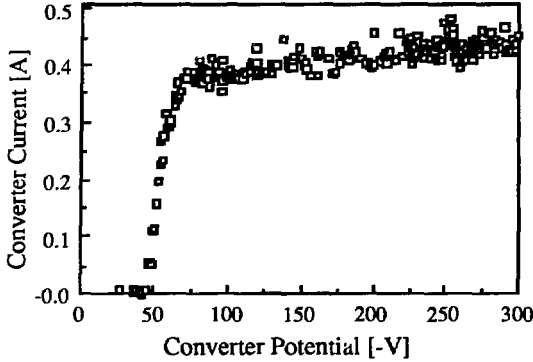


Fig. 3.6. The current drawn by the converter versus the converter potential. The ambient hydrogen pressure is 0.1 Pa. The magnetic field used to confine the plasma is 200 Gauss and the arc current is 20 A and the arc voltage is -100 V.

instantaneously to the surface due to the strong magnetic field parallel to the converter, which is used to confine the plasma column. Only a fraction of these electrons can escape along the sides of the converter to the grounded shieldings. Therefore, we expect that the electrical current to the converter gives a good measure of the flux of positive ions drawn by the surface.

The ion saturation current density, J_{sat} , can be calculated using the expression

$$J_{\text{sat}} \approx n_i e \sqrt{\frac{k T_e}{m_i}} \quad [3.5]$$

where k is the Boltzmann constant, T_e is the temperature of the electrons and m_i is the hydrogen-ion mass. Langmuir-probe measurements yielded an electron temperature of 2 eV.²³ Neglecting the experimental observation in Fig. 3.6, that the current not fully saturates, this yields a plasma density in the vicinity of the converter of the order of 10^{11} cm^{-3} , which is sufficiently low to have a negligible attenuation of the negative ion beam on its way to the detector.²³

Fig. 3.7 shows the measured mass distribution of the extracted negative ion beam for a converter potential of -200 V and a pure hydrogen discharge. Only H^- ions are present in the spectrum. It is remarked that one would not expect to see any Ba^- ions in the extracted beam because the affinity level of barium in the ground state is

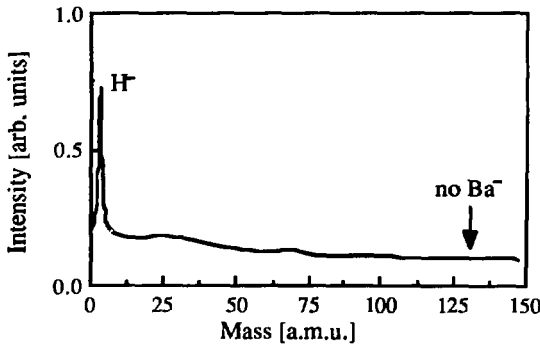


Fig. 3.7. The mass distribution of the "self-extracted" negative-ion beam. The operating pressure is 0.1 Pa, the converter bias is -200 V, the confining magnetic-field is 200 Gauss, the arc voltage is -100 V and the arc current is 20 A.

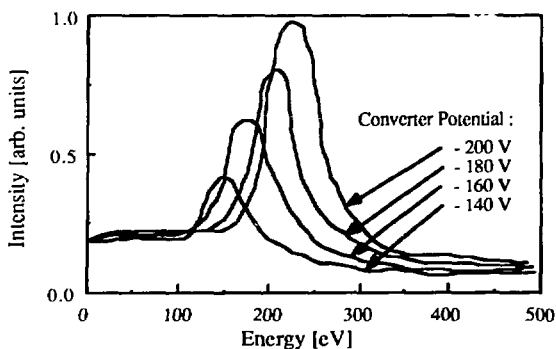


Fig. 3.8. The energy distribution of the "self-extracted" negative hydrogen ion beam for various converter potentials, ranging from -140 to -200 V. The operating pressure is 0.1 Pa, the confining magnetic field is 200 Gauss, the arc voltage is -100 V and the arc current is 20 A.

positive. Moreover, this implies that Ba^- ions cannot be formed via resonant charge exchange with a barium surface. Measurements of the energy of the extracted beam give insight in the production mechanism of the negative ions. If the particles arrive at the detector with an energy (in eV) significantly larger than the converter potential, this implies that they were scattered from the converter surface. Note, that the final energy depends on the incident species; H^+ , H_2^+ or H_3^+ . Negative ions formed via scattering of H_3^+ will acquire a maximum energy of 1.3 times the converter potential, for H_2^+ it is 1.5 and for H^+ it is 2 times the converter potential. Particles having an energy of the order of the converter potential have escaped from the surface with a low initial energy, i.e., they have been sputtered. Fig. 3.8 shows the energy distribution of the extracted beam for four different converter potentials ranging from -140 to -200 V. Firstly, the peak height is seen to increase with increasing converter potential. This is consistent with Fig. 3.6, where we see an increase of the current drawn by the converter with increasing converter potential in this range. Secondly, from the distributions it is clear that the particles initially leave the surface with a low energy, which indicates that they were sputtered from the surface. Only a small contribution of reflected particles are observed in the tail of the distribution, which is partly related to the employed "self-extraction" technique. Sputtered H^- ions leave the converter surface with a low initial energy and are subsequently accelerated across the plasma sheath normal to the surface. Therefore, the angular distribution of these particles is expected to be sharply peaked normal to the surface. On the other hand, scattered particles leave the surface with a relatively large energy and therefore, the angular distribution for these ions is expected to be less sharply peaked. Since only particles leaving normal to the converter surface can enter the detector, sputtered particles thus have a higher probability of being detected.

The conversion efficiency, which is defined as the extracted negative-ion current divided by the current drawn by the converter, gives a means to compare different surface conversion sources. It ranges from 2.5 to 5.5 % for sources which operate with cesium vapor injection and a tungsten or molybdenum converter.^{5,25,26} In Fig. 3.9 we plotted the conversion efficiency obtained with our barium converter as a function of the converter potential, for various arc currents. For low converter

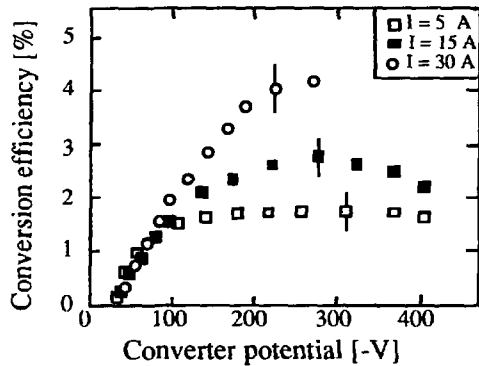


Fig. 3.9. The conversion efficiency as a function of the converter potential for arc currents ranging from 5 to 30 A. The operating pressure is 0.1 Pa, the arc voltage is -100 V and the confining magnetic field is 200 Gauss.

potentials it increases and for higher potentials it saturates. The efficiencies we measure coincide with the range of conversion efficiencies which have been measured elsewhere using cesium vapor injection. The conversion efficiency exhibits an interesting dependence on the arc current. Increasing the arc current increases the plasma density and thus the current which is drawn by the converter. The latter causes the negative ion current to increase. It is not expected to lead to an increase of the conversion efficiency. However, from Fig. 3.9 we see an increase in conversion efficiency with increasing plasma density. We shall discuss this nonlinear behavior of the extracted negative ion current in the next section.

In Ref. 7 we showed that for a cesiated porous tungsten converter in contact with a pure hydrogen plasma, the conversion efficiency drastically increased after admitting a heavy gas, like xenon or argon, to the discharge vessel. To see whether this enhancement of the conversion efficiency is also obtainable with a pure barium converter, we seeded the pure hydrogen discharge with argon. This was done by admitting argon to the vacuum vessel with a known back ground pressure. Part of the argon gas is ionized in the discharge and contributes to the incident current to the converter. The measured conversion efficiency versus the argon back ground pressure is shown in Fig. 3.10. No significant increase or decrease of the

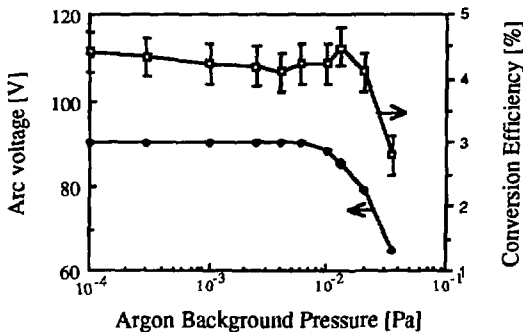


Fig. 3.10. The conversion efficiency versus the back-ground pressure of argon for an argon seeded hydrogen plasma. The arc current is 30 A and the arc voltage is -100 V. The confining magnetic field is 200 Gauss and the operating pressure is 0.3 Pa. The converter is biased at -170 V.

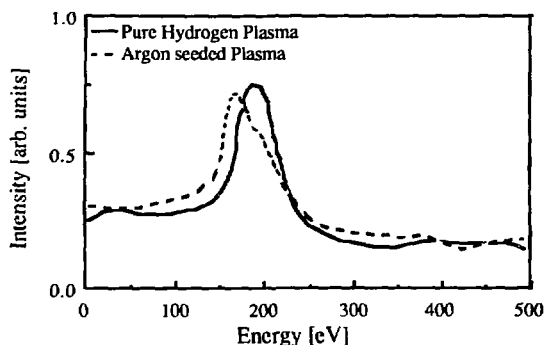


Fig. 3.11. The energy distribution of the "self-extracted" negative-ion beam. The solid line is for a pure hydrogen plasma, the dashed line is for an argon seeded plasma with an argon pressure of 0.02 Pa. The arc current is 30 A, the arc voltage is -100 V, the confining magnetic field is 200 Gauss and the operating pressure is 0.3 Pa. The converter is biased at -170 V.

conversion efficiency is observed. Note that for an argon pressure of 0.05 Pa, the arc starts to run on argon. This is illustrated in Fig. 3.10, where we see a rapid decrease of the arc voltage as a function of the argon pressure for values above 8×10^{-3} Pa.

In Fig. 3.11, the energy distribution of the "self-extracted" beam is shown for a pure hydrogen plasma and for an argon seeded plasma. At this point it is worthwhile to note that the positive hydrogen ion species distribution hardly changes due to the presence of argon ions for argon pressures below 3×10^{-2} Pa. For an argon-seeded hydrogen-discharge, the peak of the distribution lies closer to the energy which corresponds to the converter potential. Note, that the shape of the distribution changes for these two cases, however, the integral over the entire energy range is more or less the same. An explanation for this constant value of the conversion efficiency, which is in contrast with our cesiated porous tungsten converter, is probably related to a decrease of the hydrogen coverage of the converter after admitting argon to the discharge vessel. We shall elaborate further on this subject in the following section.

3.5. Discussion

In the first part of this section we shall compare the results obtained with our barium converter with more conventional cesium-seeded sources. An important issue is the effect of adding a heavy gas to the discharge to increase the sputtered flux of hydrogen from the surface. The second part deals with the increasing conversion efficiency with increasing arc current.

3.5.a. The conversion efficiency

In table 3.2 we have collected some results obtained with other surface-conversion sources. The important parameter in this table is the conversion efficiency, η_H^* , which is defined as the extracted negative-ion current divided by the positive-ion current drawn by the converter. Our measurements show that with a barium converter the conversion efficiency is roughly the same as with more

Table 3.2 The (optimum) converter potential V_c , the current density J_{sat} drawn by the converter and the conversion efficiency in a number of negative-ion sources.

V_c [V]	J_{sat} [mA/cm ²]	η_H^* [%]	Reference
-125	320	3.8	3
-160	100	5.5	5
-200	80	3.6	7
-130	48	4.0	25
-210	71	2.5	26
-200	183	4.2	This chapter

conventional converters. In section. 3.2, we deduced that this is partly related to the width of the conduction band, i.e., the Fermi energy of the metal electrons. Due to the relatively high Fermi energy of barium compared to cesiated tungsten, hydrogen atoms leaving the surface with an energy in the range of 50 till 250 eV have a relatively high ionization probability. Whereas, in the case of cesiated tungsten, the ionization probability decreases with increasing energy in this range. Furthermore, as we already noted in the introduction, it is resonable to assume that the dynamical cesium coverage of a tungsten or molybdenum converter, in contact with a cesium seeded hydrogen plasma, is not the "optimum" cesium coverage of 0.6 monolayers. The latter also partly explains why the conversion efficiencies obtained with a barium converter are roughly the same as for a more conventional cesiated converter. In spite of the similar values for the conversion efficiency, however, a surface conversion source equipped with a barium converter is favorable over conventional cesium seeded sources, where the large amount of cesium gives rise to electrical break downs in the extraction system.

In Ref. 7 it was concluded that the role of cesium in a conventional surface conversion source is not only to lower the work function of the converter surface, but also to sputter hydrogen from the surface. It was shown that after admitting argon or xenon to a pure hydrogen discharge, the negative-ion conversion efficiency strongly increased. This is related to the fact that firstly, these heavy ions have a larger sputter coefficient, so that more hydrogen atoms leave the surface and secondly, the sputtered particles leave the surface with a relatively low initial energy: for xenon a maximum of 3 percent of the incident energy of the xenon ions, for argon a maximum of 10 %. Therefore, the angular distribution becomes sharply peaked in the direction normal to the surface where these ions are "self-extracted". However, for a pure barium converter we observed no increase in the conversion efficiency. We relate this to a reduction of the hydrogen coverage, as will be discussed next.

3.5.b. The hydrogen coverage of the converter surface

In section 3.4 we showed the conversion efficiency as a function of the converter potential for various arc currents in the range of 5 to 30 A. At that point we noted that the conversion efficiency increases with arc current, which was not expected. A possible explanation of this observation is that the hydrogen coverage of the converter surface is a function of the current drawn by the converter. We will

elaborate further on this subject in the following.

We assume that the detected negative-ion current solely consists of hydrogen atoms which have been sputtered from the surface. This assumption is justified if one looks at the energy distribution of the extracted beam, see Fig. 3.8. The flux of particles leaving the surface, Φ_{Hsput} , is equal to the incoming flux multiplied by the sputtercoefficient for hydrogen on at the surface adsorbed hydrogen, $\Gamma_{\text{H-H}}$. Normally, a sputtercoefficient is based on the sputtering of a solid body, e.g. a concentration of the order of 10^{23} atoms/cm³. For our system we have to take into account that the concentration of hydrogen at the surface is expected to be lower. Therefore, we have to include a term which describes the probability of hitting a hydrogen atom. This probability is equal to the ratio of the actual concentration, $C(z,t)$, at the surface and the hydrogen saturation coverage; $c(z,t) = C(z,t)/c_{\text{sat}}$. Here $c(z,t)$ is the relative hydrogen concentration, which is a function of time, t , and place, z , in the barium bulk, where $z=0$ represents the surface. Φ_{Hsput} can then be calculated with

$$\Phi_{\text{Hsput}} = c(z=0,t) \Gamma_{\text{H-H}} \Phi_{\text{H}^+}, \quad \Phi_{\text{H}^+} = \sum_{i=1}^3 \Phi_{\text{H}_i^+} \quad [3.6]$$

where $\Gamma_{\text{H-H}}$ denotes the sputter coefficient for stimulated desorption of hydrogen atoms by incoming hydrogen ions, Φ_{H^+} is the total incident flux of all hydrogen ion species, $\Phi_{\text{H}_i^+}$ are the incident fluxes of H_i^+ ions and $c(z=0,t)$ is the relative hydrogen concentration at the surface. A fraction, η_{H} , of the sputtered flux becomes negatively charged. The conversion efficiency can thus be written as

$$\eta_{\text{H}}^* = \eta_{\text{H}} c(z=0,t) \Gamma_{\text{H-H}}. \quad [3.7]$$

Since $\Gamma_{\text{H-H}}$, and η_{H} are believed to be independent of the incoming flux and on the contamination with hydrogen of the surface, we conclude that the increasing conversion efficiency is related to a changing hydrogen concentration at the converter surface. In our view, the only non-linear process which could be responsible for an increase of the hydrogen coverage of the converter surface with increasing flux of positive hydrogen ions onto the surface, is diffusion of hydrogen in barium. Peterson and Hammerberg reported a value for the diffusion coefficient of hydrogen in barium of 3×10^{-5} cm²/s for a temperature of 200 °C.²⁷

Our starting point for the model is the assumption that we have a half infinite slab of barium which is exposed to a homogeneous flux of protons at the surface. This effectively reduces our problem to solving the one-dimensional diffusion equation,

$$\frac{\partial c(z,t)}{\partial t} = D \frac{\partial^2 c(z,t)}{\partial z^2} \quad [3.8]$$

where $c(z,t)$ denotes the concentration of hydrogen in barium, the surface is at $z=0$, and D is the diffusion coefficient. Due to removal of barium from the surface via sputtering by incident hydrogen ions, the surface moves inwards with a velocity

$$v_{\text{sput}} = \frac{\Gamma_{\text{H-Ba}} \Phi_{\text{H}^+}}{\rho_{\text{Ba}}} \quad [3.9]$$

where $\Gamma_{\text{H-Ba}}$ denotes the sputtercoefficient for hydrogen ions on barium and ρ_{Ba} is

the density of the barium metal. This movement of the surface can be incorporated in Eq [3.8] by transforming the z-coordinate according to $z' = z - v_{\text{sput}} t$. This results in an additional term in the diffusion equation,

$$\frac{\partial c(z,t)}{\partial t} = D \frac{\partial^2 c(z,t)}{\partial z^2} + v_{\text{sput}} \frac{\partial c(z,t)}{\partial z}. \quad [3.10]$$

Furthermore, TRIM code calculations for this system show that the major part of the incoming beam is implanted into the surface ($\alpha = 84 \%$) at a depth of the order of 100 \AA .²⁸ Assuming a Gaussian implantation profile Eq. [3.8] becomes

$$\frac{\partial c(z,t)}{\partial t} = D \frac{\partial^2 c(z,t)}{\partial z^2} + v_{\text{sput}} \frac{\partial c(z,t)}{\partial z} + \frac{\alpha \Phi_{\text{H}^+}}{d\sqrt{\pi} c_{\text{sat}}} \exp\left(-\left(\frac{z-r}{d}\right)^2\right) \quad [3.11]$$

where r and d are the range and deviation of the implantation profile. This equation resembles the one used by Thompa, Carr and Seidl to calculate the surface coverage of a tungsten or molybdenum surface bombarded with cesium ions.²⁹ Substitution of numerical values clearly indicates that in our case we can neglect the second term in Eq [3.11]. Furthermore, since the diffusion rate is very high we can simplify the implantation profile by assuming that the implantation takes place at the surface, Eq. [3.11] reduces to Eq. [3.8]. At the surface we have the following boundary condition,

$$D \left. \frac{\partial c(z,t)}{\partial z} \right|_{z=0} = \frac{\alpha \Phi_{\text{H}^+} - \Phi_{\text{Hsput}} - \Phi_{\text{Hdes}}}{c_{\text{sat}}} \quad [3.12]$$

where α is the implantation fraction, Φ_{Hsput} denotes the sputter flux from the surface described by Eq. [3.6] and Φ_{Hdes} denotes the desorbed flux from the surface. The latter is equal to the surface hydrogen coverage, n_{H} , divided by the residence time τ ; $\Phi_{\text{Hdes}} = n_{\text{H}}/\tau$. The hydrogen coverage of the surface can be calculated from the relative hydrogen concentration at the surface multiplied by the hydrogen saturation coverage, n_{sat} .

The measurements show no variation on a time scale of the order of hours. Therefore, we conclude that we have reached a steady state situation which means that the concentration gradient at the surface is zero. From Eq. [3.12] and [3.6] we can directly calculate the surface coverage under these conditions, this yields

$$c(z=0,\infty) = \alpha \left(\Gamma_{\text{H-H}} + \frac{n_{\text{sat}}}{\Phi_{\text{H}^+} \tau} \right)^{-1}. \quad [3.13]$$

We can estimate, from the measurements, the hydrogen concentration at the surface in the following way. The conversion efficiency amounts to 4 %. From the energy distributions in Fig.3.9 we seen that the H-atoms leave the surface with an average energy of the order of 20 eV. According to Fig. 3.2, these atoms have an ionization probability of about 15 %. This corresponds with a surface hydrogen coverage of 30 % of the saturation coverage for an incident flux of 200 mA/cm^2 . With this value and Eq.[3.13] we can calculate the residence time τ , which amounts to $5 \times 10^{-4} \text{ s}$. To check whether this value is resonable, we used the following equation to calculate the desorption energy, Q ,

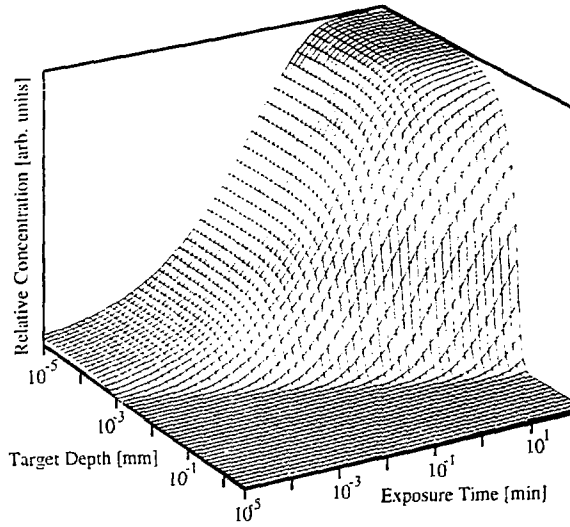


Fig. 3.12. The calculated hydrogen concentration as a function of the depth of the barium surface and the exposure time. The target is exposed to a incident positive ion current of 100 mA/cm².

$$\tau = \tau_0 \exp\left(\frac{Q}{kT}\right) \quad \tau_0 \approx 10^{-13} \text{ s}, \quad kT \approx 0.05 \text{ eV} \quad [3.14]$$

which yield a desorption energy of 1.1 eV. This seems quite resonable. An other important item which has to be checked is the time scale of the diffusion process. Therefore, we solved the time dependent diffusion equation with a boundary condition according to Eq. [3.12];

$$\begin{aligned} \frac{\partial c(z,t)}{\partial t} &= D \frac{\partial^2 c(z,t)}{\partial z^2}, & c(z,0) &= 0, \quad c(\infty,t) = 0, \\ D \frac{\partial c(z,t)}{\partial z} \Big|_{z=0} &= \Phi_{H^+} \left(\frac{\alpha}{c_{sat}} - \Gamma_{H-H} c(z=0,t) - \frac{c(z=0,t) n_{sat}}{\Phi_{H^+} \tau} \right) \end{aligned} \quad [3.15]^\dagger$$

This Equation can be solved analytically using Laplace transformations, the method is described in appendix 3.1, the result is

$$\begin{aligned} c(z,t) &= \frac{\alpha}{a} \left(\operatorname{erfc}\left(\frac{z}{\sqrt{D t}}\right) - \exp\left(\frac{a \Phi_{H^+} z}{D} + \frac{(a \Phi_{H^+})^2 t}{D}\right) \operatorname{erfc}\left(a \Phi_{H^+} \sqrt{\frac{t}{D}} + \frac{z}{\sqrt{D t}}\right) \right) \\ \text{with } a &= \Gamma_{H-H} + \frac{n_{sat}}{\Phi_{H^+} \tau}. \end{aligned} \quad [3.16]^\dagger$$

In Fig. 3.12 we have plotted the concentration profile as a function of time. We can see that after about 5 minutes the concentration of hydrogen at the surface is constant in time, whereas in the bulk, hydrogen still moves inwards. In Fig. 3.13 we plotted the calculated relative hydrogen coverage (i.e. the ratio of the hydrogen concentration at the surface and the saturation concentration) according to Eq.

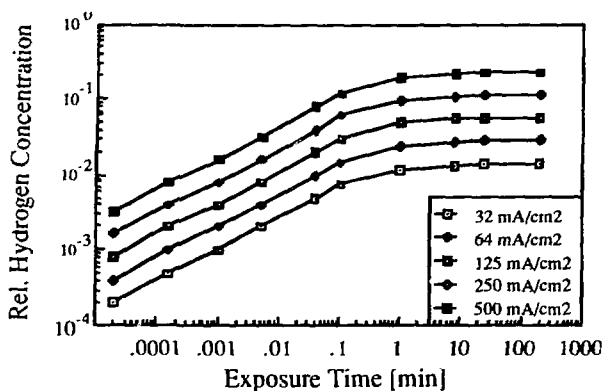


Fig. 3.13. The calculated ratio between the hydrogen concentration at the barium surface and the saturation concentration as a function of exposure time for incident fluxes ranging from 20 to 140 mA/cm².

[3.16] of the surface as a function of the time for incoming positive hydrogen ion currents ranging from 30 to 500 mA/cm². For n_{sat} we assumed that each surface barium atom can be covered by one hydrogen atom, this gives a value of 6×10^{14} #/cm². The curves have been calculated for a surface temperature of 230 °C. We see that as a function of time the hydrogen coverage of the surface initially increases and reaches saturation for times larger than 10 min. This equilibrium coverage is a function of the incoming flux of positive hydrogen ions onto the surface.

Using Eq. [3.7] and the expression of Bodansky in order to calculate the sputtercoefficient $\Gamma_{\text{H-H}}$, taking the ionization probability η_{H} to be 15 % for sputtered particles according to Fig. 3.2, we are able to calculate the conversion efficiency as a function of the converter potential for various arc currents. The result of this calculation is depicted in Fig. 3.14. An arc current of 5 A corresponds with an current density of hydrogen ions to the surface of 40 mA/cm² and an estimated surface temperature of 230 °C. For 15 A arc current these values are 100 mA/cm² and 240 °C and for 30 A, 200 mA/cm² and 244 °C. In the calculations we did not take into account the increase of the surface temperature with increasing converter potential. Comparing the calculated conversion efficiency in Fig. 3.14 with the measured efficiencies in Fig 3.9 shows a reasonable qualitative and quantitative agreement between theory and experiment. Note, that we used the activation energy according to Eq. [3.14] which was calculated using experimental and theoretical data.

This model permits us to estimate the conversion efficiency for barium exposed to much higher incident currents. For an incident current of 800 mA/cm² the *estimated* conversion efficiency is around 7 % for an estimated surface temperature of 260 °C. This corresponds with a produced negative ion current of about 60 mA/cm². According to Dimov and Belchenko, this current density may be increased by a factor of two to three using geometrical focussing.

The last item we want to discuss in this section is the seeding of the hydrogen plasma with argon in order to increase the sputter rate of hydrogen from the surface. Measurements showed no effect of the seeding on the produced negative ion current. We can include the additional sputtering of argon into our model by

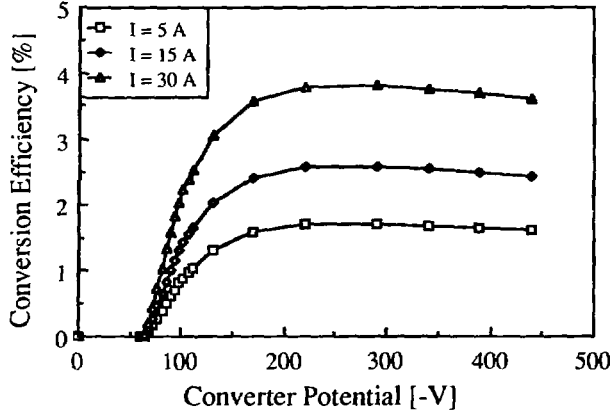


Fig. 3.14. The calculated conversion efficiency as a function of the converter potential for arc current of 5, 15 and 30 A. The desorption energy of hydrogen from barium is calculated from the measurements.

subtracting $\Phi_{Ar\text{sput}} = \Gamma_{Ar-H} c(z=0, t=\infty) \Phi_{Ar^+}$ from the left hand side of Eq. [3.12]. The resulting coverage can be written as

$$c(0, \infty) = \alpha \left(\Gamma_{H-H} + \Gamma_{Ar-H} \frac{\Phi_{Ar^+}}{\Phi_{H^+}} + \frac{n_{sal}}{\Phi_{H^+} \tau} \right)^{-1} \quad [3.17]$$

where it is clear that seeding the discharge with argon decreases the hydrogen coverage of the surface. Apparently, the increase of the sputter rate is compensated by a decrease of the hydrogen coverage of the surface. The net effect of seeding the plasma with hydrogen is negligible. However, hydrogen atoms sputtered by argon leave the surface with a lower energy compared by those sputtered by hydrogen, therefore, despite the fact that the conversion efficiency does not increase, the emittance of the source may improve.

3.6. Summary

We have shown, both experimentally and theoretically, that a surface source equipped with a pure barium metal converter gives negative ion yields, which are comparable with more conventional cesium-seeded sources. This approach eliminates a main drawback of cesium seeded sources, namely the large amount of cesium needed for efficient operation. From our theoretical study, we concluded that the high electron density of barium compared to cesium is responsible for the observed high negative-ion yields. Furthermore, experiments as well as model calculations, indicate that the hydrogen coverage of the converter increases with the increasing flux of positive hydrogen ions to the surface. This implies, that increasing the plasma density increases the conversion efficiency of the source. For a pure hydrogen discharge in contact with a cesiated porous tungsten converter, such a behavior was not observed.²⁶ According to the model, the time scale of the diffusion process is controlled by the factor $(a\Phi_{H^+})^2/D$. Since there is a good

agreement between the time scale of the experiments and that of the model we conclude that this factor is correct. The only two less known values in this factor are the sputtercoefficient Γ_{H-H} and the desorption time τ . If we chose Γ_{H-H} and fit the measurements to obtain the desorption time τ we obtain a good qualitative and quantitative agreement between theory and experiment. Furthermore, with this model we can estimate the produced negative ion current for high incident currents; for 800 mA/cm² it is *estimated* that a current of 60 mA/cm² can be produced without geometrical focussing.

Acknowledgments

The authors wish to thank, H. J. Timmer for his technical support, R. M. A. Heeren, S. Sman and C. Leguijt for their assistance during the various stages of the experiment, J. P. Gauyacq and J. J. C. Geerlings for useful suggestions concerning the model calculations on the resonant charge exchange, and F. Vitalis for solving the time-dependant diffusion equation. The work described here was performed as part of the research program of the association agreement between the Stichting voor Fundamenteel Onderzoek der Materie (FOM) and EURATOM, with financial support from the Nederlandse Organisatie voor Wetenschappelijk Onderzoek (NWO) and EURATOM.

Appendix 3.1

In this section we will solve the time dependant diffusion equation as formulated by Eq. [3.15]. Our problem is defined as

$$\frac{\partial c}{\partial t} = D \frac{\partial^2 c}{\partial z^2}, \quad D \frac{\partial c}{\partial z} \Big|_{z=0} = \Phi_H^+ \left(\frac{\alpha}{c_{\text{sat}}} - a c(0,t) \right), \quad c(z,0) = 0, \quad c(\infty,t) = 0 \quad [3.A1]$$

where a is defined similar to Eq. [3.16]. The Laplace transform of $c(z,t)$, denoted as c^* , yields

$$c^*(z,s) = \int_0^\infty e^{-st} c(z,t) dt = -\frac{1}{s} \int_0^\infty c(z,t) de^{-st} = \frac{1}{s} \int_0^\infty c_t(z,t) dt \quad (s : \mathbb{C}) \quad [3.A2]$$

since $c(z,0) = 0$. With $c_t(z,t) = D c_{zz}(z,t)$ this reduces our problem to

$$c^*(z,s) = \frac{D}{s} c^*_{zz}(z,s) \quad \text{thus} \quad c^*(z,s) = A(s) \exp(-z \sqrt{\frac{s}{D}}). \quad [3.A3]$$

Back transformation of $c^*(z,s)$ for $z=0$ yields

$$c(0,t) = \frac{1}{2\pi i} \int e^{st} A(s) ds \quad [3.A4]$$

Note, that this can be done since $c(\infty,t) = 0$. Differentiating Eq. [3.A3] with respect to z and applying the boundary conditions for $z=0$ gives

$$D c_z(0,t) = \frac{\sqrt{D}}{2\pi i} \int_L e^{st} A(s) \sqrt{s} ds = \Phi_{H^+} \left(\frac{\alpha}{c_{sat}} - \frac{a}{2\pi i} \int_L e^{st} A(s) ds \right) \quad [3.A5]$$

where L is some path in the complex plane. Back Laplace transformation of Eq. [3.A5] yields an expression for $A(s)$ which combined with Eq. [3.A3] gives the concentration profile;

$$A(s) = \frac{\alpha \Phi_{H^+}}{s c_{sat} (a \Phi_{H^+} + \sqrt{sD})} \quad [3.A6]$$

thus

$$c(z,t) = \frac{\alpha \Phi_{H^+}}{2\pi i c_{sat}} \int_L \frac{\exp\left(st - z \sqrt{\frac{s}{D}}\right)}{s (a \Phi_{H^+} + \sqrt{sD})} ds. \quad [3.A7]$$

The latter integral can be solved according to Abramowitz & Stegun (formula 29.3.89) and results in Eq. [3.16].

References

- ¹ Yu. I. Belchenko, G. I. Dimov and V. G. Dudnikov, Nucl. Fus. **14** (1974) 113.
- ² E. J. Britt, J. L. Desplat, M. Korrinda and K. N. Leung, J. Vac. Sci. Technol. A **3** (1985) 1241.
- ³ A. I. Hershcovitch, V. K. Kovarik and K. Prelec, Rev. Sci. Instrum. **57** (1986) 827.
- ⁴ J. N. M. van Wunnik, J. J. C. Geerlings, E. H. A. Granneman and J. Los, Surf. Sci. **131** (1983) 17.
- ⁵ K. N. Leung and K. W. Ehlers, Rev. Sci. Instrum. **53** (1982) 803.
- ⁶ J. L. Desplat and C. A. Papageogopoloulos, Surf. Sci. **92** (1980) 97.
- ⁷ C. F. A. van Os and P. W. van Amersfoort, Appl. Phys. Lett. **50** (1987) 662.
- ⁸ P. W. van Amersfoort, Ying Chung Tong and E. H. A. Granneman, J. Appl. Phys. **58** (1985) 2317.
- ⁹ G. S. Tompa, W. E. Carr and M. Seidl, Appl. Phys. Lett. **49** (1986) 1511.
- ¹⁰ K. F. Wojciechowski, Surf. Sci. **55** (1976) 246.
- ¹¹ R. Gomer and L. W. Swanson, J. Chem. Phys. **38** (1963) 1613.
- ¹² J. W. Gadzuk, Surf. Sci. **6** (1967) 133.
- ¹³ B. Rasser, J. N. M. van Wunnik and J. Los, Surf. Sci. **118** (1982) 697.
- ¹⁴ B. Rasser and M. Remy, Surf. Sci. **93** (1980) 223.
- ¹⁵ J. N. M. van Wunnik, R. Brako, K. Makoshi and D. M. Newns, Surf. Sci. **126** (1983) 618.
- ¹⁶ J. J. C. Geerlings, P. W. van Amersfoort, L. F. Tz. Kwakman, E. H. A. Granneman, J. Los and J. P. Gauyacq, Surf. Sci. **157** (1985) 151.
- ¹⁷ Landolt-Bornstein, *Atom und Molecular Physik*, 1. Teil, 1. Band, (Springer Verlag, Berlin 1950) p. 401.
- ¹⁸ P. W. van Amersfoort, J. J. C. Geerlings, L. F. Tz. Kwakman, A. Hershcovitch, E. H. A. Granneman and J. Los, J. Appl. Phys. **58** (1985) 3566.
- ¹⁹ N. D. Lang and A. R. Williams, Phys. Rev. B **18** (1987) 616.
- ²⁰ J. K. Nørskov, Phys. Rev. B **20** (1979) 446.
- ²¹ P. W. van Amersfoort, J. J. C. Geerlings, R. Rodink, E. H. A. Granneman and J. Los, J. Appl.

- Phys. **59** (1986) 241.
- 22 C. F. A. van Os, R. M. A. Heeren and P. W. van Amersfoort, Appl. Phys. Lett. **51** (1987) 1495.
- 23 C. F. A. van Os, E. H. A. Granneman and P. W. van Amersfoort, J. Appl. Phys. **61** (1987) 5000.
- 24 J. Bodansky, Nucl. Instr. Meth. in Phys. Res. **B 2** (1984) 587.
- 25 J. W. Kwan, G. D. Ackerman, O. A. Anderson, C. F. Chan, W. S. Cooper, G. J. de Vries, A. F. Lietzke, L. Soroka and W. F. Steele, Rev. Sci. Instrum. **57** (1986) 831.
- 26 B. Piosczyk and G. Dammertz, Rev. Sci. Instrum. **57** (1986) 840.
- 27 D. T. Peterson and C. C. Hammerberg, J. Less-Common Metals, **16** (1968) 457.
- 28 J. P. Biersack and W. Eckstein, Appl. Phys. (Berlin) **A34** (1984) 73.
- 29 C. S. Tompa, W. E. Carr and M. Seidl, Appl. Phys. Lett. **48** (1986) 1048.

†: Note, a printing error occurred in the publication of these formula, they should read:

$$\begin{aligned} \frac{\partial c(z,t)}{\partial t} &= D \frac{\partial^2 c(z,t)}{\partial z^2}, & c(z,0) &= 0, \quad c(\infty,t) = 0, \\ D \frac{\partial c(z,t)}{\partial z} \Big|_{z=0} &= \Phi_{H^+} \left(\frac{\alpha}{c_{sat}} - \frac{\Gamma_{H-H} c(z=0,t)}{c_{sat}} - \frac{c(z=0,t) n_{sat}}{c_{sat} \Phi_{H^+} \tau} \right) \end{aligned} \quad [3.15]$$

and

$$\begin{aligned} c(z,t) &= \frac{\alpha}{a c_{sat}} \left(\operatorname{erfc} \left(\frac{z}{\sqrt{D t}} \right) - \exp \left(\frac{a \Phi_{H^+} z}{D} + \frac{(a \Phi_{H^+})^2 t}{D} \right) \operatorname{erfc} \left(a \Phi_{H^+} \sqrt{\frac{t}{D}} + \frac{z}{\sqrt{D t}} \right) \right) \\ \text{with } a &= \frac{1}{c_{sat}} \left(\Gamma_{H-H} + \frac{n_{sat}}{\Phi_{H^+} \tau} \right). \end{aligned} \quad [3.16]$$

SURFACE CONVERSION AT A CESIATED TUNGSTEN SURFACE

A fundamental study of the formation of negative hydrogen ions at a cesiated surface is presented. The surface (converter) consists of a porous tungsten plate through which liquid cesium can diffuse in order to obtain the surface coverage which evolved from calculations of the cesium coverage of a tungsten surface immersed in a cesium seeded discharge. This gives an efficient replenishing of the cesium sputtered from the surface. Therefore, a full monolayer coverage is always maintained with this converter. Energy distributions of the extracted negative ion beam show that the dominant formation process is negative ionization of hydrogen atoms sputtered from the converter surface. In this system the implanted hydrogen ions are trapped in the tungsten surface layers which results in a saturation of the converter with hydrogen. This could be calculated analog to the modelling done for a pure barium metal converter on the assumption that the process is sputter dominated rather than diffusion dominated. However, the hydrogen at the surface is sandwiched between the cesium adlayer and the tungsten surface. Measurements show that the conversion efficiency (i.e. the ratio of the extracted negative ion current and the positive ion current on the surface) scales with the sputter coefficient of hydrogen on adsorbed cesium. The derived ionization probability for resonant charge exchange agrees well with earlier model calculations derived from experimental data obtained in a UHV experiment.

4.1. Introduction

Research on thermonuclear fusion invoked a considerable research effort in the formation of negative ions either via surface conversion or by means of volume production or a combination of these two basically different processes. The interest in this subject is related to the need of intense neutral hydrogen or deuterium beams with an energy of the order of 1 MeV. These beams serve to heat, diagnose and drive the fusion plasma. At these energies, the neutralization efficiency of positive ions is very small.¹ However, for negative ions, the neutralization is of the order of 60 percent which makes negative ions interesting as an intermediate step in the production of intense high-energy beams of neutral atoms. In this paper, we present a fundamental study on the negative ion production process in a surface conversion source. In particular a source with uses a converter surface covered with cesium to provide the necessary low work function.

One of the first surface conversion experiments was done by Belchenko *et al.*, who extracted a beam of negative hydrogen ions from a magnetron source.² These were produced on the cathode surface. It was generally believed that the conversion process could be better controlled if it was separated from the plasma production process. Therefore, in most subsequent experiments the negative ions are produced on an isolated electrode, the so-called converter.^{3,4,5,6} The converter should have a small work function to obtain a high negative ion yield. This can be achieved via

adsorption of a sub monolayer cesium on a metal substratum.⁷ Cesium vapor is usually injected into the discharge chamber for this purpose.

In a typical negative-ion source, the converter is biased at a negative potential V_c of a few hundred Volts, so that it draws a flux of positive hydrogen ions from the surrounding plasma. A fraction of these ions is scattered. Furthermore, adsorbed hydrogen atoms are sputtered from the converter surface by incident positive plasma particles. The scattered and sputtered hydrogen particles can be ionized via charge exchange with the metal surface. Negative ions thus formed are accelerated across the plasma sheath, a process known as "self-extraction".⁸ The ionization process is operative over a distance of a few times the Bohr radius a_0 , which is small with respect to the sheath thickness. The latter is typically a few μm in an intense discharge. Therefore, the charge exchange process between metal surface and hydrogen atom is not influenced by the sheath potential.

Insight into the conversion process can be obtained from the energy distribution of the extracted ions. Leung and Ehlers measured this distribution for a converter made from polycrystalline molybdenum, which was cesiated via vapor deposition.⁹ Van Bommel *et al.* did a similar study using different converter materials, mono crystalline as well as polycrystalline.¹⁰ It was found in both studies that the distribution has a dominant peak at an energy of roughly $e|V_c|$ eV. This implies that the particle energy close to the surface is small compared with the sheath potential, which suggests that negative ions are primarily produced via sputtering of adsorbed atoms. Negative ions produced via scattering would leave the source with an energy of roughly $2e|V_c|$ eV, in particular when the converter is made from a heavy element. Recent calculations of Belchenko and Kupriyanov on the energy distribution of hydrogen atoms leaving the surface confirm this experimental observation.¹¹

The abundance of sputtered particles in the extracted beam is related to the applied geometry in the extraction region. The extraction aperture is usually placed in a plane parallel to the converter surface, so only those particles emitted under more or less normal angles to the surface are able to leave the source. Close to the converter the angular spread is considerable, both for scattered and sputtered ions. It is reduced by the electric field in the plasma sheath, which increases the "normal energy" by an amount $e|V_c|$ eV. The reduction is higher at a smaller initial energy, which leads to the conclusion that the geometry favours the extraction of sputtered ions. Note that it cannot be concluded that the formation of negative ions via sputtering is also favoured. Wada *et al.* rotated the converter in such a way, that the normal no longer pointed into the direction of the extraction aperture, and measured a significant contribution of scattered particles to the negative ion yield.¹²

In a geometry as described above, the production of a large flux of sputtered atoms is important to get a high negative ion yield. This is one of the subjects studied here for the case of a porous tungsten converter with liquid cesium flowing through it. This set-up has evolved from model calculations of the cesium coverage of a tungsten surface immersed in a cesium seeded discharge. With the afore mentioned set-up we obtained a full monolayer coverage of the tungsten surface, independent of the plasma characteristics and the converter bias. This stable converter composition enabled us to model the hydrogen sputtering process in a

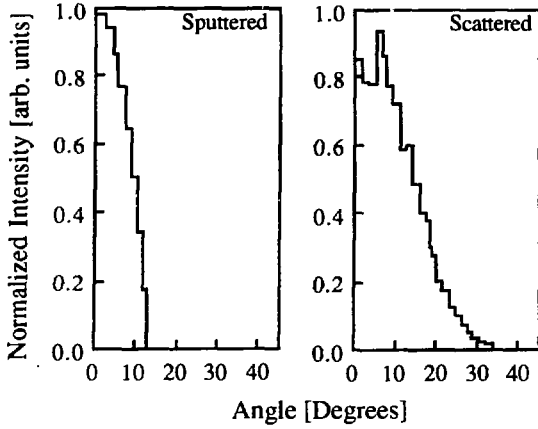


Fig. 4.1 The angular distribution of negative hydrogen ions after acceleration across the plasma sheath for sputtered and reflected atoms from a full cesium layer on a tungsten surface.

way analog to the the modelling done for a pure barium metal converter. In fact, the proposed model is a specific solution of the general modified diffusion equation derived for the barium converter.

4.2. Theory

The negative ion current density, J_{H^-} , can in its most general form be described as a integration over the parallel, v_{\parallel} , and normal velocity, v_{\perp} , of an ionization probability multiplied by the flux of hydrogen atoms leaving the surface and an attenuation factor;

$$J_{H^-} = \int_0^{\infty} dv_{\perp} \int_0^{\infty} dv_{\parallel} \eta_H(v_{\perp}, v_{\parallel}) \Phi_H(v_{\perp}, v_{\parallel}) \exp\left(-\int_0^L dl \sum_i n_i \sigma_i(v_{\perp}, v_{\parallel})\right) \quad [4.1]$$

where $\eta_H(v_{\perp}, v_{\parallel})$ denotes the ionization probability, $\Phi_H(v_{\perp}, v_{\parallel})$ denotes the flux of hydrogen atoms leaving the surface and the exponent is an attenuation factor which describes the stripping of negative ions on molecules and plasma particles with their respective densities, n_i , and cross sections, $\sigma_i(v_{\perp}, v_{\parallel})$.

In a practical surface conversion source, only negative ions leaving more or less normal to the surface are collected. $\Phi_H(v_{\perp}, v_{\parallel})$ is a sum of particles which are reflected from the surface and particles which are sputtered or recoiled. Recent work on the surface production of negative ions has illustrated that the negative ions are dominantly formed via a combination of sputtering and recoiling.¹³ Both processes result in hydrogen atoms leaving the surface with a relatively low energy, of the order of a few tenth's of an eV. Subsequently, these particles are accelerated across the plasma sheath which gives them an angular distribution which is peaked around the normal. Reflected particles however, have an angular distribution which is less peaked around the normal since they have an energy of the same order as the sheath potential before they are accelerated across the plasma sheath. This is illustrated in Fig. 4.1 which shows the calculated angular distribution of hydrogen

particles reflected from a cesiated tungsten surface using TRIM and hydrogen atoms sputtered from the surface.¹⁴ In these simple calculations we assumed that all particles, regardless of their transverse and normal energy, are negatively ionized and subsequently accelerated across the plasma sheath. In view of the difference in angular distribution of sputtered and reflected particles, $\Phi_H(v_\perp, v_\parallel)$ can be simplified by the assumption that only sputtered or recoiled hydrogen atoms contribute.

If the pressure in the surface conversion source is of the order of a few mTorr and the plasma density is below 10^{12} cm^{-3} then the attenuation term can be neglected if the path length, L , the negative ions travel is below 10 cm.^{15,16} Furthermore, on the assumption that the detection angle of our collector is small, we don't have to integrate over the parallel velocity. Moreover, since we have constrained ourselves to sputtered particles, we may simplify our integration by taking an average energy with which the hydrogen atoms leave the surface. Eq. [4.1] then reduces to

$$J_{H^-} = \int_0^{\infty} dv_\perp \eta_H(v_\perp) \Phi_H^*(v_\perp) = \int_0^{eV_c} \frac{dE}{\sqrt{2E}} \eta_H(E) \Phi_H^*(E) \approx \eta_H(\langle E \rangle) \Phi_H^* \quad [4.2]$$

where V_c denotes the converter potential, $\langle E \rangle$ the average energy of the sputtered particles and Φ_H^* the sputtered flux. In the following two sections we will discuss the two remaining factors, namely the ionization probability and the sputtered flux.

4.2.a. Ionization probability

The process of forming a negative ion via interaction with a low work function surface is generally known as resonant charge exchange. This process has been studied experimentally as well as theoretically for the last decades. We will briefly discuss the process and give an expression for the ionization probability in the so-called stationary phase approximation.

The affinity level of a hydrogen ion lowers when it comes in the vicinity of a metal surface due to the attractive interaction with its image in the metal plane. This lowering can be expressed as a function of the atom metal surface separation, z by a $0.25(z + k_s)^{-1}$ dependence, where k_s denotes the screening length of the metal electrons expressed in atomic units.¹⁷ Due to this lowering, at short distances the affinity level drops below the work function of the metal surface. At this point electrons from the metal may tunnel through the potential barrier and populate the affinity level. The tunneling frequency depends exponentially on the height and the width of the barrier. In other words electrons tunnel between the affinity level and the metal conduction band with a certain transition frequency $\omega(z)$ which is an exponentially decaying function of the distance, z , between atom and metal.

Via this process of resonant population, the atom has a certain charge state, $N^-(z)$, in the vicinity of the surface. When this atom moves away from the surface part of this charge state decays depending on the normal velocity of the atom. If the atom moves very slow, almost adiabatically, it will lose all of its charge. On the other hand if the atom moves very fast with respect to the transition frequency no

charge will be build up and also in this case no negative ion will be formed. In the intermediate range we expect some probability of forming a negative ion. This ionization probability can be calculated using the stationary phase approximation which yields¹⁸

$$\eta_H(E) = \eta_H'(v_\perp) = \frac{1}{v_\perp} \int_{z_0}^{\infty} N^-(z) \omega(z) \exp \left(\frac{-1}{v_\perp} \int_z^{\infty} \omega(z') dz' \right) dz. \quad [4.3]$$

Where $N^-(z)$ is an occupation probability depending mainly on the position of the affinity level with respect to the Fermi level, which is a function of z . With this expression, the ionization probability can be calculated as a function of the energy of the hydrogen atom leaving normal to the surface. Using the experimental data from scattering experiments, under grazing angles of incidence, of van Wunnik *et al.*¹⁹ and of van Amersfoort *et al.*²⁰ we can determine the screening length and use Eq. [4.3] to calculate the ionization probability. The result of this calculation is shown in Fig. 3.2, chapter 3 together with curves obtained in a similar way for a tungsten surface covered with only half a monolayer of cesium and for a pure barium surface. For sputtered particles, which have energies around 10 eV for a converter potential of -200 V, the ionization probability is of the order of 10 percent.

4.2.b. Sputtered flux

In this section we will elaborate on the properties of the flux of sputtered and recoiled particles. Generally, the sputtered flux is equal to an incident flux multiplied by a sputter coefficient. However, in this case we are interested in the sputtered flux of hydrogen particles from a surface. So in this case a description with a "solid body" sputter coefficient is not appropriate. Van Os, van Amersfoort and Los reported the use of a solid body sputter coefficient multiplied by the probability of hitting a hydrogen atom located at the surface.¹³ This probability is related to the relative hydrogen concentration at the surface,

$$\Phi_H^* = \frac{c_H}{c_{sat}} \Gamma_{H-H} \Phi_H^+ \quad [4.4]$$

where c_H denotes the hydrogen concentration at the surface, c_{sat} is the hydrogen saturation coverage, Γ_{H-H} is the sputter coefficient for hydrogen on adsorbed hydrogen and Φ_H^+ is the incident flux of positive hydrogen ions. The concentration of hydrogen at the surface is due to implantation of the energetic hydrogen ions. This incident flux also erodes the tungsten surface with gives the surface an inward velocity,

$$v_{sput} = \frac{\Gamma_{H-w} \Phi_H^+}{\rho_w} \quad [4.5]$$

where ρ_w denotes the volume particle density of tungsten. This movement of the surface causes implanted hydrogen to be liberated. A second important proportion

is the diffusion of hydrogen in the converter material. These two processes can be captured in the following diffusion equation,

$$\frac{\partial c(z,t)}{\partial t} = D \frac{\partial^2 c(z,t)}{\partial z^2} + v_{\text{sput}} \frac{\partial c(z,t)}{\partial z} + \frac{\alpha \Phi_{\text{H}^+}}{c_{\text{sat}} d \sqrt{\pi}} \exp\left(-\left(\frac{z-r}{d}\right)^2\right) \quad [4.6]$$

where we assumed a Gaussian implantation profile. $c(z,t)$ denotes the relative concentration of hydrogen in the bulk with respect to the surface ($z=0$), D is the diffusion coefficient for implanted particles in the tungsten bulk, r and d are the range and deviation of the implantation profile respectively and α is the implanted fraction.

This equation has two regimes: a diffusion controlled regime and a regime which is sputter dominated. In which of the two regimes we are working depends on which term we may neglect at the right hand side of Eq. [4.6]. We can express the ratio of the multiplication constants of the differentials in the equation as a dimensionless number

$$\kappa = \frac{D}{v_{\text{sput}} w}, \quad [4.7]$$

where w is a typical dimension in the process, e.g. the converter thickness. An example of a process in the diffusion dominated regime is a barium converter in a surface conversion source.¹³ In this case one can neglect the second term on the right hand side of Eq. [4.6] and assume that the entire implanted flux is collected at the surface. This reduces Eq. [4.6] to a simple diffusion equation with boundary conditions, which can be solved analytically as has been shown by van Os, van Amersfoort and Los.¹³ If the process is sputter dominated then we can neglect the first term in Eq. [4.6] and solve the equation. In view of the experimental observation that the conversion efficiency is constant as a function of time, we conclude that a stationary situation has evolved, which means that the left hand term in Eq. [4.6] is equal to zero. We will present an analytical solution of this sputter dominated model with the discussion of the experimental data.

4.3 Experimental arrangement

The set-up of the experiment is shown in Fig. 4.2, the system is discussed in great detail in Ref. 21. In summary, the plasma is produced with a hollow cathode arc discharge. The plasma is confined by an axial magnetic field of 200 Gauss. It is bent in a U-shape to avoid pollution of the converter with cathode material. The source contains two cathodes, however the experiments are done using only a single one. The arc current can be varied from 5 to 35 A.

The converter potential can be biased from 0 to -350 V with respect to the anode potential. This potential serves as extraction voltage for positive ions diffusing into the plasma sheath as well as acceleration potential for the formed negative ions. This method is generally referred to as "self-extraction". The formed negative ions are collected in a Faraday cup after removal of electrons by means of a magnetic field. Furthermore, the Faraday cup can be replaced by a magnetic analyzer with which the mass and energy distribution of the "self-extracted" negative ion beam can be measured. The resolution for energy measurements is $\Delta E/E = 13.4\%$. After

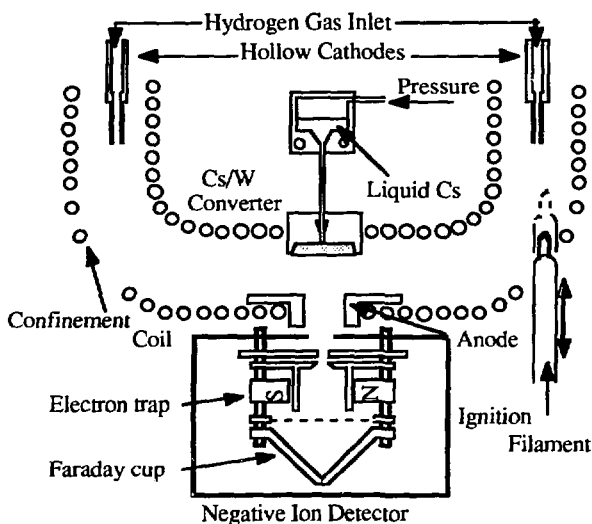


Fig. 4.2 Experimental arrangement of the Amsterdam Light Ion Conversion Experiment (ALICE).

acceleration of the incident particles to 1 keV the mass distribution can be determined, with a resolution of $\Delta m/m = 19.9\%$. It is also possible, by reversing all potentials of the detector, to extract directly a positive current from the plasma.

In the following we will first present model calculations for a tungsten surface immersed in a cesium seeded plasma. This is a well known method for obtaining a cesium coverage of the surface in order to lower the work function. From the calculations of the cesium coverage in such a system, it is clear that maintaining an optimum, i.e. half a monolayer-, coverage is difficult and puts a severe constraint on the operation regime of the converter bias and plasma parameters. Therefore, we chose for a different type of converter with cesium coverage which will be described in the second part of this section.

4.3.a. Cesium coverage of a tungsten surface immersed in a cesium seeded hydrogen discharge

A schematic view of the deposition process at a conversion surface immersed in a cesium seeded discharge is shown in Fig. 4.3. The converter is covered with θ_{Cs} monolayers of cesium. It is biased at a negative potential V_c with respect to the anode potential. The associated electric field is concentrated in a thin layer, the so-called plasma sheath. The sheath thickness is typically a few μm in the type of sources relevant for our calculations.

The surface is exposed to a flux of thermal cesium atoms, positive cesium ions and hydrogen ions. Calculations of the mean free path for ionization of thermal cesium atoms in a hydrogen plasma show that with a vapor injection scheme all cesium atoms are ionized before they reach the converter surface. Therefore in the model only cesium ions and hydrogen ions are used as the incoming fluxes. The

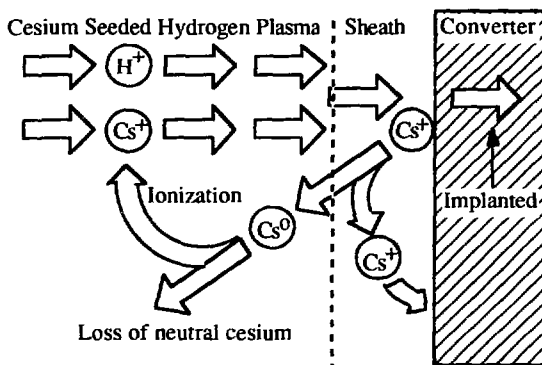


Fig. 4.3 A schematic presentation of the various flows of neutral and ionized cesium particles towards the converter surface.

corresponding fluxes are denoted as Φ_{Cs} and Φ_H , respectively. The presence of molecular ions (i.e. H_2^+ or H_3^+ ions) is neglected. A fraction of all incident cesium particles is trapped at the surface, a fraction is implanted in the tungsten and the remaining fraction is scattered. Furthermore, adsorbed particles are sputtered by incident cesium ions and protons, which are accelerated by the negative converter potential. There are thus two effects that contribute to a flux of cesium particles leaving the surface. These are either neutral or positively charged. The ion component returns to the surface due to the electric field in the plasma sheath. The neutral component does not feel the electric field and flows to the plasma. Note that it is implicitly assumed here that the mean free path for ionization is larger than the sheath thickness. The returning ions initiate a new step of trapping, scattering and sputtering phenomena. Consequently, a loop structure in the adsorption process develops. One loop is shown in Fig. 4.3. The neutral component in each loop flows to the plasma.

The evolution of the cesium coverage is calculated as follows. The surface is exposed to the involved fluxes for dt seconds and the loop structure initiated by this exposure. A rate equation is obtained from a balance of source and sink terms. The equilibrium coverage due to adsorption can be found by determining the time independent solution of this rate equation. Van Amersfoort *et. al* found for the coverage due to the adsorption;²²

$$\theta_{Cs,a} = (1-\alpha) \frac{\{P(E_i, \theta_{Cs}) + \eta_{Cs}(\theta_{Cs})[1-P(E_i, \theta_{Cs})]\} \Phi_{Cs}}{\{1-\eta_{Cs}(\theta_{Cs})\} \{\Gamma_{Cs-Cs}(E_i, \theta_{Cs})\Phi_{Cs} + \Gamma_{H-Cs}(E_i, \theta_{Cs})\Phi_H\}} \quad [4.8]$$

where α is the implanted fraction, E_i is the incident energy, $P(E_i, \theta_{Cs})$ is the trapping probability for cesium ions and $\eta_{Cs}(\theta_{Cs})$ is the ionization degree of the sputtered cesium particles as a function of the surface coverage. $\Gamma_{Cs-Cs}(E_i, \theta_{Cs})$ and $\Gamma_{H-Cs}(E_i, \theta_{Cs})$ are the sputter coefficients, respectively for incident cesium and hydrogen ions on an adsorbed cesium layer on tungsten.

So far we did not discuss the consequences of the cesium ions that are implanted into the tungsten surface. Tompa, Carr and Seidl set up a model to calculate the equilibrium coverage due to implantation.²³ Their model is based upon a differential equation analogous to Eq. [4.6]. The only difference is that they accounted for the effect that implanted cesium particles in the tungsten bulk result

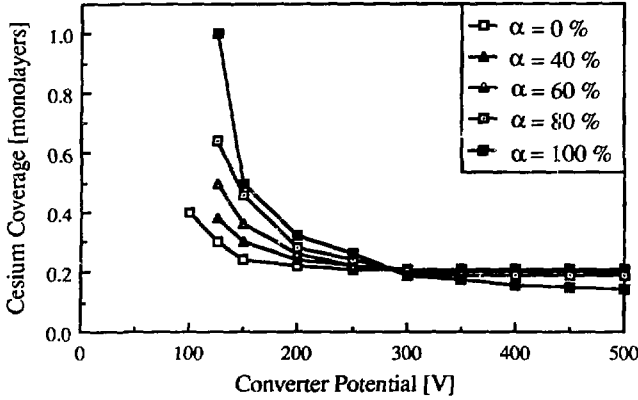


Fig. 4.4 The calculated cesium coverage of the converter surface as a function of the converter potential for various implantation fractions.

in a rearrangement of the tungsten. For hydrogen as incident particles, this effect can be neglected. In their model we defined the incoming flux as $\Phi_{in} = \Phi_H + \alpha \Phi_{Cs}$. For the cesium coverage, only the sputtering of the target material by hydrogen ions is relevant, implantation of hydrogen into the tungsten surface is not described. If diffusion is neglected, the result of this model is the following analytical expression

$$\theta_{Cs,i} = \frac{\kappa \alpha}{(\Gamma_{Cs-w}(E_i) + \beta \Gamma_{H-w}(E_i))} \quad [4.9]$$

where κ can be calculated from the measurements of Tompa *et al.* and $\Gamma_{Cs-w}(E_i)$ and $\Gamma_{H-w}(E_i)$ are the sputter coefficients for incident cesium and hydrogen ions on tungsten, respectively.²⁴ The factor β is defined by $\Phi_H = \beta \Phi_{Cs}$. This gives an additional term in the time independent solution of the rate equation. The resulting coverage can be written as the following implicit equation,

$$\theta_{Cs} = (1-\alpha) \frac{\{P(E_i, \theta_{Cs}) + \eta_{Cs}(\theta_{Cs})[1-P(E_i, \theta_{Cs})]\} \Phi_{Cs}}{\{1-\eta_{Cs}(\theta_{Cs})\} \{\Gamma_{Cs-Cs}(E_i, \theta_{Cs})\Phi_{Cs} + \Gamma_{H-Cs}(E_i, \theta_{Cs})\Phi_H\}} + \frac{\kappa \alpha}{(\Gamma_{Cs-w}(E_i) + \beta \Gamma_{H-w}(E_i))} \quad [4.10]$$

This equation can be written as a term which describes the coverage as a result of the adsorption process $\theta_{Cs,a}$ and a term which describes the coverage as a result of the implantation process $\theta_{Cs,i}$

$$\theta_{Cs} = (1-\alpha) \theta_{Cs,a} + \alpha \theta_{Cs,i} \quad [4.11]$$

The implantation fraction α determines which of the two processes, adsorption or implantation, is dominant. In the following we will present numerical solutions of this equation.

The incoming positive ions reach the converter with an energy E_i , which is proportional to the converter potential V_c minus the plasma potential V_p ,

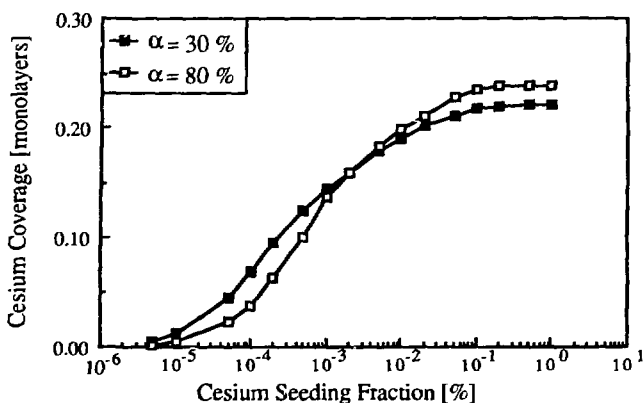


Fig. 4.5 The calculated cesium coverage of the converter surface as a function of different cesium seeding fractions for a converter potential of -150 V.

$E_i = e |V_c - V_p|$ eV. For our hydrogen discharge the plasma potential amounts roughly -50 V. In Fig. 4.4 the calculated cesium coverage is shown as a function of the converter potential for various implantation fractions α . The cesium ion contribution to the total ion current on the converter, $\Phi_{Cs}/(\Phi_{Cs} + \Phi_H)$, is taken equal to 1 %. For $\alpha = 100\%$ the curve agrees with the measurements of Tompa *et al.* For $\alpha = 0$ the curve coincides with the calculations of van Amersfoort *et al.* From TRIM calculations we derived an implantation fraction of around 80 % for the energy range 30-300 eV. Note that the implantation fraction is constant over this energy range. Using the known relation between cesium coverage and work function we observe a minimum in the work function for a converter potential of the order of -130 V for an implantation fraction of 80 %. Van Wunnik *et al.* showed that a lower work function results in a higher H^- ion yield.¹⁹ The existence of a maximum in the extracted H^- current as a function of the converter potential has been observed in various sources employing a vapor injection scheme.^{3,4} In Fig. 4.5, the coverage is plotted for different cesium fractions in the discharge for a typical converter potential of -250 V. For low fractions we see an increase of the coverage with increasing fractions and for higher fractions the coverage saturates. From this figure we may conclude that it is not useful to "overdose" the discharge with cesium to obtain a higher coverage.

4.3.b. Porous tungsten converter with liquid cesium supply

In view of the considerations and calculations shown above, a cesium coverage independent of the converter potential cannot be obtained using a cesium vapor deposition method. From the calculations it is clear that the only method of increasing the coverage is to increase the flux of neutral cesium atoms towards the surface. The method we choose to increase this flux is to use liquid cesium diffusing through a porous converter.

The converter is made from sintered tungsten with a porosity of 20%. Behind

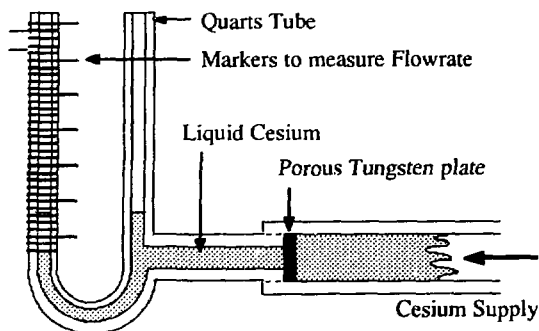


Fig. 4.6 The quartz-tube used to measure the flowrate of cesium through a porous tungsten disk. The entire set-up is heated to 100 °C.

the porous tungsten plate is a reservoir with liquid cesium which can diffuse through the plate. The reservoir can be pressurized with argon gas. In order to check whether this method is feasible we set-up a small experiment as depicted in Fig. 4.6. It consists of a quartz flow tube in which a porous disk with a thickness of 1 mm. is mounted and a vertical quartz flow tube to measure the flow of cesium through the disk. The whole system is mounted into a vacuum vessel and evacuated to 10^{-7} Torr. After heating of the entire system to about 100 °C, liquid cesium is admitted from the right side of the quartz tube and pressurized to force it through the porous disk. Under these conditions a flow rate of the order of 10^{18} atoms $\text{cm}^{-2} \text{s}^{-1}$ was measured. The latter is more than three orders higher than the rate with which cesium is removed from the surface via sputtering.

It appeared in running the source with this converter that after saturating the porous tungsten with cesium it was not necessary to pressurize the reservoir to maintain the cesium coverage. Apparently, the concentration gradients at the surface are sufficiently large to replenish all cesium which is removed via sputtering. Even after seeding the discharge with heavy ions like xenon or argon, no depletion of the surface coverage was observed. The latter could be checked experimentally by applying pressure to the reservoir and thus enhancing the cesium flow towards the surface. If the surface coverage would have been depleted it would instantly be replenished and one should be able to see an effect in the extracted negative ion current. Since, reducing the coverage in the range between a full monolayer and a half monolayer, lowers the work function which enhances the ionization probability and therefore the negative ion yield.

4.4. Experimental results

With the magnetic analyzer, described in detail in Ref.13, the energy and mass spectra of the self extracted negative ion beam have been measured. From the energy distribution in Fig. 4.7 it is found that most of the detected particles are produced via sputtering from the converter surface, since the peak energy amounts roughly $|V_c - V_{\text{extr}}|$ eV. For negative ions produced via reflection an energy of $|2V_c - V_p - V_{\text{extr}}|$ eV is expected, where V_{extr} denotes the (negative) bias of the detector to suppress electrons from the plasma. V_{extr} is of the order of the plasma potential V_p ,

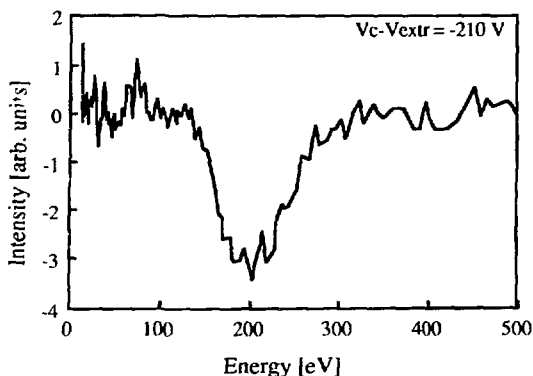


Fig. 4.7 The energy distribution of the "self-extracted" beam for a potential difference of -210 V.

which is of the order of -50 V.

In the mass distribution in Fig. 4.8 of the extracted negative ion beam only H^- ions are observed. This is expected because surface production of Cs^- ions is not very probable due to the small velocity with which Cs neutrals leave the surface. Furthermore, it is impossible to detect Cs^- ions which might be formed in the bulk plasma because no active extraction from the plasma takes place.

The position of the peak in the energy distribution as a function of the potential difference between converter and detector is shown in Fig. 4.9. The straight line denotes the energy expected for particles produced via sputtering. The error in the position of the peak is of the order of 20 %. For potential differences greater than 200 V the peak position follows the straight line indicating that in this case the production mechanism is fully dominated by sputtering. Below 200 V potential difference the peak position falls above the straight line with an increasing deviation for lower potential differences. This indicates that for these lower potential differences, the scattering of particles gives a noticeable contribution in the produced negative ion current. This can be seen in the measured energy distribution

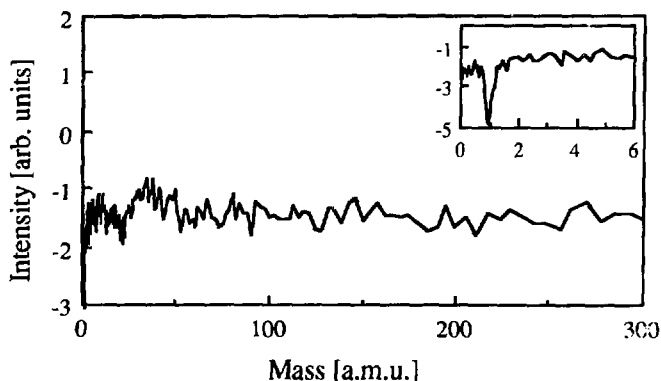


Fig. 4.8 The measured mass distribution of the "self-extracted" negative ion beam.

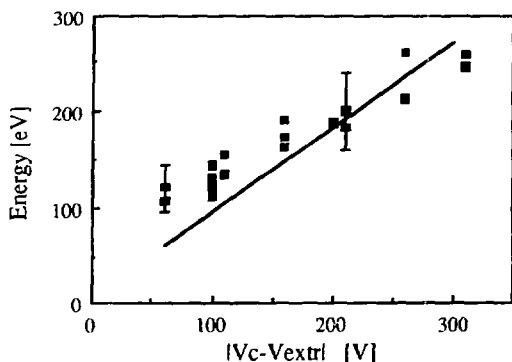


Fig. 4.9 The measured position of the peak in the energy distribution vs the potential difference between converter surface and detector.

in Fig. 4.7 where a high energy tail is present.

The measurements of the conversion efficiency (i.e. the ratio of the extracted negative ion current and the positive ion current incident on the converter surface) depicted in Fig. 4.10, as earlier reported by van Os, Granneman and van Amersfoort, show an increase at low converter potentials and a saturation at higher potentials.¹⁹ Although, the measurements taken for different arc currents are not identical, no clear dependence is seen as a function of the arc current, i.e. the positive ion current density on the converter surface. This behavior is in sharp contrast with the measurements of the conversion efficiency as a function of the arc current for a barium metal converter.¹³ The values obtained for the conversion efficiency are an order of magnitude lower than values obtained with cesium seeded discharges. Furthermore, no clear optimum is observed as a function of the converter potential, whereas in the other sources an optimum for V_c between -100 and -200 V is reported. The latter is probably related to the scheme we used to obtain a surface coverage of cesium. This coverage is independent of the discharge characteristics and the converter bias, whereas, the afore mentioned maximum in conversion efficiency was observed in sources using a cesium vapor deposition method. In section 4.3.a. we showed that with such a method the cesium coverage (i.e. the work function of the converter surface) is a function of the converter bias which accounts for the observed maximum.

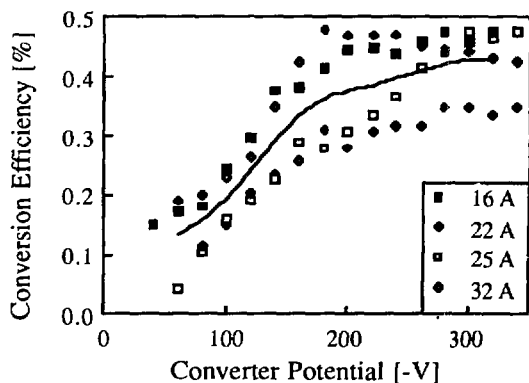


Fig. 4.10 The conversion efficiency as a function of the converter potential for various arc currents. The solid line represents the average of the conversion efficiency over the different arc currents.

4.5 Discussion

The conversion efficiency, as shown in Fig. 4.10, is independent of the arc current and therefore independent of the incoming flux. We showed in a previous report¹³ that in the case of a diffusion dominated process (e.g. barium) the conversion efficiency increases with increasing incoming flux. The diffusion coefficient for hydrogen in barium is $3 \cdot 10^{-9} \text{ m}^2 \text{ s}^{-1}$ at $T=470 \text{ K}$ ²⁵, whereas for hydrogen in tungsten it is only $10^{-15} \text{ m}^2 \text{ s}^{-1}$ ²⁶. Taking into account that our converter consists of 80% tungsten we can conclude that in the case of our cesium/tungsten converter the diffusion term in Eq.[4.6] is negligible. The resulting equation then reduces to:

$$\frac{\partial c(z,t)}{\partial t} = v_{\text{sput}} \frac{\partial c(z,t)}{\partial z} + \frac{\alpha \Phi_{\text{H}^+}}{c_{\text{sat}} d \sqrt{\pi}} \exp\left(-\left(\frac{z-r}{d}\right)^2\right) \quad [4.12]$$

The solution of [4.13], as described in the appendix, can be written as:

$$c(z,t) = \frac{\alpha \rho_w}{2c_{\text{sat}} \Gamma_{\text{H-W}}} \left(\text{erf}\left(\frac{z+v_{\text{sput}}t-r}{d}\right) - \text{erf}\left(\frac{z-r}{d}\right) \right) \quad [4.13]$$

At the surface ($z=0$) and at infinite time t this solution becomes:

$$c(0,\infty) = \frac{\alpha \rho_w}{2c_{\text{sat}} \Gamma_{\text{H-W}}} \left(1 + \text{erf}\left(\frac{r}{d}\right) \right) \approx \frac{\alpha}{\Gamma_{\text{H-W}}} \quad [4.14]$$

TRIM code simulations show that both the range, r , and deviation, d , of the implantation profile scale with the energy E [eV] of the incoming particles in the region we are working in, with an amount $r/d=1.4 E$. From Fig. 4.11, which shows the behavior of $c(z,t)$ according to Eq. [4.13] we can conclude that after a few seconds the tungsten is saturated with implanted hydrogen, which means that we can neglect the process in the bulk and only have to consider the surface processes. Furthermore, it is seen from Eq. [4.13] that in the case of a very small sputter velocity the contribution of the sputter dominated process becomes negligible and we have to take into account the diffusion term again.

Substitution of numerical values in Eq. [4.14] gives a steady state concentration near the surface of about 30 times the number density of tungsten. This is from a physical point of view rather unsatisfying. Therefore, a closer analysis has been undertaken to check whether diffusion of hydrogen in the grains of the sintered porous tungsten reduces this high concentration. In calculation this process we assumed a semi infinite cylinder (the tungsten grain) which front side is exposed to a flux of hydrogen ions. The boundary condition is chosen such that the concentration at the wall of the cylinder is zero. This is a justifiable assumption if one considers that all grains are surrounded by liquid cesium. Once a hydrogen particle diffuses into the liquid cesium it will be removed very quickly either via

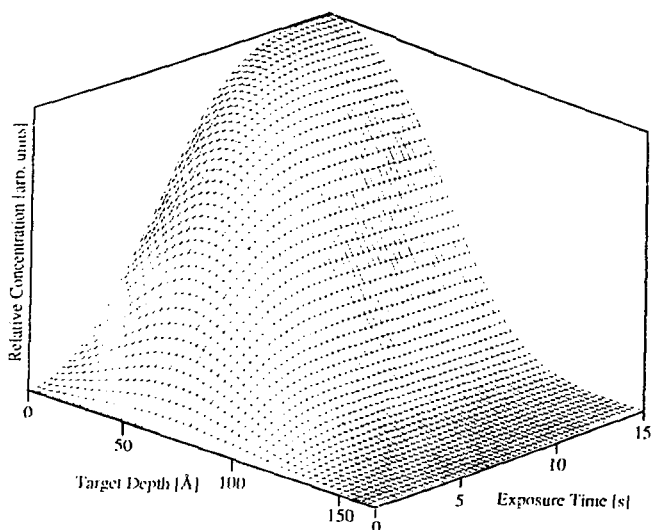


Fig. 4.11 The calculated relative hydrogen concentration as a function of place in the converter bulk and exposure time.

rapid diffusion in the liquid cesium or via diffusion along the cesium-tungsten interface.

For a cylinder diameter of $10\ \mu\text{m}$ and an incident flux of $10^{17}\ \text{cm}^{-2}$ a steady state concentration at the surface of $0.48 \times 10^{23}\ \text{cm}^{-3}$ is calculated. For a larger cylinder diameter the concentration increases and for a smaller diameter it decreases. Increasing the incident flux also increases the concentration. The average grain size in the porous tungsten is of the order of $10\ \mu\text{m}$. From this simple reasoning we see that for an incident flux of $10^{17}\ \text{cm}^{-2}$, which is equal to about $20\ \text{mA/cm}^2$ we saturate the tungsten grains with hydrogen. The incident fluxes of the experiments reported here were all above $20\ \text{mA/cm}^2$ so we may conclude that we always have a fully with hydrogen saturated converter surface.

At the surface the hydrogen is sandwiched between the cesium monolayer²⁷ and the tungsten surface, therefore we should take the sputter coefficient for incident particles on cesium rather than on hydrogen. In other words, it is assumed that the removal of one cesium atom from the surface results in the liberation of one hydrogen atom. Based on this assumption we can rewrite Eq. [4.4] using Eq. [4.2] as

$$\Phi_{\text{H}^-} = \eta_{\text{H}} \Gamma_{\text{H-Cs}} \Phi_{\text{H}^+} \quad [4.15]$$

where η_{H} is the ionization probability. With this assumption the conversion efficiency can be written as:

$$\eta_{\text{H}^+} \approx \eta_{\text{H}} \Gamma_{\text{H-Cs}} \quad [4.16]$$

The sputter coefficient can be calculated as a function of the energy of the incident

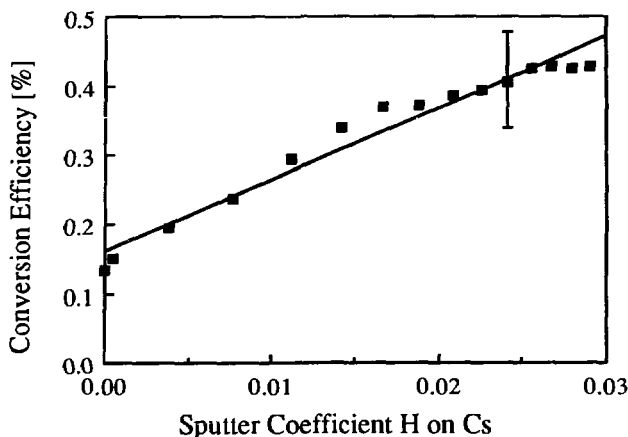


Fig. 4.12 The conversion efficiency as a function of the sputter coefficient for hydrogen on adsorbed cesium. The datapoints are averaged over the arc currents.

particles (i.e the converter potential) with the formulas of Bohdanský.²⁸ Fig. 4.12 shows the conversion efficiency as a function of the sputter coefficient for hydrogen on a full monolayer of cesium adsorbed on tungsten. From a linear regression we find for the ionization probability $\eta_H = 0.10 \pm 0.03$, which is in good agreement with model calculations based on resonant charge transfer, see Fig. 3.2, chapter 3.

The conversion efficiencies obtained with our porous cesium/tungsten converter are an order of magnitude lower (0.5 %) than those obtained with sources with a cesium vapor injection scheme (2-5 %), see table 3.2, chapter 3. In the case of cesium vapor injection there is a high Cs^+ ion density in the discharge. To investigate the role of Cs^+ ions we admitted a rare gas (Xe or Ar) to the discharge to simulate the sputtering effect of the Cs^+ ions. Van Os and van Amersfoort²⁹ did such an experiment which showed an increase of an order of magnitude of the conversion efficiency with increasing heavy ion flux as depicted in Fig. 4.13. We can understand this by examining the sputter coefficient for Ar^+ and Xe^+ on

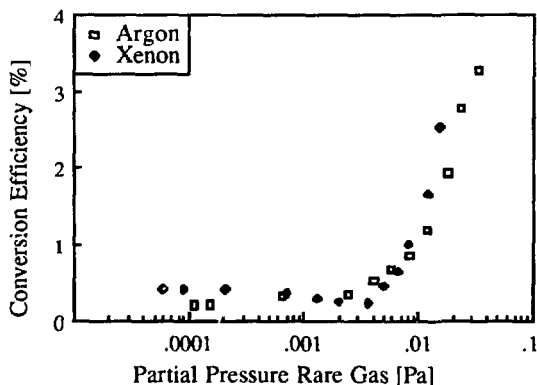


Fig. 4.13 The measured conversion efficiency as a function of the partial Ar and Xe pressure admitted into the discharge vessel.

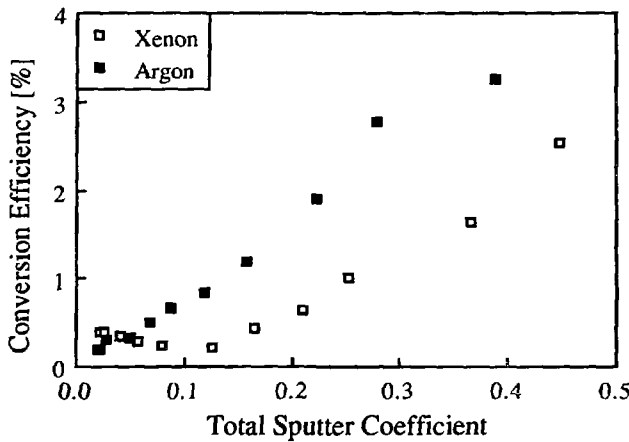


Fig. 4.14 The conversion efficiency as a function of the total sputter coefficient for a xenon or argon seeded hydrogen discharge.

cesium/tungsten, which is a factor of 100 larger than for H^+ on cesium/tungsten. Fig. 4.14 shows the dependence of the conversion efficiency on the total sputter coefficient Γ_{tot} ,

$$\Gamma_{tot} = f_{rare} \Gamma_{rare-Cs} + f_H \Gamma_{H-Cs} \quad [4.17]$$

where f_{rare} and f_H are the abundances of rare gas and H^+ ions respectively, with $f_{rare}+f_H=1$. Assuming again that every sputtered cesium atom results in one sputtered hydrogen atom and plotting the conversion efficiency as a function of the sputter coefficient in a similar way as described above only using now the total sputter coefficient instead of the sputter coefficient of hydrogen on cesium we arrive at an ionization probability of $\eta_H = 0.09 \pm 0.01$ (see Fig. 4.14). This value is consistent with the earlier determined value and in good agreement with the calculated ionization probability according to Fig. 3.2, chapter 3.

4.6. Conclusions

Summarizing, the values obtained from our surface conversion source for the ionization probability for the resonant formation of a negative hydrogen ion agree well with earlier model calculations on resonant charge exchange and experiments done in a UHV experiment. The only assumption used in obtaining the ionization probability is that each cesium atom sputtered from the surface results in the release of one hydrogen atom. This assumption seems reasonable if one considers that the hydrogen at the surface is sandwiched between the cesium adlayer and the tungsten surface. That the majority of the negative ions collected in our detector is produced via sputtering is confirmed by measurements of the energy of the negative ions. It appeared that at the surface these particles have an energy of the order of a few tenths of an eV which means that they are produced via a combination of sputtering and recoiling and not via direct backscattering.

Model calculations of the cesium household for a solid converter immersed in a

cesium seeded discharge show that the cesium coverage of the converter is a strong function of the converter bias. The set-up we used, a porous tungsten converter with liquid cesium diffusing through it, always has a full monolayer coverage of cesium due to the efficient replenishing of the sputtered cesium. Moreover, this arrangement results in a low cesium content of the hydrogen discharge which enabled us to study the effect of heavy ion sputtering in the negative ion production mechanism.

Model calculations on the hydrogen household of the converter show that the surface layers are saturated with hydrogen due to the very low diffusion coefficient of hydrogen in tungsten. The hydrogen located near the surface can only be liberated via removal of tungsten from the surface by means of sputtering. In this case we call the negative ion formation process *sputter dominated*. This is in contrast with experiments done with a barium converter, due to the high diffusion coefficient for hydrogen in barium no saturation occurs, this regime is *diffusion dominated*. In the latter case, the conversion efficiency is an almost linear function of the incident positive hydrogen ion flux on the surface, whereas for a cesium/tungsten converter no such increase is observed.

Acknowledgements

The authors gratefully acknowledge H.J. Timmer for his technical assistance during the experiments and R.M.A. Heeren for his help in the calculations of the cesium coverage. This work is part of the research program of the association agreement between the Stichting voor Fundamenteel Onderzoek der Materie (FOM) and EURATOM, and was made possible by financial support from the Nederlandse Organisatie voor Wetenschappelijk Onderzoek (NWO) and EURATOM.

Appendix 4.1

Here we will solve the equation as formulated by Eq. [13]. Our problem is defined as

$$\frac{\partial c(z,t)}{\partial t} = v_{\text{sput}} \frac{\partial c(z,t)}{\partial z} + K \exp\left(-\left(\frac{z-r}{d}\right)^2\right) \quad \text{with} \quad K = \frac{\alpha \Phi_{H^+}}{c_{\text{sat}} d \sqrt{\pi}} \quad [4.A1]$$

With $z, t \geq 0$. The surface is at $z=0$, $z>0$ is into the bulk. The initial condition is $c(z,0)=0$, the boundary condition is $c(\infty,t)=0$. Using the method of characteristic equations we find

$$-v_{\text{sput}} \partial t = \partial z \Rightarrow v_{\text{sput}} t + z = \gamma \quad [4.A2]$$

$$K \exp\left(-\left(\frac{z-r}{d}\right)^2\right) \partial z = -v_{\text{sput}} \partial c \Rightarrow c + K' \operatorname{erf}\left(\frac{z-r}{d}\right) = \beta. \quad [4.A3]$$

Where,

$$K' = \frac{K d \sqrt{\pi}}{2 v_{\text{sput}}} = \frac{\alpha \rho_w}{2 c_{\text{sat}} \Gamma_{H-W}} \quad \text{and} \quad v_{\text{sput}} = \frac{\Gamma_{H-W} \phi_{H^+}}{\rho_w} \quad [4.A4]$$

Setting $\beta = f(\gamma)$ we find:

$$c + K' \operatorname{erf} \left(\frac{z-r}{d} \right) = f(v_{\text{sput}}t + z) . \quad [4.A5]$$

The initial condition then gives:

$$f(z) = K' \operatorname{erf} \left(\frac{z-r}{d} \right) \quad [4.A6]$$

and therefore, with argument $v_{\text{sput}}t + z$ instead of z in Eq.[4.A6], we find finally:

$$c(z,t) = \frac{\alpha \rho_w}{2c_{\text{sat}} \Gamma_{\text{H-W}}} \left(\operatorname{erf} \left(\frac{z+v_{\text{sput}}t-r}{d} \right) - \operatorname{erf} \left(\frac{z-r}{d} \right) \right) \quad [4.A7]$$

The concentration is determined except for a single constant. However at $z=\infty$ Eq.[4.A7] already gives $c(\infty,t) = 0$ (boundary condition), which means this constant is zero.

References

- 1 K.H. Berkner, R.V. Pyle and J.W. Stearn, Nucl. Fusion **15** (1980) 1346.
- 2 Yu.I. Belchenko, G.I. Dimov and V.G. Dudnikov, Nucl. Fusion **14** (1974) 113.
- 3 E.J. Britt, J.L. Desplat, M. Korrington and K.N. Leung, J. Vac. Sci. Technol. A **3** (1985) 1241.
- 4 A.I. Hershcovitch, V.J. Kovarik and K. Prelec, Rev. Sci. Instrum. **57** (1986) 827.
- 5 J. Kwan, G.D. Ackerman, O.A. Anderson, C.F. Chan, W.S. Cooper, G.J. deVries, A.F. Lietzke, L. Soroka and W.F. Steele, Rev. Sci. Instrum. **57** (1986) 831.
- 6 B. Piosczyk and G. Dammertz, Rev. Sci. Instrum. **57** (1986) 840.
- 7 J.L. Desplat and C.A. Papageorgopoulos, Surf. Sci. **92** (1980) 97.
- 8 K.N. Leung and K.W. Ehlers, Rev. Sci. Instrum. **53** (1982) 803.
- 9 K.N. Leung and K.W. Ehlers, J. Appl. Phys. **52** (1981) 3902.
- 10 P.J.M. van Bommel, K.N. Leung and K.W. Ehlers, J. Appl. Phys. **56** (1984) 751.
- 11 Yu.I. Belchenko and A.S. Kupriyanov, Revue Phys. Appl. **23** (1988) 1885.
- 12 M. Wada, R.V. Pyle and J.W. Stearns, *Proc. of the 3rd Int. Symp. on Production and Neutralization of Negative Ions and Beams*, Upton, NY, 1983, AIP Conf. Proc. **111**, p247.
- 13 C.F.A. van Os, P.W. van Amersfoort and J. Los, J. Appl. Phys. **64** (1988) 3863.
- 14 J.P. Biersack and W. Eckstein, Appl. Phys. (Berlin) A **34** (1984) 73.
- 15 M.S. Huq, L.D. Doverspike and R.L. Champion, Phys. Rev. A **27** (1983) 2831.
- 16 J.S. Risley and R. Geballe, Phys. Rev. A **9** (1974) 2485.
- 17 R. Gomer and L.W. Swanson, J. Chem. Phys. **38** (1963) 1613.
- 18 J.J.C. Geerlings, P.W. van Amersfoort, L.F.Tz. Kwakman, E.H.A. Granneman, J. Los and J.P. Gauyacq, Surf. Sci. **157** (1985) 151.
- 19 J.N.M. van Wunnik, J.J.C. Geerlings, E.H.A. Granneman and J. Los, Surf. Sci. **131** (1983) 17.
- 20 P.W. van Amersfoort, J.J.C. Geerlings, R. Rodink, E.H.A. Granneman and J. Los, J. Appl. Phys. **59** (1986) 241.
- 21 C.F.A. van Os, E.H.A. Granneman and P.W. van Amersfoort, J. Appl. Phys. **64** (1987) 5000.
- 22 P.W. van Amersfoort, Ying Chun Tong and E.H.A. Granneman, J. Appl. Phys. **58** (1985) 2317.
- 23 C.S. Tompa, W.E. Carr and M. Seidl, Appl. Phys. Lett. **48** (1986) 1048.
- 24 C.S. Tompa, W.E. Carr and M. Seidl, Appl. Phys. Lett. **49** (1986) 1511.
- 25 D.T. Peterson and C.C. Hammerberg, J. Less-Common Metals **16** (1968) 457.

- ²⁶ *Diffusion and Defect Data* **9** (1974) 244.
- ²⁷ C.A. Papageorgopoulos and J.M. Chen, *Surf. Sci.* **39** (1973) 283.
- ²⁸ J. Bohdanský, *Nucl. Instr.&Meth. in Phys. Res. E2* (1984) 587.
- ²⁹ C.F.A. van Os and P.W. van Amersfoort, *Appl. Phys. Lett.* **50** (1987) 662.

TRANSPORT OF NEGATIVE IONS THROUGH A BUCKET SOURCE

An experimental study on the production of negative ions at a pure barium surface mounted in a multicusp bucket source is presented. The conversion efficiency, i.e. the ratio of the extracted negative ion current and the positive ion current incident on the surface, for deuterium and for hydrogen have been measured as a function of source pressure, converter bias and distance between conversion surface and extraction aperture. The conversion efficiency for deuterium is somewhat larger when compared to hydrogen. The conversion efficiencies obtained agree with a model taking into account the concentration of hydrogen in the barium surface layers. The cross sections which were measured for the stripping of negative ions by neutral gas agreed well with values from literature. The experimentally determined divergence of the surface produced beam was 4.5° for hydrogen and 3.6° for deuterium at an energy of 100 eV. At a source pressure of 5 mTorr, the volume produced negative ion current could be enhanced by 10 %, for 1 mTorr this enhancement was of the order of 25 %.

5.1. Introduction

For the next generation of fusion devices, it is necessary to develop a negative-ion based neutral beam injector for effective plasma heating and current drive.^{1,2} Negative ion currents of the order of 100 A with an energy of at least 500 keV are needed for this purpose.³ At the high energy required, the neutralization probability for D_3^+ is of the order of 20 percent, for D_2^+ 10 percent and less than 2 percent for D^+ ions. However, for negative ions the neutralization probability is as high as 60 percent for a gas target which makes these ions essential for neutral beam production.

At present, two methods to obtain large currents of negative ions are extensively studied; volume production and surface conversion. The first process is studied in magnetically filtered multicusp sources.^{4,5,6,7,8} The magnetic filter is used to separate the plasma production region (driver region) with a high electron temperature, and the extraction region with a low electron temperature. The negative ions are extracted from the latter region. The production mechanism is believed to be a two step process: firstly the generation of highly vibrationally excited hydrogen molecules followed by dissociative attachment with slow electrons in the extraction region.

The second process is studied in basically two different experimental configurations. The first method is mounting a surface (the converter) in a multicusp source and running the source with a cesium seeded discharge.^{9,10} The other approach is to use a hollow cathode arc to produce a highly ionized plasma which is brought into contact with a surface.^{11,12,13} Both methods employ a tungsten or molybdenum surface covered by cesium to lower the work function and thereby enhance the negative ion yield.¹⁴ Recently, experiments on scattering a proton beam

from a barium surface under UHV conditions showed it to be a good candidate to replace the conventional cesium covered surfaces.¹⁵ Application of a pure barium metal converter in a surface conversion source, which uses an hollow cathode arc discharge, proved to be quite successful.¹⁶ The conversion efficiency (i.e. the ratio between the extracted negative ion current and the positive ion current incident on the converter surface) for a barium converter was of the same order as conversion efficiencies obtained with more conventional cesium covered converters.

This paper deals with the use of a barium converter in an magnetically filtered multicusp volume source. The primary goal of the experiments was to expose the converter to a high incident flux of positive ions to verify the theoretical diffusion model set-up at the FOM institute in Amsterdam.¹⁷ Some of the details of this model are presented in the next section. A second area studied was the transport of the surface produced negative ions through the source into the movable accelerator. Finally, this paper describes the enhancement of the total extracted negative ion current by the combination of volume- and surface production at low source pressures.

5.2. Theoretical considerations regarding surface ionization

Generally, a surface conversion source consist of two components, a plasma source and a metal electrode, the so-called converter, which is brought into contact with the plasma. The converter is usually biased at a negative potential of the order of a few hundreds of volts which extracts positive ions from the surrounding plasma. This incident positive ion current can be converted into a negative one via surface conversion. The production of these ions is dominated by the following two processes. Firstly, the conversion of a hydrogen atom moving away from the barium surface into a negative ion and secondly the production of the flux of hydrogen atoms moving away from the surface.

The first process is called resonant charge exchange and has been widely studied, theoretically¹⁸ as well as experimentally¹⁹, for a molybdenum or tungsten surface covered with half a monolayer of cesium. Only recently, theoretical and experimental work on resonant charge exchange with a barium surface has been carried out.¹⁶ In the following section we will briefly explain the important parameters of the resonant charge exchange.

The second process, the mechanism responsible for the flux of hydrogen atoms leaving the surface has recently been modeled in terms of implantation, sputtering and diffusion of hydrogen into barium.¹⁷ A brief summary of the model will be given in the last part of this section and the importance of the time-scale of the experiments will be explained.

5.2.a. Resonant charge exchange (RCE)

As mentioned before, the converter surface is exposed to a flux of positive ions from the surrounding plasma. In the vicinity of the surface, these ions are effectively neutralized, probably via resonant neutralization into an excited state, followed by Auger deexcitation to the ground state. Since, these atoms have an energy of the order of a few hundred eV, most of them will be implanted into the

surface. According to TRIM (TRansport of Ions in Matter) calculations, about 84 % will be implanted.²⁰ However, the incoming particle may sputter an already adsorbed atom from the surface. These atoms combined with the directly backscattered atoms may become negatively charged via resonant charge exchange.

Close to the surface, the affinity level of the hydrogen atom is shifted downwards due to the attractive interaction with its image in the metal. At these distances the affinity level is below the work function of the metal, i.e. the level is resonant with the metal conduction band. This means that electrons can tunnel between the metal conduction band and the broadened affinity level. Important parameters are the electronic characteristics of the surface, the work function, the Fermi energy and the atomic affinity level. All three parameters depend on the species used. For barium the work function is 2.5 eV and the Fermi energy is 3.65 eV, the affinity level for hydrogen and deuterium is 0.75 eV. If the atoms move adiabatically away from the surface, the probability that a stable negative ion is formed is zero. However for higher velocities, this probability is non zero. Therefore, another important quantity is the velocity (or energy) with which the atom leaves the surface. In the low energy range we expect an increase of the ionization probability with energy. Model calculations showed an ionization probability of 15 % for an energy of 200 eV.¹⁵

5.2.b. Implantation, sputtering and diffusion at the converter surface

The converter surface is exposed to a flux of positive hydrogen ions, which arrive at the surface with an energy of the order of a few hundred eV. Most of these ions will be implanted. Due to the high diffusion rate of hydrogen in barium ($D = 3 \times 10^{-5} \text{ cm}^2/\text{s}$ at 200 °C), the implanted particles will be transported into the bulk of the barium. After some time, a quasi stationary situation evolves where the flux of implanted particles into the surface is equal to the sum of the flux of desorbing hydrogen molecules from the surface and the flux of sputtered hydrogen atoms from the surface. The latter two fluxes depend strongly on the concentration of hydrogen atoms in the first layers of the barium surface. The model set-up to describe the process of reaching this quasi stationary situation resulted in a better understanding of the experimental results obtained with a surface conversion source at the FOM institute.¹⁷ The most important quantity which can be calculated with this model is the flux of sputtered hydrogen atoms from the surface.

The dependences that were found and which are of interest for the present work are (i) the time to reach a quasi stationary situation is of the order of ten minutes, independent of the incoming flux, and (ii) increasing the flux of incoming positive hydrogen ions onto the surface gives a stronger than linear increase of the sputtered flux due to the increase in the concentration of hydrogen in the barium. Both effects are depicted in Fig. 3.13, chapter 3, which is taken from Ref. 17. In this figure, the relative hydrogen concentration is plotted as a function of the time the barium surface is exposed to the hydrogen flux for various values of this incoming flux. Since, the Culham set-up consists of a source pulsed on for three seconds it is important to realize the effect of a short exposure time of the converter to positive

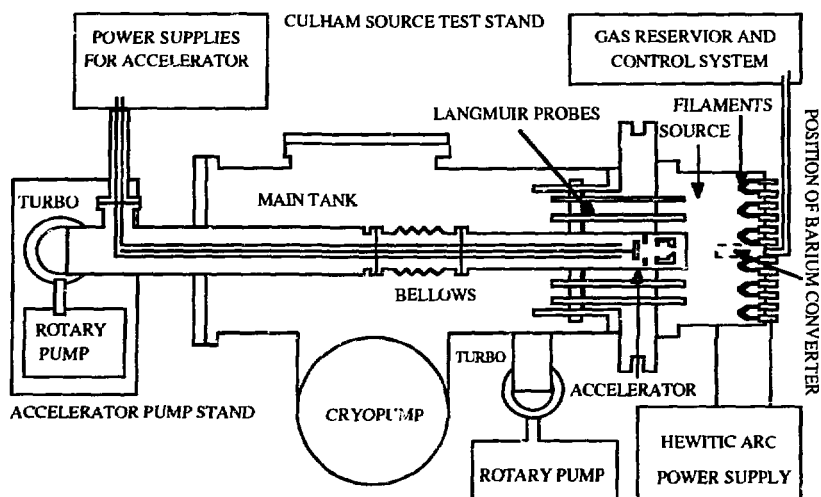


Fig. 5.1 The source test stand, shown as a sectional schematic, at Culham laboratory. The accelerator and 16 Langmuir probes can be moved into the source. The supporting vessel is cryo pumped. The accelerator itself is separately pumped with a turbo pump down to 10^{-6} Torr. The Hewitic arc supply is capable of producing currents up to 1500 A for a pulse length of 3 seconds. The dimensions of the P. I. N. I. source are roughly $60 \times 30 \times 20 \text{ cm}^3$.

hydrogen ions. In this short time no quasi stationary situation evolves, thus the concentration of hydrogen is lower which results in a lower sputtered flux and therefore a smaller negative ion yield. Note that it was not possible to run the Culham source test stand in a DC-mode to obtain a stationary situation.

5.3. Experimental arrangement

The experimental source test stand at Culham has been modified for the investigation of surface conversion. The first part of this section covers the existing experimental apparatus used for research on the volume production of negative ions from a P.I.N.I. (Plug In Neutral Injector) bucket plasma source. The second part deals with the modifications of the P.I.N.I.-source and a description of the converter module.

5.3.a. The Culham source test stand

The experimental source test stand is shown as a sectional schematic in Fig. 5.1. The power supplies associated with the test stand are capable of operating a bucket type source at arc currents of up to 1500 A for pulses of three seconds or less duration. The source itself is a standard P.I.N.I. ion source as used for positive ion production, with certain of the wall mounted permanent magnets, which are normally used to enhance the plasma confinement, reorientated to provide a magnetic filter field.

The filter field effectively divides the source into two regions, a dense plasma

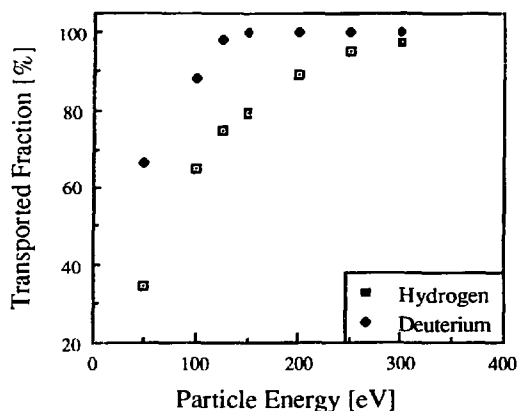


Fig. 5.2 Results of trajectory calculations for the accelerator. Shown is the transported fraction of the negative ion beam as a function of its energy for hydrogen and for deuterium.

with high electron temperature in the region containing the filaments and a less dense plasma with lower electron temperature in the region adjacent to the extraction plane.

The accelerator and the 16 Langmuir probes depicted in Fig. 5.1 can be moved into the source in order to measure the homogeneity of the produced plasma not only in a plane parallel to the extraction plane, but also perpendicular to this plane. The extraction aperture used was 3 mm in diameter. This feature enabled us to study the divergence of the surface produced negative ion beam.

The accelerator employed in the source test stand is designed for the acceleration and transport of energetic negative ions of the order of a few kV's. It basically consists of three grids equipped with magnets to reduce the extracted electron current. The magnetic fields present in this accelerator influence the trajectories of the "self-extracted" negative ions coming from the surface since they have energies of the order of only a few hundred eV. Therefore, trajectory calculations on the transport of these particles through the accelerator are necessary to calculate the truncation of the incident beam. The NEGTRACE code, developed at Culham Laboratory, has been used for this calculation. Fig. 5.2 shows the calculated transported fractions as a function of the particle energy. Note, that especially a hydrogen ion beam with an energy below 150 eV is strongly attenuated. All experimental results collected in the next section have been corrected for the transport properties of the accelerator.

5.3.b. The barium converter

The converter was designed and constructed at the FOM institute in Amsterdam. The design criteria were; (i) the size of the total assembly should be very small compared to the total bucket volume to minimise the disturbance to the plasma, (ii) it should not be possible to cover the converter surface with tungsten evaporated from the filaments and (iii) the converter should be capable of dissipating at least 400 Watt/cm².

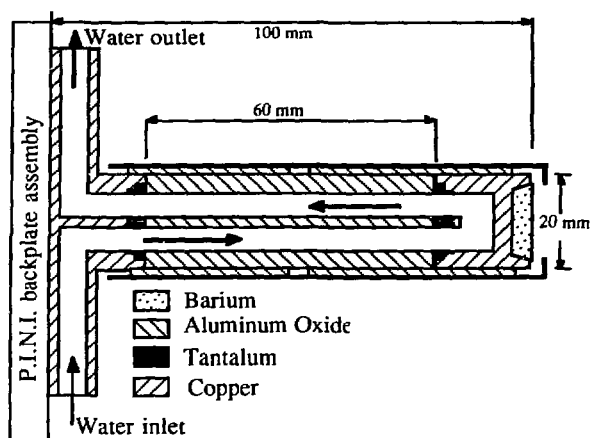


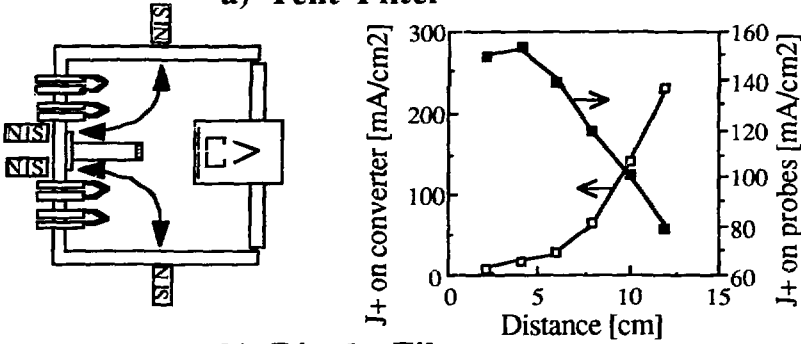
Fig. 5.3 The schematic set-up of the barium converter module. The whole system is water cooled and all insulating surfaces are protected by tantalum shieldings. The total area of the barium surface is of the order of 3 cm^2 .

The final assembly is shown schematically in Fig. 5.3. The whole system is mounted from the backplate of the P.I.N.I. source using the cooling tubes as a support. The cooling tubes are fed through the mounting holes of the middle two filaments, which had to be removed. In fact four of the 24 filaments were removed to maintain a symmetric configuration. The total surface area of the converter is about 3 cm^2 and only this surface is biased. All insulators are shielded with tantalum foil to prevent damage. A thermocouple is situated approximately 1.5 mm below the barium surface to monitor its temperature. The barium surface itself is produced by milling a reservoir in a copper substrate and filling it with liquid barium to obtain the desired good heat contact. After cooling the surface is flattened and polished to a grainsize of $10 \mu\text{m}$. The barium surface is cleaned *in situ* by bombarding the surface with argon ions, directly extracted from a pure argon plasma.

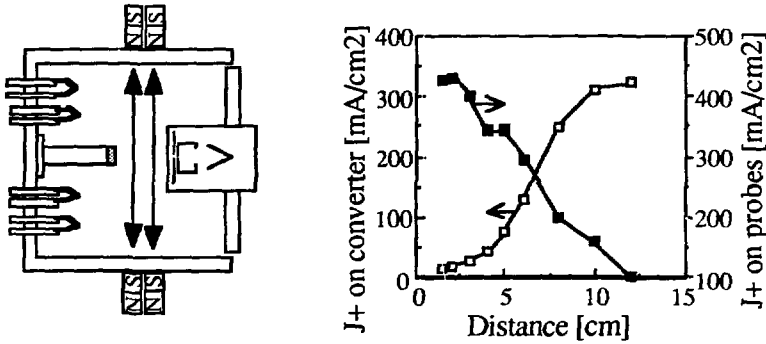
5.4. Experimental results

This section is divided into four parts. The first part deals with the extraction of the positive ion current onto the surface as a function of accelerator converter-surface distance for various magnetic filter geometries. The second part deals with the actual conversion taking place at the surface and the third part describes measurements on the transport of locally, at the barium converter surface, produced negative ions through the P.I.N.I. source to the accelerator. The last part deals with the enhancement of the extracted volume produced negative ion current when biasing the converter. We are able to separate the volume and surface produced negative ions simply by biasing the accelerator. For a non biased accelerator, only the "self-extracted" surface produced negative ions will be collected in the accelerator. When the accelerator is biased, both surface and volume produced negative ions are collected.

a) Tent Filter



b) Dipole Filter



c) Checkerboard

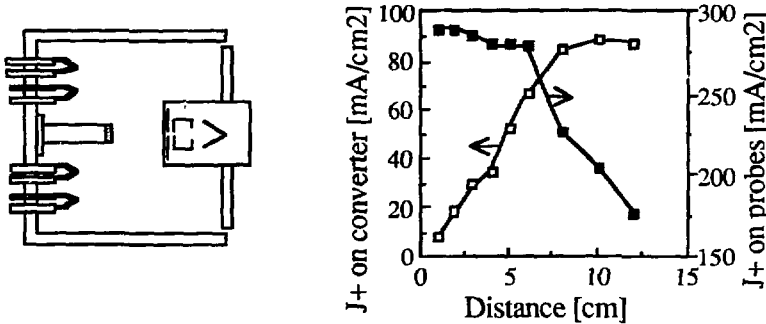


Fig. 5.4 The extracted positive ion current density on the converter and on the Langmuir probe is shown as a function of the distance between the extraction aperture of the accelerator and the converter surface for three different magnetic configurations. Note, the difference in the vertical axes. Also shown schematically are the arrangements of the magnets to obtain a) a tent filter, b) a dipole filter and c) no filter (a checkerboard). Not drawn are the magnets producing the multicusp field at the backplate and sideplates of the source.

5.4.a. Extracted positive ion current density reaching the surface

Data is presented in Fig. 5.4, for the positive ion current collected by the converter and a Langmuir probe adjacent to the accelerator as the accelerator was moved into the source. For graph a) the source was configured with a tent filter, for b) a dipole filter and for c) without a magnetic filter. For all three cases the source was operated with a filling pressure of 5 mTorr. First of all we see an increase in the positive current density measured by the Langmuir probe when moved into the source. This is consistent with measurements done without a converter located within the source body.²¹ However, for all three magnetic geometries the current to the converter decreases when the accelerator is moved inwards. In the case of a dipole filter (b) this decrease is noticeable even when the accelerator is move inwards only a few cm, whereas for an essentially field free source (c) the decrease is moderate. The difference in the obtained current density is related to the fact that with a dipole filter (b) the converter is located inside the driver region where the plasma density is large, whereas with a tent filter (a) the converter is located in the extraction region with a corresponding lower plasma density. In the filter free situation (c) the plasma is not confined very well which results in a even lower extracted current density by the converter.

For all three magnetic configurations, we measured an unexpected decrease of the positive ion current density at the converter surface as the accelerator was moved inwards. With the reversely biased accelerator, extracted positive ion current showed the same behavior with distance. So we conclude that the plasma density between the converter surface and the accelerator actually decreases with decreasing distance converter-accelerator. Only the steepness of the decrease varies with the type of magnetic filter used. The tent filter has the strongest effect and the field free source the weakest.

These results may be explained qualitatively in terms of the electric field within the plasma which causes a plasma drift towards the frontplate of the source from the backplate. The axial magnetic field has been measured experimentally and is of a significant magnitude in the filter region of a source when a dipole filter is present. As the accelerator is moved into the source it will partially "short circuit" the plasma and the requirements then exists that the same potential drop occurs across the reduced distance to the accelerator. This increased electric field would cause an increased drift of the plasma towards the accelerator thereby reducing the current of ions moving in the opposite direction towards the barium surface. In principle, the enhanced drift of plasma particles towards the accelerator (where they are neutralized), results in a depletion of the plasma density between the converter surface and the accelerator. For short distances between the converter surface and the accelerator, there would also be a geometrical shielding effect of the surface by the accelerator.

Our goal of exposing the converter surface to high current densities could therefore not be reached. However, we were able to check whether the time dependencies, which followed from the model calculations, were correct. Furthermore, studies of the transport of the surface produced negative ions through the multicusp ion source have been undertaken.

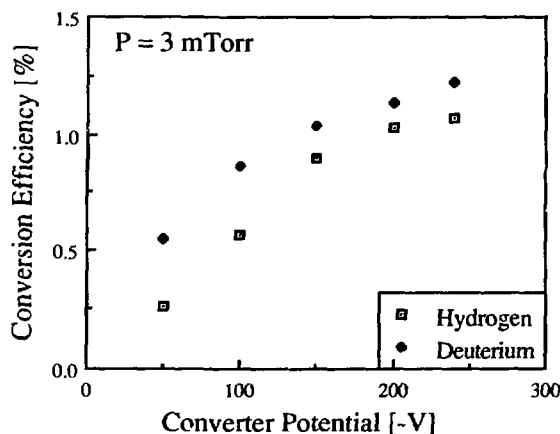


Fig. 5.5 The conversion efficiency for hydrogen and deuterium as a function of the converter potential. The distance between the converter surface and the extraction aperture is 1 cm and the filling pressure is 3 mTorr. The arc current is this case is 750 A and the arc voltage is of the order of 80 V.

5.4.b. Surface production of negative ions

At an accelerator converter-surface distance of one cm we measured the conversion efficiency as a function of the converter potential. The conversion efficiency is defined as extracted negative ion current density divided by the incident positive ion current density. Fig. 5.5. shows the result of this measurement for deuterium and for hydrogen. The pressure in the source was 3 mTorr, the arc voltage 80 V and the arc current 750 A. The pulse length was three seconds and the magnetic filter geometry used was a "tent" filter. The conversion efficiency increases with converter potential with a tendency to saturate at high potentials. From Fig. 5.5 one can see that the formation of D^- ions is somewhat more efficient compared to the formation of H^- ions.

It is of interest to compare the conversion efficiencies for hydrogen and deuterium for particles leaving the surface with the same normal velocity. In doing so one finds a difference of almost a factor of two for low velocities (≈ 100 eV/nucleon) and a factor of 1.3 for higher velocities (> 200 eV/nucleon). From scattering experiments we know that the negative ion formation probability for hydrogen is the same as for deuterium.^{22,23} Therefore, this difference must be attributed to the following; (i) the sputter coefficient for deuterium is higher than for hydrogen so the sputtered flux is larger,²⁴ and (ii) the diffusion coefficient of deuterium may be smaller than that for hydrogen which results in a higher concentration of deuterium in the barium surface layer.²⁵ Both arguments result in a larger flux of deuterium atoms leaving the surface, and since the ionization probability for hydrogen and deuterium moving with the same velocity is equal, this results in a higher conversion efficiency for deuterium compared to hydrogen.

5.4.c. Transport of surface produced negative ions

The Culham source test stand enables us to study the transport of the locally

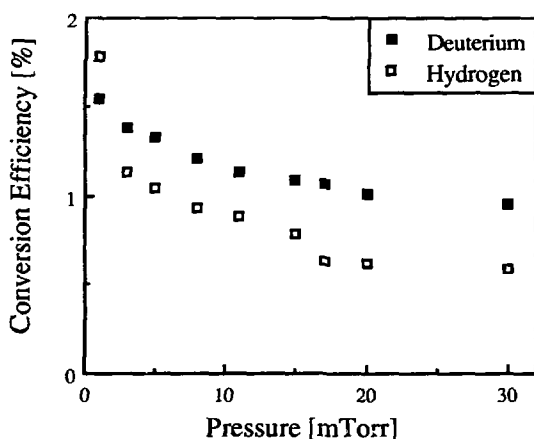


Fig. 5.6 The conversion efficiency for hydrogen and deuterium as a function of the filling pressure of the source at a fixed distance accelerator-converter of 1 cm. The positive ion current onto the converter surface is held constant over the entire pressure range. The arc current is typically 750 A and the arc voltage is of the order of 80 V. The converter potential is -240 V.

produced negative ions through the P.I.N.I. source by either varying the source gas pressure and keeping the positive ion current to the converter constant, or by varying the distance between the extraction aperture and the conversion surface.

In Fig. 5.6 we varied the gas pressure in the source and measured the conversion efficiency at an accelerator-converter separation of 1 cm. In doing this experiment we kept the positive ion current density received at the converter constant to within 10 percent. A bucket plasma has only a very low degree of ionization, typically less than a few percent, therefore, the observed decrease in conversion efficiency with gas pressure is related to "stripping" of negative ions due to collisions with the neutral gas molecules. For the measured current I ;

$$I = I_0 \exp\left(-\int_L N \sigma_n dl\right) \quad [5.1]$$

where I_0 is the negative ion current produced at the surface, N is the neutral gas density, σ_n is the cross section for neutralization of negative ions and L is the path length which the negative ions travel. The results contained in Fig. 5.6 have been obtained for a converter potential of -240 V, which means that the "self-extracted" negative ions have an energy ranging from 240 to 480 eV. The cross sections we find from the experimental data are; for hydrogen $\sigma_n = 0.9 \times 10^{-15} \text{ cm}^2$ and for deuterium $\sigma_n = 0.6 \times 10^{-15} \text{ cm}^2$. The estimated error in these cross sections is 15 percent.

Huq, Doverspike and Champion reported a cross section for the attenuation of a D^- ion beam of 200 eV in D_2 of $0.55 \times 10^{-15} \text{ cm}^2$.²⁶ For a 200 eV H^- ion beam travelling through H_2 they reported a value of $0.62 \times 10^{-15} \text{ cm}^2$. However, Risley and Geballe reported a value of $0.8 \times 10^{-15} \text{ cm}^2$.²⁷ In view of the large energy

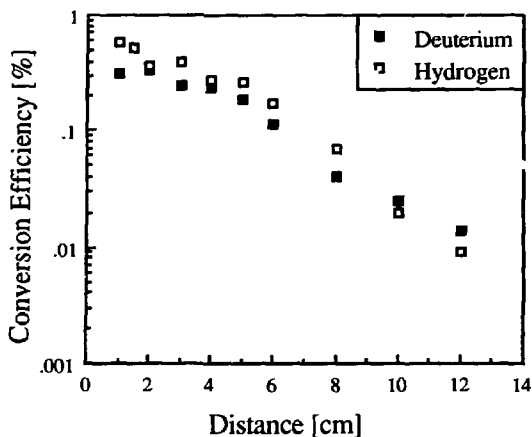


Fig. 5.7 The conversion efficiency for hydrogen and deuterium as a function of the distance between the extraction aperture and the converter surface. The converter potential is -100 V and the source filling pressure is 5 mTorr. The arc current is roughly 750 A and the arc voltage is 80 V.

spread we have for the "self-extracted" negative ion beam we can state that there is good agreement between our experimental measurements and the literature. From the measurements we confirm that attenuation due to plasma particles, e.g. positive hydrogen ions and electrons, is negligible.

In Fig. 5.7 the conversion efficiency is shown as a function of the distance between accelerator and converter for a converter potential of 100 V and a gas pressure of 5 mTorr. In order to derive the divergence of our "self-extracted" negative ion beam we have to correct the measured conversion efficiency for the following processes. First of all we took into account the attenuation of the negative ions due to the neutral gas. For deuterium we used a value for the neutralization cross section σ_n of $0.5 \times 10^{-15} \text{ cm}^2$ and for hydrogen we took a value of $0.6 \times 10^{-15} \text{ cm}^2$.^{26,27} We cannot use the afore mentioned measured neutralization cross sections since these were obtained for a converter potential of -240 V. Secondly we took into account the collection angle of the accelerator. At a given distance the collection angle of the accelerator is such that it "sees" more than just the negative ion emitting converter surface which leads to an additional reduction in the collected negative ion current. From the kink in the curves in Fig. 5.7 we derive that the distance at which this effect appears is about 5 cm. Based upon the geometry of the accelerator we arrive at a collection angle of 12.5° , which corresponds to a distance of 4.6 cm at which the afore mentioned effect becomes apparent.

Applying all corrections and assuming that we have a homogeneous beam, we arrive at a divergence of the "self-extracted" negative ion beam of 4.5° for hydrogen and 3.6° for deuterium at a converter potential of 100 V. Since we know at which point these negative ions are born and what the divergence is at that point we are able to estimate the emittance of the surface produced beam. For hydrogen

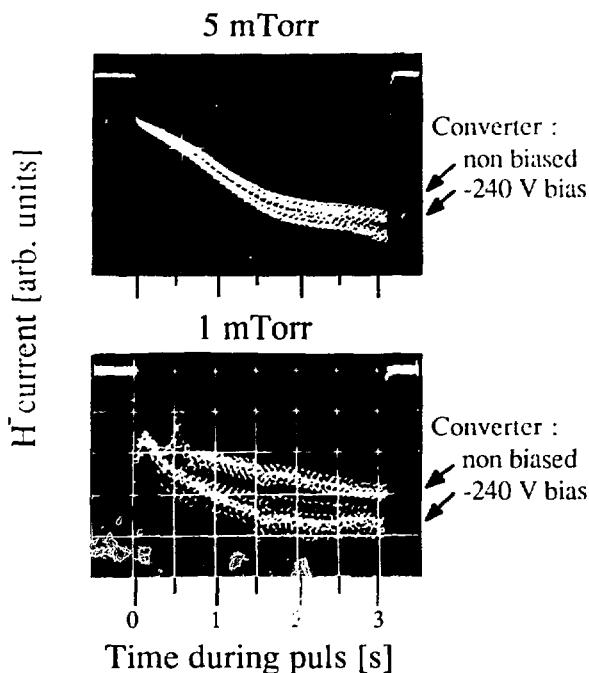


Fig. 5.8 Oscilloscope readings of the extracted negative ion current during the pulse for an acceleration potential of 10 kV. The upper traces are measured for a source filling pressure of 5 mTorr, whereas the lower traces are obtained for a source filling pressure of 1 mTorr. Both photos contain two traces, one without biasing the converter and the second with a converter bias of -240 V.

we estimate an emittance of 780π mm mrad for deuterium 620π mm mrad, both at a beam energy of 100 eV.

5.4.d. Enhancement of volume produced negative ion current

So far we have only described the results from measurements made on the surface produced negative ions. This was achieved by analysis of the "self extracted" current produced at the surface. When, however, we applied a high positive voltage to the accelerator we were also able to extract negative ions from the plasma itself. Fig. 5.8 shows two photographs taken from an oscilloscope reading of the extracted negative ion current with and without bias on the converter. For a source filling pressure of 5 mTorr we see an increase of the volume produced negative current by about 10 percent after biasing the converter. Note that during the pulse the negative ion current increases. This is due to an increase of the plasma density, caused by an increase in the arc current, which occurs because no feedback mechanism exists to reduce the filament current as the filaments are heated by the discharge. For a pressure of 1 mTorr this effect is even more pronounced; with an increase of the order of 25 percent. Both traces have been recorded with hydrogen as the filling gas and a converter bias of -240 V and 10

Table 5.1. Extracted negative ion current densities for the P. I. N. I. source with and without the converter mounted. The source filling pressure is in all cases 5 mTorr.

	Filter type	Arc current [A]	Arc voltage [V]	Current density [mA/cm ²]
Without converter:	Dipole	600	120	8.5
	Tent	600	120	3 - 7.5*
With converter:				
non biased	Dipole	750	100	5.8
biased at -240 V	Dipole	750	100	6.5

*) The numbers indicated are the lowest and highest values measured with several different tent filter geometries.

V. For completeness, we have collected some measured extracted negative ion densities with and without a converter mounted in the P. I. N. I. source in Table 5.1. It is not possible to directly compare the extracted current density for the case the barium converter is mounted and when no converter is present since the data presented in Fig. 5.4 indicates that the plasma is disturbed by the presence of the converter. No data is available on the extracted negative ion current from a P. I. N. I. source with no converter mounted for a source filling pressure of 1 mTorr.

5.5. Discussion

The time dependence of the theoretical model, set up at the FOM institute in Amsterdam, has been checked on the 3 second pulse-length test stand at the Culham Laboratory. For approximately similar converter to extractor separation, current density on the converter surface and gas pressure, we measured at Culham a conversion efficiency of 0.21 % (pressure is 3 mTorr and distance to travel 4 cm), whereas at the FOM institute, a conversion efficiency of 1.0 % was measured (pressure 0.8 mTorr and separation 11.6 cm).

The difference, almost a factor of five, can be deduced from the diffusion model calculations by taking the ratio of the hydrogen concentration at infinite time (DC operation) and the concentration after 3 seconds exposure (see Fig. 5.1). In doing so we find a factor of 4 which agrees with the measured ratio taking into account that one expects a difference due to the divergence of the beam (At Culham we took a distance of 4 cm, whereas at the FOM institute we measured at 12 cm) and due to the difference in the degree of ionization of the plasma (at Culham <3 % and at the FOM institute > 50 %).

Furthermore, the experiments at Culham show that the divergence of the surface produced negative ion beam is of the order of 4° at an energy of 100 eV, which corresponds to an emittance of the order of 700 π mm mrad. Accelerating this beam to 40 keV gives an emittance of 35 π mm mrad. This is rather large compared to a volume produced beam, which has a typical emittance of the order of 2 π mm mrad at 40 keV.

In addition, we have shown that the surface conversion process for deuterium is somewhat more efficient when compared to hydrogen. This is in contrast with the

results obtained for volume production where it is found that the extracted deuterium current is approximately a factor of one over square root two of the hydrogen current under similar conditions.

In conclusion, we have shown that by using a converter mounted in a volume production source, an enhancement of the negative ion current density can be obtained. This is advantageous for increasing the negative ion current at low source pressure. However, it should be noted that due to the significant plasma drift in the P.I.N.I. source, the positive current density reaching the converter surface was small, resulting in a small contribution of the surface produced negative ions to the total extracted negative current. The latter observation is the reason why the negative ion current density obtained with a P.I.N.I. source without a converter mounted (see Table 5.1) is higher compared to our results even with a biased converter. However, it is generally known that the volume produced negative ion current density decreases as the extraction aperture increases. For surface conversion, there is no reason to believe that this decrease also occurs. This means that a P.I.N.I. source with a biased barium converter will give a higher yield for a larger extraction aperture even compared to a P.I.N.I. source without a converter mounted. This could not be checked experimentally since no larger extraction aperture was possible. Continuation of this research into the tandem production of negative ions (a combination of volume and surface production) is, therefore, only considered worthwhile if the present low positive ion current densities reaching the surface can be increased.

Acknowledgements

The authors wish to thank D.C. Clark and G.O.R. Naylor for their help in running the source test stand, R.W.M. Loos for the construction of the converter module and Culham Laboratory for giving the necessary support and permission for doing these experiments. Furthermore, EURATOM is acknowledged for their funding of the travelling involved. The work described here was performed as part of the association agreement between the Stichting voor Fundamenteel Onderzoek der Materie (FOM) and EURATOM, with financial support from the Nederlandse Organisatie voor Wetenschappelijk Onderzoek (NWO) and EURATOM.

References

- 1 S. Yamamoto et. al., 11th Conf. on Plasma Physics and Controlled Fusion Research, Kyoto (1986).
- 2 W.S. Cooper et. al., *Proc. 12th Symposium on Fusion Engineering*, Monterey (1987) p294.
- 3 H. Horiike, Y. Ohara, Y. Okumura, T. Shibata and S. Tanaka, Japan Atomic Energy Research Report, JEARI-M 86-064 (1986).
- 4 K.N. Leung, K.W. Ehlers, C.A. Hauck, W.B. Kunkel and A.L. Lietzke, *Rev. Sci. Instrum.* **59**, 453 (1988).
- 5 A.J.T. Holmes, L. M. Lea, A.F. Newman and M.P.S. Nightingale, *Rev. Sci. Instrum.* **58**, 223 (1987).

- 6 J.R. Hiskes, Comments At. Mol. Phys. **19**, 59 (1987).
- 7 M. Bacal, A.M. Bruneteau and M. Nachman, J. Appl. Phys. **55**, 15 (1984).
- 8 Y. Okumura, Proc. 11th Symposium on ISLAT,87, Tokyo (1987) p267.
- 9 K.N. Leung and K.W. Ehlers, Rev. Sci. Instrum. **53**, 803 (1982).
- 10 J.W. Kwan, G.D. Ackerman, O.A. Anderson, C.F. Chan, W.S. Cooper, G.J. de Vries, A.F. Lietzke, L. Soroka and W.F. Steele, Rev Sci. Instrum. **57**, 831 (1986).
- 11 A.I. Hershcovitch, V.J. Kovarik and K. Prelec, Rev. Sci. Instrum. **57**, 827 (1986).
- 12 C.F.A. van Os, E.H.A. Granneman and P.W. van Amersfoort, J. Appl. Phys. **61**, 5000 (1987).
- 13 Yu.I. Belchenko and A.S. Kupriyanov, *Proc. of the 3rd European workshop on Production and Application of Light Negative Ions*, February 17-19, Amersfoort, The Netherlands, p133-140.
- 14 J.L. Desplat and C.A. Papageogopoloulos, Surf. Sci. **92**, 97 (1980).
- 15 C.F.A. van Os, H.M. van Pinxteren and J. Los, *Proc. of the 3rd European workshop on Production and Application of Light Negative Ions*, February 17-19, Amersfoort, The Netherlands, p166-169.
- 16 C.F.A. van Os, R.M.A. Heeren and P.W. van Amersfoort, Appl. Phys. Lett. **51**, 1495 (1987).
- 17 C.F.A. van Os, P.W. van Amersfoort and J. Los, Accepted for publication in J. Appl. Phys. **64**, 3863 (1988).
- 18 J.N.M. van Wunnik, J.J.C. Geerlings, E.H.A. Granneman and J.Los, Surf. Sci. **131**, 17 (1983).
- 19 J.J.C. Geerlings, P.W. van Amersfoort, L.F.Tz. Kwakman, E.H.A. Granneman, J.Los and J.P. Gauyacq, Surf.Sci. **157**, 151 (1985).
- 20 J.P. Biersack and W. Eckstein, Appl. Phys. (Berlin) **A34**, 73 (1984).
- 21 L.M. Lea, A.J.T. Holmes, G.O.R. Naylor and D.C Clark, JDC meeting march 1988, unpublished.
- 22 J.N.M. van Wunnik, J.J.C. Geerlings, E.H.A. Granneman and J. Los, Surf. Sci. **131**, 17 (1983).
- 23 J. Los, E.A. Overbosch and J. van Wunnik, *Proc. of the second International Symposium on the Production and Neutralization of Negative Hydrogen Ions and Beams*, Brookhaven, New York (1980) p23-p31.
- 24 J. Bodansky, Nucl. Instrum. Meth. in Phys. Res. **B 2**, 587 (1984).
- 25 H. Katsuta, s. Komishi and H. Yoshida, J. of Nucl. Mat. **116**, 244 (1983).
- 26 M.S. Huq, L.D. Doverspike and R.L. Champion, Phys. Rev. **A27**, 2831 (1983).
- 27 J.S. Risley and R. Geballe, Phys. Rev **A9**, 2485 (1974).

HIGH FLUX SURFACE CONVERSION AT A BARIUM SURFACE

Experiments on the production of negative hydrogen ions via surface conversion for incident positive hydrogen ion currents in the range of 0.2 to 1 A/cm² are reported. The conversion efficiency, i.e. the ratio of the produced negative ion current and the positive ion current on the converter shows a strong temperature dependence and has a maximum for a positive ion current density of about 0.5 A/cm². Due to the limited magnetic confinement of the intense hydrogen plasma, the base pressure of these experiments was of the order of 50 mTorr which resulted in very large losses of negative ions due to stripping. With correction for these losses, we obtained a conversion efficiency of the order of 8 percent which corresponds to a surface produced negative ion current density of the order of 60 mA/cm².

6.1. Introduction

The dynamic interaction of plasma particles with a metal surface is employed in various devices, among which are etch or deposition reactors for fabrication of semiconductor components or corrosion resistant coatings, and surface conversion sources. The latter devices are used to produce intense beams of negatively charged (light) ions. These serve as intermediate step in the production of intense neutral beams, which can be used for additional heating or diagnosis of fusion plasmas. The experimental data in this paper are obtained using a surface conversion source.^{1,2,3,4} In this type of device, a metal electrode (the so-called converter) is negatively biased at a potential of typically a few hundred volts with respect to the plasma. This causes plasma ions to be accelerated towards the surface, where they impinge under normal angle of incidence. At the energies involved, most of the incoming ions are implanted into the surface. At the surface, adsorbed hydrogen particles can be sputtered by incoming ions, which results in a flux leaving the surface. If the characteristics of the surface permit resonant charge exchange between the sputtered particles and the metal, then part of the sputtered beam is negatively charged. These negative ions are accelerated over the plasma sheath and subsequently "self-extracted" through an aperture.⁵

To obtain reasonable probabilities for negative ion formation, the work function of the converter surface should be small, typically below 3 eV.⁶ Recent work has shown that a pure barium metal surface fulfills this requirement.⁷ The work function of a barium metal is 2.5 eV which is about 1 eV larger when compared to a Tungsten or Molybdenum surface covered with half a monolayer of cesium. However, it has been shown that the high density of states (Fermi energy) of barium compensates for the higher work function.⁸ Furthermore, extensive modeling of the dynamic hydrogen concentration at the surface of a barium converter exposed to an intense flux of positive hydrogen ions, shows that the conversion efficiency (i.e. the ratio between the surface produced negative ion

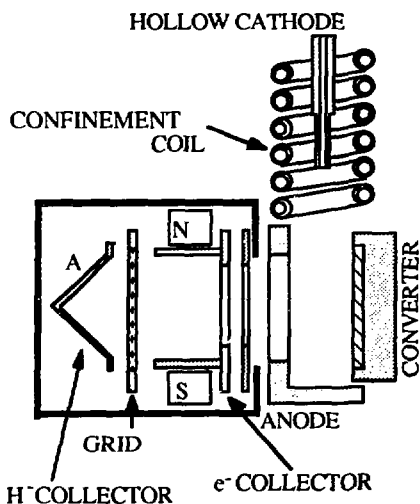


Fig. 6.1. Experimental set-up of the MEGA Light Ion Conversion Experiment (MEGALICE).

current density and the positive ion current density on the surface) scales with this current. The higher the incident flux the higher the conversion efficiency. Van Os, van Amersfoort and Los showed that for a positive ion current density of 0.2 A/cm^2 a conversion efficiency of 4.2 percent was obtainable.⁹ In this situation, model calculations showed that the hydrogen concentration was only a few percent of the saturation concentration which means that no saturation has occurred yet. This letter describes the results obtained with an upscaled surface conversion source which is capable of delivering of the order of 1 A/cm^2 of positive hydrogen ions on a barium surface in a DC mode.

For a current density of the order of 1 A/cm^2 one needs a plasma density in the vicinity of the converter surface of the order of $5 \times 10^{12} \text{ cm}^{-3}$. The set-up we use to obtain this high plasma density is to use a Hollow Cathode Arc (HCA) discharge and placing the converter surface as close as possible to the cathode. This set-up is shown schematically in Fig. 6.1 and is basically a redesign of our surface conversion source ALICE (Amsterdam Light Ion Conversion Experiment) which has been described extensively in literature.² The surface produced negative ions are collected in Faraday cup A after removal of electrons by means of a small magnetic field ($\approx 100 \text{ Gauss}$) perpendicular to the extracted beam. A compromise had to be made in the magnetic confinement of the HCA plasma which resulted in an operation pressure of the order of 50 mTorr . Secondly, with this set-up, Tantalum evaporated from the cathode can be deposited on the converter surface thus reducing the negative ion yield. Table 6.1 shows the difference in operating parameters for this set-up called MEGALICE (MEGA Light Ion Conversion Experiment) and the operation parameters of ALICE. Note, that due to the higher operation pressure, the mean free path for negative hydrogen ions is greatly reduced due to stripping on hydrogen molecules, a problem also observed in volume sources.^{10,11,12}

Table 6.1. The operation parameters for MEGALICE and ALICE.

	MEGALICE	ALICE	unit
Operating Pressure	40..55	3..7	mTorr
Plasma density in the vicinity of converter	$\approx 3 \times 10^{12}$	$\approx 10^{11}$	cm^{-3}
Mean free path for H^- :			
a. Due to molecules	≈ 0.5	> 100	cm
b. Due to electrons	> 500	$> 14 \times 10^3$	cm
c. Due to positive ions	> 30	$> 10^3$	cm
Magnetic confinement field	200..500	150..350	Gauss
Arc current	10..100	5..35	A
Positive ion current density at converter	200..1200	20..230	mA/cm^2

6.2. Experiments

The experimental procedure we used is as follows. The HCA discharge is started on argon and the converter surface is biased negatively while monitoring the current of the converter. Since the sputtercoefficient for argon on a barium target is of the order of unity, we are effectively sputter cleaning the surface. The latter is observed experimentally by a gradual increase of the converter current, as a function of time, due to removal of barium oxides and barium hydroxides. After some time, typically of the order of 20 minutes, the converter current saturates, which means that we have obtained a clean barium surface. At this point the HCA discharge is switched to hydrogen and the currents in the detector are monitored.

First of all we measured the negative ion current as a function of time for different arc currents. We observe a sharp rise, a maximum and then a gradual drop of the negative ion current as a function of time. For low arc current (≈ 20 A) we observe a 10 percent decrease from the maximum value of the negative ion current in about 5 minutes, for high arc current (≈ 60 A) this 10 percent decrease takes about 18 minutes. In view of this difference in time scale, it is reasonable to believe that this decrease is related to the pollution of the surface with tantalum. Increasing the arc current only increases the sputterrate of tantalum a little due to the relatively small increase of the ionization degree in the hollow cathode, whereas, the sputterrate of tantalum from the barium converter increases linearly with arc current. This in effect means that for increasing arc current the net supply of tantalum to the surface decreases which explains for the difference in the time constants mentioned before.

Secondly, the conversion efficiency was measured as a function of the incident flux of positive hydrogen ions. The converter voltage we used was -300 V and the measurements were taken at the peak value for the negative ion current vs time, in view of the afore mentioned problem of the pollution of the barium surface with tantalum. In order to compare these results with the measurements obtained for the conversion efficiencies in the earlier set-up, ALICE, we corrected the obtained negative ion current densities for stripping on molecules. The cross section we used is $1 \times 10^{-15} \text{ cm}^2$, which results in a correction factor for the conversion efficiency

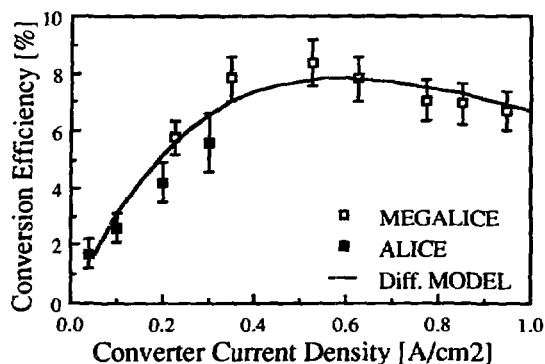


Fig. 6.2. The conversion efficiencies for ALICE and MEGALICE as a function of the incident positive ion current density. The operation pressure for ALICE is 3 mTorr and for MEGALICE 50 mTorr, the conversion efficiencies for MEGALICE have been corrected for stripping of negative ions on molecules. The converter potential in all cases is -300 V. The solid line is the result of model calculation assuming a linear increase of the surface temperature with incident positive ion flux. The probability for negative surface ionization used in the calculations is 12 percent.

of 620 ± 60 .¹³ The results for the conversion efficiency for MEGALICE are depicted together with earlier results from ALICE in Fig. 6.2.

6.3. Discussion

The two curves for ALICE and MEGALICE do not exactly join up, this is probably related to a difference in temperature of the surface and a possible contribution to the surface hydrogen coverage by adsorption of molecules for the latter experiment. For low positive ion current densities we observe an increase of the conversion efficiency with increasing positive ion current on the converter. Around 0.5 A/cm^2 a maximum is observed and a slowly decreasing conversion efficiency from this point on. In Fig. 6.2 also shows a theoretical curve based on our diffusion model. In calculating this curve we assumed a linear increase of the temperature with incident flux. The curve follows the trend in the experimental data. We will briefly discuss this model in the following and show that for incident fluxes above 0.5 A/cm^2 a much better agreement can be obtained.

In order to understand why the conversion efficiency decreases for higher converter current densities we have to look in detail what determines the conversion efficiency. Energy distributions of the self extracted beam show that the majority of the negative ions collected are formed via a sputtering and/or recoiling process at the converter surface.⁹ Based on this observation we have argued that the conversion efficiency is equal to an ionization probability multiplied by a sputtercoefficient. The latter coefficient can be treated as a solid body sputter coefficient multiplied by a probability of hitting a hydrogen atom at the surface. Or more practical, the solid body sputter coefficient multiplied by the relative hydrogen concentration in the top layers of the barium converter. This yields for

the conversion efficiency,

$$\eta_H^* = \frac{\Phi_{H^-}}{\Phi_{H^+}} = \frac{\eta_H \frac{c_H}{c_{sat}} \Gamma_{H-H} \Phi_{H^+}}{\Phi_{H^+}} = \eta_H \Gamma_{H-H} \frac{c_H}{c_{sat}} \quad [6.1]$$

where Φ_{H^+} is the incident flux, η_H is the probability for negative surface ionization, c_H denotes the hydrogen concentration, c_{sat} the hydrogen saturation concentration, Φ_{H^-} the negative ion yield and Γ_{H-H} the sputtercoefficient for hydrogen on a "solid" hydrogen target. Since the solid body sputter coefficient Γ_{H-H} and the ionization probability η_H are independent of the incident flux and the temperature of the surface, we believe that the observations mentioned above are related to a changing hydrogen concentration at the surface.

In Ref. 9 we described a model, with which the hydrogen concentration can be calculated, based upon zero net flux of hydrogen at the surface, or rather, the implanted flux is equal to the sum of the desorbed and sputtered flux;

$$\alpha \Phi_{H^+} = \Phi_{Hsput} + \Phi_{Hdes} \quad [6.2]$$

where α denotes the implantation fraction, and Φ_{Hsput} and Φ_{Hdes} are the sputtered and desorbed fluxes respectively. The sputtered flux, Φ_{H^-} is given in Eq. [6.1]. For the desorbed flux we can write,

$$\Phi_{Hdes} = \frac{n_H}{\tau} \approx \frac{n_{sat} c_H}{\tau}, \quad \tau = \tau_0 \exp(Q/kT_s), \quad \tau_0 \approx 10^{-13} \text{ s} \quad [6.3]$$

where n_H denotes the surface hydrogen coverage, τ the residence time of hydrogen on the surface, Q is the binding energy of hydrogen on barium and T_s is the surface temperature. Combining these equations yields the hydrogen coverage at the barium surface,

$$\frac{c_H}{c_{sat}} = \alpha \left(\Gamma_{H-H} + \frac{n_{sat}}{\tau \Phi_{H^+}} \right) - 1 \approx_{>T_s} \frac{\Phi_{H^+} \alpha \tau}{n_{sat}} = \frac{\Phi_{H^+} \alpha \tau_0}{n_{sat}} \exp\left(\frac{Q}{kT_s}\right) \quad [6.4]$$

One can see that the hydrogen concentration is a direct function of the incoming positive hydrogen ion flux and the temperature of the surface. In practice these two parameters are coupled since an increase in current density on the surface also increases the power input at the surface thus resulting in a higher temperature. Apparently, we are working in a range in which the temperature becomes so high that via desorption the hydrogen concentration drops resulting in a lower conversion efficiency. Therefore, the decrease in Fig. 6.2 is interpreted as due to a decrease in c_H .

The experimental data for the temperature dominated regime (i.e. for positive ion current densities on the converter above 0.5 A/cm^2) permits us to estimate the surface binding energy according to Eq. [6.4] combined with Eq. [6.1] From the exponential fit in Fig. 6.3 of the conversion efficiency, in this regime, divided by the incoming positive hydrogen ion flux versus the reciprocal surface power dissipation, which is proportional to the surface temperature, we are able to estimate the surface binding energy for hydrogen on barium, Q , which amounts to $1.3 \pm 0.25 \text{ eV}$. This is a reasonable value for a binding energy and consistent with an

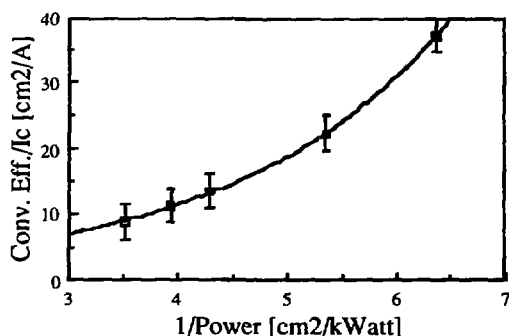


Fig. 6.3. The conversion efficiency divided by the incident positive ion current density versus the reciprocal adsorbed power on the converter. Only the measurements for a incident positive ion current above 0.5 A/cm^2 are used. The solid line is an exponential fit of the experimental data.

earlier estimate based upon the experimental results obtained from ALICE.

6.4. Summary

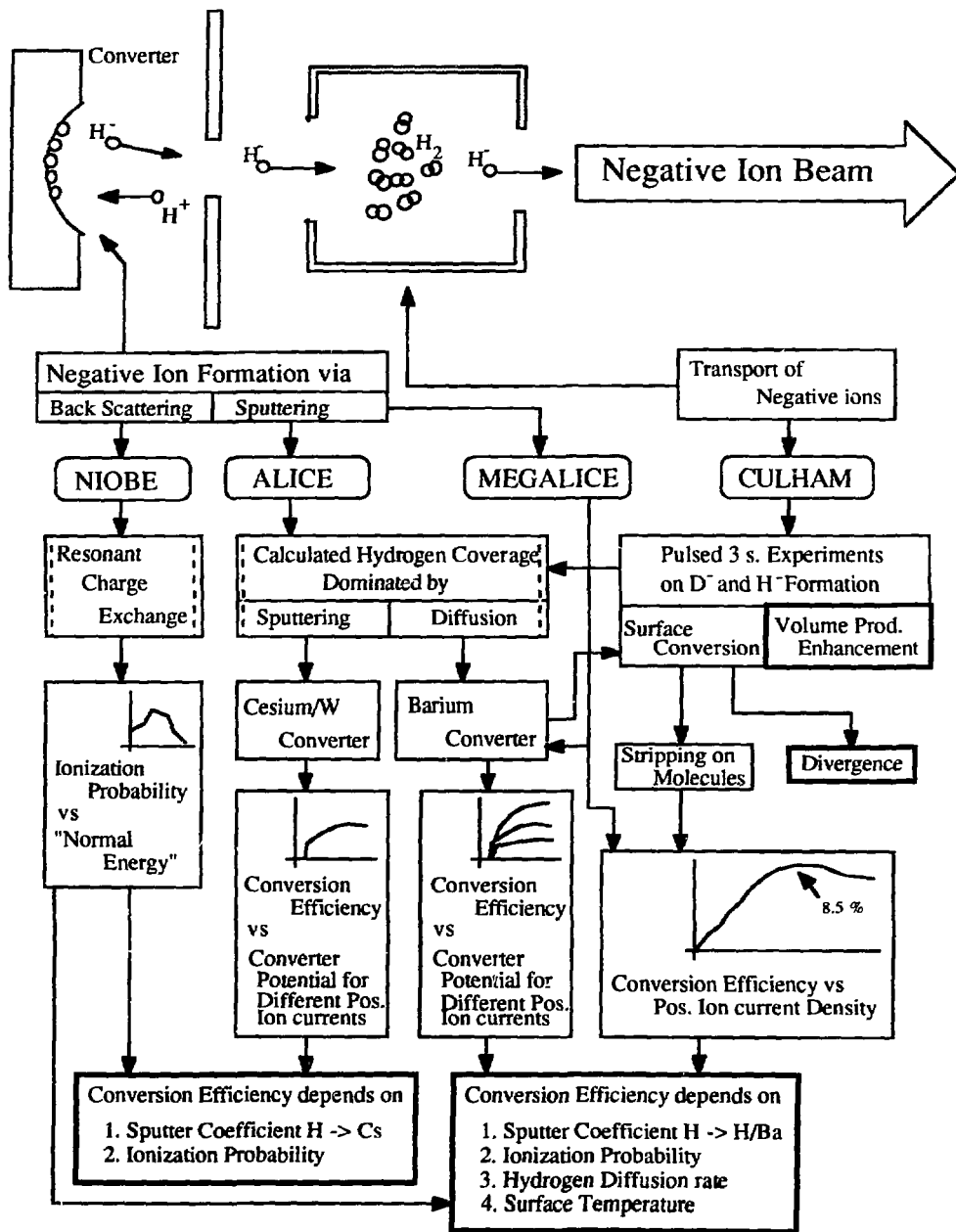
Summarizing, our experimental data shows that the conversion efficiency scales with the incoming positive ion flux as predicted by our diffusion model. For high temperatures of the converter surface, desorption of hydrogen reduces the hydrogen concentration which reduces the conversion efficiency. Further experiments with a better confined HCA discharge in order to reduce the operating pressure and a more efficient cooling of the converter are necessary. In a surface conversion source there is no need for a high neutral gas pressure in contrast to a volume source. Therefore, if the pressure can be lowered, a surface source equipped with a barium converter can deliver a higher negative ion current at a lower gas loading of the accelerator when compared to a volume source. The maximum conversion efficiency which can be obtained, which requires a low surface temperature, is equal to the negative ion formation probability which is in the range 10-15 percent. For an incident current density of 1 A/cm^2 this yields a negative ion current density of 100 to 150 mA/cm^2 . However, a detailed study of the extracted beam properties are needed to investigate the viability of this type of source for use in neutral beam lines. These afore mentioned studies are in preparation.

Acknowledgements

The authors gratefully acknowledge H.J. Timmer for transferring ALICE into MEGALICE. This work is part of the research program of the association agreement between the Stichting voor Fundamenteel Onderzoek der Materie (FOM) and EURATOM, and was made possible by financial support from the Nederlandse Organisatie voor Wetenschappelijk Onderzoek (NWO) and EURATOM.

References

- ¹ Yu. I. Belcherko, G.I. Dimov and V.G. Dudnikov, Nucl. Fus. **14** (1974) 113.
- ² C.F.A. van Os, E.H.A. Granneman and P.W. van Amersfoort, J. Appl. Phys. **61** (1987) 662.
- ³ E.J. Britt, J.L. Desplat, M. Korringa and K.N. Leung, J. Vac. Sci. Technol. A **3** (1985) 1241.
- ⁴ A. I. Herscovitch, V.K. Kovarik and K. Prelec, Rev. Sci. Instrum. **57** (1986) 827.
- ⁵ K. N. Leung and K.W. Ehlers, Rev. Sci. Instrum. **53** (1982) 803.
- ⁶ J.N.M. van Wunnik, J.J.C. Geerlings, E.H.A. Granneman and J. Los, Surf. Sci. **131** (1983) 17.
- ⁷ C.F.A. van Os, R.M.A. Heeren and P.W. van Amersfoort, Appl. Phys. Lett. **51** (1987) 1495.
- ⁸ C.F.A. van Os, H.M. van Pinxteren and J. Los, *Proceedings of the III European Workshop on Production and Application of Light Negative Ions*, p. 166, Amersfoort, Feb. 17-19, 1988.
- ⁹ C.F.A. van Os, P.W. van Amersfoort and J. Los, J. Appl. Phys. **64** (1988) 3863.
- ¹⁰ A.J.T. Holmes, L.M. Lea, A.F. Newman and M.P.S. Nightingale, Rev. Sci. Instrum. **58** (1987) 223.
- ¹¹ M. Bacal, A.M. Bruneteau and M. Nachman, J. Appl. Phys. **55** (1984) 15.
- ¹² Y. Okumura, *Proc. 11th Symposium on ISAT 87, Tokyo* p.267, 1987.
- ¹³ C.F.A. van Os, A.W. Kleyn, L.M. Lea, A.J.T. Holmes and P.W. van Amersfoort, Accepted for publication in Rev. Sci. Instrum (MS A88389).



SUMMARY

Recent design studies of future nuclear fusion reactors emphasize the need for current drive and additional heating of the fusion plasma. One proposed method for current drive is Neutral Beam Injection (NBI). The anticipated beam energy of such a system is of the order of 1 MeV, which makes the use of positive ions as intermediate particles impractical in view of the very low neutralization cross section at this high energy. However, negative ions have a neutralization probability at these energies of about 60 %. This observation invoked a worldwide research effort in the development of high current negative ion sources. Two methods are pursued; *volume production* and *surface conversion*. Research on the fundamentals of the latter method is discussed in this thesis.

Surface conversion can be described as a two electron transfer from a metal surface to a positive hydrogen ion, scattering from the surface. The incident positive ion is neutralised at a distance of around $10 a_0$ from the metal surface, resulting in a excited hydrogen atom. Closer to the surface the atom is Auger deexcited. In the vicinity of the metal surface, the affinity level of the hydrogen atom lowers due to the attractive image potential. At very short atom metal-surface separation, the affinity level crosses the work function of the metal surface. Which means that the electronic states in the metal conduction band are in resonance with the affinity level, and electrons can tunnel through the Coulomb barrier between the atom and the metal surface conduction band and form a negative ion. This process is generally referred to as *resonant charge exchange*.

It is common knowledge, that resonant charge exchange is very sensitive to the work function of the metal surface; the lower the work function the higher the probability of forming a negative ion. For this reason, the metal surface used in research on charge transfer is made from tungsten or molybdenum covered with a (sub)monolayer of cesium. The work function of such a system can be as low as 1.45 eV and it has been shown that up to 67 % of hydrogen atoms scattering from such a surface can be transformed into negative ions. Chapter 2 describes a well defined UHV scattering experiment in which a different surface is used; pure barium, which has a work function of 2.5 eV. The negative ion fractions obtained with this surface amounted up to 35 %, which is quite unexpected. The explanation for this high value lies in the density of electronic states (i.e. the Fermi energy) of the metal conduction band. The high Fermi energy results in an increase of the transition frequency which explains the high negative ion formation probability observed, although the optimum negative ion formation probability with respect to the incident energy is shifted to higher energies. Due to the relatively high work function of barium the charge exchange process takes place very close to the surface. This can lead to interferences in the charge exchange process as discussed in chapter 2.

The high negative ion formation probabilities mentioned above, resulted in the

development of so-called *surface conversion sources* based on the physical principle discussed above. Such a source basically consists of a hydrogen discharge which is in contact with a negatively biased low work-function surface. Positive hydrogen ions are accelerated across the plasma sheath perpendicular to the surface and can either reflect from or penetrate into the surface. The incident flux also sputters already present hydrogen atoms and molecules from the surface. The reflected and sputtered particles can become negatively ionized in their outgoing trajectory. Once a negative ion is formed it is accelerated again across the plasma sheath into the accelerator, a process called "self-extraction".

Chapter 3, 4 and 6 describe measurements with our surface conversion source ALICE (Amsterdam Light Ion Conversion Experiment) which has been operated with a cesium/tungsten and a pure barium metal converter. From the energy distribution of the formed negative ions it is concluded that the majority is produced via sputtering and/or recoiling. We have argued that the hydrogen concentration in this sputtering process predominantly determines the obtained negative ion yield. Therefore, both systems have been extensively modeled in terms of implantation, sputtering and diffusion in order to calculate the dynamic hydrogen concentration of the converter at the surface.

It is concluded from the measurements that the cesium/tungsten system is *sputter dominated*, whereas for the barium system the processes are *diffusion dominated*. Both are specific solutions of a general master equation which was formulated for the sputtering process. For both systems good agreement could be obtained between experimental observations and theoretical predictions. The maximum conversion efficiency (the ratio of the negative ion current density and the positive ion current density on the converter surface) which has been obtained with a barium converter amounted to 8.5 % for an incident positive ion current of the order of 500 mA/cm² and is the highest obtained in any DC surface conversion source at the time of writing.

The negative ions produced at the surface have to travel some distance before they enter the accelerator. The transport of these negative ions is studied in chapter 5. The dominant loss mechanism appeared to be the stripping of negative ions on hydrogen molecules. Furthermore, the divergence of a 100 eV surface produced beam has been estimated to be around 4°. The experiments have been done at Culham, England, with a bucket plasma source (P.I.N.I., Plug In Neutral Injector) in which a barium converter was mounted. Biasing the converter in this source gave an enhancement of the volume produced negative ion current up to 25 % at low source filling pressures.

SAMENVATTING (SUMMARY IN DUTCH)

Uit onderzoek op het gebied van kernfusie in de vorm van een hoog energetische plasma opgesloten in een torodiaal magneetveld, blijkt dat er gezocht moet worden naar een methode om het fusieplasma te stuwen en tevens te verhitten om ontsteking en "steady state" fusie te bereiken. Eén van de vier methoden, die in dit onderzoek genoemd worden, is het inschieten van neutrale bundels (NBI, Neutrale Bundel Injectie). De bundelenergie moet om en nabij de 1 MeV zijn om door te kunnen dringen tot het centrum van het fusieplasma. Het gebruik van positieve ionenbronnen voor dit doel is vrijwel onmogelijk vanwege de lage neutralisatiekans bij deze hoge energieën. Een oplossing van dit probleem is het gebruik van negatieve ionen als tussenstap in de produktie van de neutrale bundel. De neutralisatiekans is voor negatieve ionen bij deze hoge energie ongeveer 60 %. Deze constatering heeft geleid tot wereldwijd onderzoek op het gebied van negatieve ionenbronnen die in staat zijn een grote stroom te leveren. Hiervoor staan twee methodes ter beschikking; *volume produktie* en *oppervlakte omlading*. In dit proefschrift wordt onderzoek naar de fundamentele eigenschappen van de laatstgenoemde methode beschreven.

Oppervlakte omlading is in feite het overbrengen van twee elektronen uit een metaaloppervlak naar een positief waterstofatoom wat daaraan reflecteert. In de inkomende baan wordt eerst het positieve waterstofion geneutraliseerd en vervolgens vindt dicht bij het oppervlak Auger deëxcitatie plaats. Op zo'n korte afstand tot het oppervlak zal het affiniteitsnivo van het waterstofatoom verlaagd zijn ten gevolge van de attractieve spiegelbeeldpotentialiaal. Zeer dicht bij het oppervlak zal het affiniteitsnivo onder de werkfunctie van het metaal liggen, waardoor het mogelijk wordt dat een elektron dat vanuit het metaal door de Coulomb barrière heendringt, het affiniteitsnivo bezet. Het omgekeerde kan ook gebeuren, zodat er sprake is van een resonante bezetting van het affiniteitsnivo. Wanneer het waterstofatoom zich verwijderd van het metaaloppervlak kan een gedeelte van de lading terugvloeien naar het metaal. Hierdoor zal slechts een gedeelte van de atomen omgeladen worden naar een negatief ion. Dit proces wordt resonante ladingsruil genoemd.

Het is algemeen bekend dat resonante ladingsruil sterk afhankelijk is van de werkfunctie van het metaaloppervlak; hoe lager deze is des te groter wordt de kans op de vorming van een negatief ion. Dit is de reden waarom onderzoek aan resonante ladingsruil voornamelijk werd gedaan aan wolfram en molybdeen oppervlakken bedekt met een halve monolaag cesium. De werkfunctie voor zo'n oppervlak is 1.45 eV en een vormingskans van negatieve ionen van 67 % is waargenomen voor waterstofionen verstrooid aan zo'n oppervlak. Hoofdstuk 2 beschrijft onderzoek in een goed gedefinieerde UHV-opstelling waarin een waterstofbundel wordt verstrooid aan een *bariumoppervlak* welke een werkfunctie heeft van 2.5 eV. Ondanks deze relatief hoge werkfunctie, werden vormingskansen

tot 35 % waargenomen. Een verklaring voor deze opmerkelijke ontdekking kan worden gevonden in de hoge dichtheid van elektronische toestanden in het bariummetaal (Fermi-energie). Door deze hoge dichtheid wordt de overgangsfrequentie hoger waardoor meer negatieve ionen worden gevormd dan verwacht; de optimum vormingskans is echter verschoven naar een hogere energie van de gereflekteerde deeltjes. Door de relatief hoge werkfunctie van het barium is de ladingsruil sterk gelokaliseerd bij het oppervlak waardoor interferenties, zoals beschreven in hoofdstuk 2, kunnen optreden.

De hoge vormingskans van negatieve ionen die met resonante ladingsruil werd waargenomen, resulteerde in de ontwikkeling van zogenaamde *oppervlakte omladings bronnen*. In principe bestaat zo'n bron uit een waterstofontlading die in contact wordt gebracht met een oppervlak met een lage werkfunctie (de omlader) dat op een negatieve spanning wordt gezet. Door deze spanning worden positieve ionen uit het plasma geëxtraheerd. Deze kunnen reflektoren van danwel penetreren in het omladeroppervlak. De binnenkomende stroom van ionen kan tegelijkertijd aan het oppervlak geadsorbeerd waterstof verwijderen (sputteren). De gereflekteerde en gesputterde deeltjes kunnen omgeladen worden via resonante ladingsruil. Zodra een negatief ion gevormd is, zal het door de omladerspanning versneld worden in de richting van de extraktieopening: "zelf-extractie".

Hoofdstuk 3,4 en 6 beschrijven metingen de oppervlakte- omladingsbron ALICE (Amsterdam Light Ion Conversion Experiment), waarmee de eigenschappen van een gecesieerde wolframomlader en een pure bariumomlader zijn onderzocht. Metingen van de energieverdeling van de geproduceerde negatieve ionen laten zien dat sputteren het dominante productieproces is. Een belangrijke parameter in het sputterproces is de aanwezige hoeveelheid waterstof aan het omladeroppervlak. Voor beide omladeroppervlakken zijn uitgebreide modellen opgezet om deze concentratie te berekenen.

Hoofdstuk 4 laat zien dat voor een gecesieerde wolframomlader deze concentratie voornamelijk wordt bepaald door de erosiesnelheid van het wolfram; in andere woorden: het verwijderen van wolfram door sputteren. We noemen dit model dan ook *sputter-gedomineerd*. Hoofdstuk 3 en 6 laten zien dat voor een bariumomlader de concentratie bepaald wordt door diffusie van waterstof in het barium, een *diffusie-gedomineerd* model. In alle gevallen werd een goede overeenkomst bereikt tussen theorie en experiment. Voor een positieve ionenstroom van 500 mA/cm^2 op het oppervlak werd een omladingsefficiëntie (verhouding tussen geproduceerde negatieve ionenstroom en positieve ionenstroom op het oppervlak) van 8.5 % waargenomen. Dit is de hoogst gemeten waarde in een DC oppervlakte omladingsbron op het moment van schrijven.

De negatieve ionen kunnen op hun weg naar de "versneller" botsen met restgas - en plasmadeeltjes, waardoor deze ionen verloren kunnen gaan. In hoofdstuk 5 wordt onderzoek beschreven naar het transport van negatieve ionen, gevormd aan een bariumomladeroppervlak, door een plasmabucketbron. Het verlies ten gevolge van botsingen met restgas bleek dominant te zijn. Als laatste werd gekeken naar het in symbiose werken van oppervlakte omlading en volume productie. Een toename van 25 % door oppervlakte omlading werd waargenomen bij een lage brondruk.

ЗАКЛЮЧЕНИЕ (SUMMARY IN RUSSIAN)

Из исследования в области ядерной фузии, в частности исследование высокoэнергической пласми оказывается нужна метода толкнуть на пласму и тоже ее раскалить, только что будет возможно достигнуть зажигания и т.н.-ого "steady state fusion" (стабильной фузии). Один из четыре метода, который называется в этой диссертации - иньекция в нейтральные пучки (NBI; Neutral Beam Injection). Энергия пучка надо пронукнуть в центре пласми - около 1 MeV. Для этой цели употребление позитивных ионных источников почти невозможно, потому что шанс нейтрализации у таких высоких температур всегда небольшой. Разрешение этого вопроса - употребление позитивных ионных источников как междустадия в производство нейтрального пучка. У такой высокой энергии шанс нейтрализации для негативных ионов - около 60 %. Это установление повело к всемерную исследованию в области негативных ионных источников, которые могут поставить много тока. Для этого имется 2 метода; (1) проивводство объема и (2) перезаряд поверхности. В этой диссертации описывается исследование к основным качествам последнего метода.

Перезаряд поверхности действительно - перевод 2 электрона из металлической поверхности в позитивный водородный атом, который рефлектирует на поверхность. Сначала позитивный водородный атом нейтрализуется на входной рулон, а потом, близ поверхности, состоится Аудер дезксситация. На таком кратком расстоянии от поверхности уворень сродства водородного атома будет понижен ради заманчивого отраженного потенциала. Очень близ поверхности уворень сродства будет под рабочей функцией металла, посредством чего будет возможно чем определенный электрон пробьет через барьера Куломба и займет уворень сродства. Обратное и возможно, так что говорит о резонирующем занятии уверения сродства. Часть заряда может течь обратно к металлу, когда водородный атом отдаляется от металлической поверхности. Вледствие этого только часть атомов перезарядит в негативные ионы. Этот процесс называется резонирующим обменом зарядом.

Это известно любому что резонирующий обмен зарядом очень нависимый от рабочей функции металлической поверхности; чем ниже этой, тем больше шанса на образование негативного иона. Это причина почему исследуют особенно обмену зарядом у поверхности вольфрана и молибдена, покрыты с половино моно- слоистой цесием. Рабочая функция такой поверхности 1.45 eV, а шанс образования ионов для водородных атомов, разбросанных над той же самой поверхностью, наблюдался на 67 %.

Вторая глава описывает исследование в одной точно определенной U.N.V.- установке, в которой пучок водорода разбрасывается на поверхность бария, чья рабочая функция 2.5 eV. Вопреки этой относительно высокой рабочей функции, наблюдался шанс на образование ионов до 35 %. Объяснение этого замечательного открытия можно найти во высокую плотность электронных положений в том же самом барии (т.н. Ферми энергия). Ради этой высокой плотности переходная частота растет, через которая образуется больше негативных ионов чем ожидало. Однако, оптимальный шанс на образование ионов изменился к высшую энергию рефлектируемых частиц. Из-за относительно высокой рабочей функции бария, обмен зарядом локализуется особенно близ поверхности, посредством чего будет возможно чем явится интерференциями, как и описывает вторая глава.

Высокий шанс на образование негативных ионов, который наблюдался у резонирующий обмен зарядом, повел к образованию т.н.-ых источников для перезаряда поверхности. В принципе такой источник существует из водородной разрядки, которая связалась с поверхностью с низкой рабочей функцией (перезарядником), которая - под тока негативного напряжения. Из-за этого напряжения экстрагируются негативные ионы из плазмы. Эти ионы могут рефлектировать или проронуть в поверхность перезарядника. Входное течение ионов одновременно может удалить абсорбируемый водород (шипеть). Через резонирующий обмен зарядом возможно перезарядить рефлектируемые и шипимые частицы. Немедленно, когда образовался один негативный ион, ускорится его в направлении открытия для экстракции: т.н. самоэкстракция.

Третье, четвертое и шестое главы описываются измерения и источник для перезаряда поверхности ALICE (Amsterdam Light Ion Conversion Experiment), с которым исследовалось качества (а) перезарядника вольфрама, покрыт с цезием, и (б) перезарядника бария. Измерения разделения энергии производных ионов оказываются, чем важнейший начин производства шипеть. В процессе шипения важный параметр есть имеющееся количество водорода на поверхности перезарядника. Для обеих поверхности перезарядов поставилось модели, чтобы рассчитать эти концентрации.

В четвертой главе можно читать, что эта концентрация у перезарядник вольфрама, покрыт с цезием, особенно определена через скорость эрозии вольфрама, в сущности вольфран удалится, вследствие процесса шипения. Этот модель называется преобладание шипения (*sputter dominated*). Третье и шестое главы описываются, что концентрация у перезарядник бария определена через диффузию водорода в барий. Этот модель называется преобладание диффузии (*diffusion dominated*). В всех случаях согласуется теория с практикой. У течение позитивных ионов 500 mA/cm² наблюдалось эффективность перезаряда 8.5 %. Сейчас, то есть высочайшая измеренная стоимость в одном "DC"- источнике для

перезаряда поверхности.

Негативные ионы могут пройти в столкновение с частицы отстального газа и пласми по пути до ускорения, отчего эти ионы пропадут. В пятой главе можно читать о исследовании к транспорту негативных ионов, образованны на поверхности перезаряда бария из одного "plasma-bucket" источника. Потеря, вследствие столкновений с отстальным газом, преобладала. Дивергенция пучка, который производился на поверхности, исследовалась. Под конец исследовалось, чтобы работать в единстве производство объема и перезаряд поверхности. Ради перезаряда поверхности у низкое давление источника наблюдалсь один прирост на 25 %.

Het onderzoek waarvan het resultaat verzameld ligt in dit boekje, kwam tot stand in samenwerking met vele mensen van het instituut. Tegenover al deze mensen wil ik hier mijn dankbaarheid uitspreken. Met name wil ik Joop Los en Henk Timmer noemen die er de afgelopen vier jaar voor zorgden dat ik op het fysische en het experimentele vlak niet te ver uit de bocht vloog. Daarnaast wil ik Arjen Deij bedanken voor het vertalen van mijn samenvatting in het Russisch.

I also would like to thank the group of Andrew Holmes at Culham Laboratories for their hospitality and for giving me the opportunity for doing the experiments discussed in Chapter 5.

CURRICULUM VITAE

Naam:	Ron van Os
Voornamen:	Carolus Franciscus Adrianus
Geboren:	4 maart 1961 te Helmond
V.W.O.	augustus 1973 tot mei 1979, ongedeeld Atheneum
W.O.	- september 1979 tot januari 1982 kandidaats N3 aan de RUU, vakken: Natuurkunde, Wiskunde en Geofysica. - september 1981 tot april 1985 doctoraal experimentele natuurkunde aan de RUU.
Promotie	- oktober 1985 tot mei 1989, FOM-Instituut voor Atoom en Molecuul Fysica, Amsterdam.